EPA

United States
Environmental Protection
Agency

Spatial and Temporal Trends of Air Pollutants in the South Coast Basin Using Low Cost Sensors

CSAM Pod Site Locations

Office of Research and Development
National Exposure Research Laboratory

Spatial and Temporal Trends of Air Pollutants in the South Coast Basin Using Low Cost Sensors

Ron Williams and Rachelle Duvall
U.S. Environmental Protection Agency
Office of Research and Development
National Exposure Research Laboratory
Research Triangle Park, NC 27711

Dena Vallano
U.S. Environmental Protection Agency, Region 9
Air Quality Analysis Office
San Francisco, CA 95105

Andrea Polidori, Vasileios Papapostolou, Brandon Feenstra, Hang Zhang
South Coast Air Quality Management District Science and Technology Advancement Office
Air Quality Sensor Performance Evaluation Center (AQ-SPEC)
Diamond Bar, CA 91765

Sam Garvey
Jacobs Technology Inc.
Tullahoma, TN 37388

Disclaimer

This technical report presents the results of work performed by the South Coast Air Quality Management District's AQ-SPEC Laboratory under contract EP-16-W-000117 and Jacobs Technology, Inc. under contract EP-C-15-008 for the National Exposure Research Laboratory, U.S. Environmental Protection Agency (U.S. EPA), Research Triangle Park, NC. It has been reviewed by the U.S. EPA and approved for publication. Mention of trade names or commercial products does not constitute endorsement or recommendation for use.

Abstract

The emergence of small, portable, low-cost air sensors has encouraged a shift toward their use and away from traditional approaches to monitoring air quality. The U.S. Environmental Protection Agency (U.S. EPA), in collaboration with t h e South Coast Air Quality Management District's (SCAQMD) Air Quality Sensor Performance Evaluation Center (AQ-SPEC), deployed custom-built sensor devices (pods) measuring fine particulate matter ($PM_{2.5}$), ozone (O_3), relative humidity, and temperature at nine locations throughout southern California from January 2017 to April 2017 to evaluate their performance under "real-life" conditions. Prior to the deployment, these pods were evaluated within the AQ-SPEC program both in the field and in the laboratory. Southern California is an ideal testing location for air quality sensor technology, as it often experiences elevated air pollutant levels resulting from gasoline and diesel engines, marine ports, and various other industries. The South Coast Air Basin's particular meteorology (frequent sunny days and little precipitation) and geography also contribute to the elevated pollution levels in the region. The goal of this project was to characterize the performance of these newly developed pods and better understand their potential applications for community monitoring. This report summarizes the AQ-SPEC field and laboratory performance evaluations of the Citizen Science Air Monitor (CSAM) sensor pods designed and developed by the EPA. In addition, this document summarizes the spatial and temporal variability of the $PM_{2.5}$ and O_3 measurements collected during the field deployment of the CSAM pods at nine monitoring locations covering approximately a 200 km^2 area in southern California.

Table of Contents

List of Tables

List of Figures

Acronyms and Abbreviations

AMS	Air Monitoring Station
AM	Atmospheric Measurements
APS	Aerodynamic Particle Sizer
AQ-SPEC	Air Quality – Sensor Performance Evaluation Center
BAM	Beta Attenuation Monitor
BAT	Best Available Technology
°C	Degrees Celsius
COTS	Commercial-off-the-shelf
CSAM	Citizen Science Air Monitor
DP	Dew point
EJ	Environmental Justice
EPA	Environmental Protection Agency
°F	Degrees Fahrenheit
FEM	Federal Equivalent Method
FRM	Federal Reference Method
hr	Hour
JARPD	Jurupa Area Recreation and Parks District
m	meter
Max	maximum
$\mu g/m^3$	Microgram per cubic meter
min	Minute
Min	Minimum
mL	Milliliter
NAAQS	National Ambient Air Quality Standards
NO	Nitric oxide
nm	nanometer
NO_2	Nitrogen dioxide
O_3	Ozone
OPC	Optical Particle Counter
ORD	Office of Research and Development
PM	Particulate matter
$PM_{1.0}$	Particles smaller than 1 µm in aerodynamic diameter
$PM_{2.5}$	Particles smaller than 2.5 µm in aerodynamic diameter
PM_{10}	Particles smaller than 10 µm in aerodynamic diameter
PM_c	Coarse Particulate matter
Ppb	Parts per billion
QAPP	Quality Assurance Project Plan
QA/QC	Quality Assurance/Quality Control
R^2	Correlation coefficient
RH	Relative humidity
RIVR	Rubidoux Air Monitoring Station
ROP	Research Operating Protocol
RTP	Research Triangle Park
SCAB	South Coast Air Basin
SCAQMD	South Coast Air Quality Management District

SE	Standard Error
SOP	Standard Operating Procedure
SO_2	Sulphur Dioxide
SSAB	Salton Sea Air Basin
STDEV	Standard Deviation
T	Temperature
TSP	Total Suspended Particles
μm	Micrometer
UV	Ultraviolet
V	Volt
VOC	Volatile Organic Compound

Executive Summary

Background

The Office of Research and Development (ORD) at EPA has been conducting a variety of both laboratory and field-based evaluations/deployments of air quality sensors and other Next Generation Air Monitors (NGAM). These efforts have included laboratory and/or field evaluations of numerous NGAM devices for measuring nitrogen dioxide (NO_2), ozone (O_3), particulate matter (PM), volatile organic compounds (VOC), and sulfur dioxide (SO_2) (Williams 2015a, Williams 2015b, Williams 2014a, Williams 2014b). The ORD has published findings from some of these efforts through its Air Sensor Toolbox for Citizen Scientists, Researchers and Developers website (www.epa.gov/air-sensor-toolbox). During recent years, air pollution sensor technology has advanced significantly. Specifically, sensors that currently are being developed are much smaller, more lightweight, and lower in cost than traditional ambient air monitoring systems. The advent of these types of sensors present an opportunity to advance EPA's strategic goals, including those of community monitoring and environmental justice. One of the potential benefits of this type of technology is the ability to deploy a larger number of sensors across a small geographic area (e.g., a neighborhood) and collect data with a level of spatial and temporal resolution that would be cost-prohibitive using traditional monitoring methods. Prime examples of such efforts include the Citizen Science Air Monitor (CSAM; Barzyk 2016, Williams 2015c) and the AirMapper (U.S. EPA, 2016) devices. All the aforementioned examples involved ORD collaboration with regional offices and local communities and/or state air quality agencies. To the greatest extent possible, technology insights from such recent projects were leveraged in this study to reduce sensor pod development costs as well as provide for project timeline savings. This project supports the development of low-cost sensor technologies that can be used for community monitoring.

Study Objectives

The main objective of this project was to fully characterize the performance of the low-cost air quality sensors devices developed by the EPA (herein referred to as pods, sensor pods, or CSAM) and to better understand their potential for community monitoring applications. The performance of the sensor pods developed by the EPA was evaluated and characterized in the field (i.e., at one of SCAQMD's air monitoring stations) and in a controlled laboratory environment (i.e., AQ-SPEC's characterization chamber). After evaluating the sensors' performance, the pods were dispersed in a nodal pattern to study the spatial and temporal patterns of multiple criteria pollutants in Southern California.

Study Approach

The EPA developed and assembled ten identical pods containing low-cost commercial-off-the-shelf (COTS) sensors for measuring PM, O_3, relative humidity (RH), and temperature (T). Each pod has AC and/or solar power functionality and internal data storage. The basic operational status of the pods was established at EPA's Research Triangle Park (RTP) laboratory in North Carolina. A research operating protocol (ROP) for operating the sensor pod was developed by EPA staff. Once the pods were deemed operational and fully functional, they were shipped to the AQ-SPEC group, which conducted an intensive field and laboratory performance evaluation of the $PM_{2.5}$, O_3, RH, and T sensors against the corresponding reference monitors. Ultimately, the pods were placed in a nodal pattern in areas of high interest to EPA Region 9 (i.e., adjacent to freeways, existing regulatory monitoring stations, and associated neighborhoods including schools, as well as emissions sources such as marine ports, airports, etc.) and operated for approximately three months from January 2017 to April 2017. The components of the EPA-designed sensor pods, selected for their known capabilities of being integrated into a sensor pod arrangement, are defined in Table A.1.

Table A.1. Sensor components in each CSAM Sensor Pod developed by EPA

Sensor / Manufacturer	Parameters Measured	Approximate total cost (per pollutant for multi-pollutant
OPC-N2 (AlphaSense)	PM_1, $PM_{2.5}$ and PM_{10}	$500
SM-50 (Aeroqual)	O_3 (Ozone)	$500
Adafruit AM 2315	Relative humidity (RH)	$200
Adafruit AM 2315	Temperature	$200
Grape Solar 1289	Solar panel	$500
Arduino Mega with Adafruit SD	Microprocessor	$400

EPA has prior experience assembling integrated sensor devices (e.g., CSAM, AirMapper) and sharing their features with all interested parties. Figures A.1 and A.2 below depict the basic CSAM pod and deployment components (sensor box, tripod, solar panel) that were used for the project.

Figure A.1. Sensor pod assembly

Figure A.2. Fully assembled pod with solar panel, battery cell, and tripod.

Each sensor component was operated according to the manufacturer's recommendations. On-board data storage (secure digital [SD] card) was used to minimize data collection issues. A weatherproof enclosure was used to contain all sensor components, with inlets protruding from the base of the enclosure. The placement of the solar panel was designed to act as a shading device to reduce the internal operating temperature of the pod. A stable tripod base provided the means to secure all components and allowed for consistent deployment across the various geographical locations. Once the devices were determined to be operating in an acceptable manner, they were delivered to AQ-SPEC for laboratory and field evaluation and then for subsequent field deployment.

The AQ-SPEC team was responsible for evaluating the sensor pods developed by ORD and then operating the pods in a nodal (spatial) pattern across Southern California in specific areas of interest to EPA Region 9 and SCAQMD. The evaluation of the sensor pods was conducted at SCAQMD field and laboratory locations.

The individual sensor components selected for the pods had been evaluated previously as part of the CAIRSENSE field tests (Jiao 2016, Jiao 2015) under ambient conditions. The performance of these same sensors in California (field/laboratory) was expected to be similar to these earlier findings. Even though both

the OPC-N2 and the Aeroqual SM-50 sensors had been tested previously by the EPA over several months, a full (e.g., field and laboratory) evaluation of these sensors at this geographic scope had not been performed prior to this effort. The current project described herein adds to EPA's knowledge base of these sensors and their performance characteristics.

This project consisted of both laboratory and field NGAM evaluation scenarios over the lifespan of the research project. The PM and ozone gas pollutant sensors were compared with the appropriate Federal Equivalent Method or Federal Reference Method (FEM or FRM, respectively) air pollutant measurement systems. Field and laboratory evaluations involving FEM/FRM monitors operated by SCAQMD's personnel were conducted under AQ-SPEC's internal quality assurance guidelines.

Conclusions

The ten CSAM pods, each one equipped with i) a $PM_{2.5}$ sensor, model OPC-N2, by Alphasense, UK; ii) an ozone sensor, model SM-50, by Aeroqual, New Zealand, and; iii) a temperature/relative humidity sensor, model AM2315, by Adafruit, were co-located and field tested alongside reference instruments for two months at one of SCAQMD's fixed ambient monitoring stations in Riverside-Rubidoux (RIVR), California. One CSAM pod developed operational issues at the onset and was not deployed. The other nine CSAM pods proved to be very reliable, with excellent data recovery and overall showed only a modest intra-model variability for $PM_{2.5}$ and a low intra-model variability for ozone, temperature, and relative humidity. Three CSAM Pods carried PM sensors that indicated a potential mischaracterization of ambient $PM_{2.5}$ mass concentration measurements compared to those from the reference instruments. The CSAM $PM_{2.5}$ sensor data for seven of the nine units tested showed a modest correlation (R^2: $0.40 - 0.60$) with substantially more costly FEM instruments (i.e., GRIMM and BAM), and overestimated the 5-minute average $PM_{2.5}$ measurements by approximately 75% as measured by the FEM GRIMM. The $PM_{2.5}$ data from two units showed a poor correlation with the FEM due to a potential PM sensor malfunction with the sensor's optics during the co-location testing period. The CSAM ozone sensor data for all nine pods showed excellent correlation (R^2: $0.80 - 0.97$) with the corresponding measurements of an FRM instrument (i.e., Thermo 49i) but underestimated the 5-minute average ozone concentrations by 10 to 50% as measured by the FRM instrument. The CSAM temperature and relative humidity measurements from the nine sensors correlated very well with the corresponding RIVR data ($R^2 > 0.80$ and $R^2 > 0.91$ for temperature and relative humidity, respectively). Upon completion of the field co-location testing, two of the CSAM pods were subsequently brought back to the AQ-SPEC laboratory for further testing. Under controlled environmental conditions in the laboratory chamber, the two CSAM Pods were very reliable and showed excellent correlation with the FEM GRIMM and FRM ozone instruments ($R^2 > 0.99$ and $R^2 > 0.95$ for $PM_{2.5}$ and ozone, respectively). However, the two PM sensors in the CSAM pods consistently overestimated the FEM readings for a wide range of $PM_{2.5}$ mass concentrations. On the contrary, the two ozone sensors in the two CSAM Pods underestimated the FRM readings for a wide range of ozone concentrations at average ambient weather conditions. Both the PM and ozone sensors in the two CSAM Pods showed good precision under more "extreme" weather conditions. When challenged with a range of nitrogen dioxide (NO_2) concentrations, the two ozone sensors in the two CSAM Pods were not affected by the presence of a potential ozone interferent gas, reporting zero values, which indicates that the two sensors may not respond to such interferences in the ambient air.

The CSAM Pods then were deployed successfully at nine locations across southern California in three distinct areas including Long Beach, Jurupa Valley, and Coachella Valley. The extended deployment and subsequent data analysis revealed some of the concerns pertaining to the long-term sensor deployment of low-cost sensors. The AQ-SPEC field and laboratory evaluation process provides a short-term study to

identify sensor performance over a specific two-month period with specific ambient conditions. As ambient air quality studies begin to involve low-cost air quality sensors for extended time periods, identifying and quantifying sensor response degradation and characterizing performance over time becomes crucially important to provide meaningful data and results. The reliability of the sensor is also important, as reductions in data recovery and sensor performance over time significantly increase the complexity related to comparing spatial and temporal differences between sensor locations. Throughout this study, the OPC-N$_2$ was found to have significant data losses with low data recovery at several sites. The ozone sensor had high data recovery, but its readings were found to degrade over the deployment period (three months in this case) when compared with reference instrumentation. Validating these sensors' performance and keeping them calibrated over time will be a significant challenge for agencies and organizations attempting to deploy sensor networks to monitor ambient air quality over a wide area. The ability to access sensor data and use real-time online dashboards remotely would provide the opportunity to automate validating procedures for cloud-based applications to properly characterize sensor failures and quantify data loss.

Lessons learned during the study period suggest that low-cost sensors like those employed here may have a role in air quality monitoring under highly controlled situations. Even so, the fact that a sensor's responsiveness can change over a fairly brief time or under varying meteorological conditions suggests that a sophisticated quality assurance program for their deployment would be useful. We observed significant changes in gas phase sensor response (~ 6 months of age) although most of the sensors' manufacturers suggest lifespans of approximately 1 year. Our experiences during this study confirmed our previous experience with these types of sensors relative to their actual lifespans.

Introduction

The AQ-SPEC group evaluated the field and laboratory performance of ten Citizen Science Air Monitor (CSAM) units (sensor pods #401-410) developed by the EPA to measure ambient $PM_{2.5}$, ozone, temperature and relative humidity. The ten CSAM units were tested in a co-location setting at the SCAQMD Rubidoux (RIVR) Air Monitoring Site (AMS) between 11/9/2016 and 01/05/2017. Results of the co-location performance testing are presented in Section 1. The performance of two of the CSAM units (406 and 409) were evaluated in post co-location testing in the AQ-SPEC laboratory chamber. The results of this evaluation are summarized in Section 2. The CSAM pods were deployed throughout Southern California for approximately three months in three distinct geographical areas including Long Beach, Jurupa Valley, and Coachella Valley. The results of this field deployment are summarized in Section 3 of this report.

1. Co-location Testing

Through the AQ-SPEC program, sensors are typically tested in the field "out-of-the-box", without prior modifications, calibrations, or checks, including zero, span, or precision checks. The sensors were operated according to the manufacturer's user guide or manual. If specified by the sensor manufacturer's user guide or manual, the sensors may have undergone routine maintenance throughout the study. Such routine maintenance may have included but was not limited to filter replacement, zero calibration, flow rate checks, date/time synchronization, and battery change. The air monitoring stations where the field testing was conducted was equipped with FRM, FEM, or best available technology (BAT) air monitoring equipment that was routinely used to measure the ambient concentrations of gaseous or particle pollutants for regulatory purposes. The low-cost sensors were deployed side by side with the FRM, FEM, or BAT monitoring equipment. The data obtained from the two monitoring methods are compared and used as the primary tool in the AQ-SPEC evaluation process of low-cost sensors. To ensure statistically relevant data sets, the sensors were deployed in triplicate and for a period of two months. Deployments in triplicate allow for a statistically robust intra-model comparability between the three sensors and for the ability to detect potential sensor failures or malfunctions. Sensors that are ruggedized and designed for ambient air monitoring purposes are typically mounted outside on the protective railing of the AMS. Sensors that are not ruggedized for inclement weather and are designed for ambient air monitoring conditions are deployed in a custom -built sensor shelter.

1.1. Methods

Before a sensor's field evaluation begins, a bench test at SCAQMD is performed. The bench test involves:

- Reviewing the sensor documentation, including the manual or operating procedures
- Evaluating the power options: cable, battery, and/or solar
- Evaluating the data acquisition options: device internal storage, laptop data logging, cloud based
- Evaluating the data output format to ensure a usable format
- Evaluating the functionality of the On/Off switch to test whether sensors turn on properly

Upon successful completion of the bench test, the sensors were brought to the SCAQMD's Riverside-Rubidoux (RIVR), CA AMS. Since the CSAM pods were ruggedized for inclement weather, the CSAM pods were set up outside of the AMS, as shown in Figure 1.1. CSAM pods #401 through #407 were mounted on tripods and were configured with solar power components. CSAM pods #408- through #410 were configured for 120V power and mounted on a safety railing next to the other CSAM units at the AMS

(Figure 1.2). It should be stated that all CSAMs had the capability of operating on land-based power. Although some of the pods had solar capability, all the pods were eventually operated on land power for consistency. The CSAM's inlets and reference monitors were within ± 2 meters of the same height. The CSAM pods were then exposed to ambient air for more than two months from 10/13/2016 to 01/05/2017 (further details on the AQ-SPEC's Field Setup and Testing Protocol can be found in Appendix B).

Figure 1.1. Co-location set-up for CSAM units #401 - #407 at Riverside-Rubidoux AMS

Figure 1.2. Co-location set-up for CSAM units #408 - #410 at Riverside-Rubidoux AMS

To ensure that the sensors were not crowding one another, care was taken to place them a minimum of 8 inches apart. The sensors were shielded from rain using their own weather-protected NEMA enclosures. After deployment, the AQ-SPEC personnel checked each of the sensors on a biweekly basis to ensure proper functionality and that the data were downloaded periodically from the sensor's SD card. All data collected by the sensors were compared to those collected from the reference monitors at that site.

The AQ-SPEC reference instrumentation at the Riverside-Rubidoux fixed AMS used for this study included:

A GRIMM Dust Monitor (model EDM 180, Ainring, Germany): The EDM 180 spectrometer provides high-resolution, real-time aerodynamic measurements of PM_{10}, $PM_{2.5}$, $PM_{1.0}$, total suspended particulate (TSP), and PM coarse (PM_c). The EDM 180 measures light-scattering at a resolution time of one minute, costs more

than $25,000   and is designated as class III equivalent method EQPM-0311-195 by the U.S. EPA.

A Met One Instruments Particulate Monitor (model BAM-1020 PM_{10} & $PM_{2.5}$, Grants Pass, OR). The BAM-1020 automatically measures and records airborne particulate concentration levels using the principle of beta ray attenuation. This method provides a simple determination of concentration in units of milligrams or micrograms of particulate per cubic meter of air, at a time resolution of one -hour,   and costs more than $20,000. The BAM-1020 is designated as an equivalent method for PM_{10} EQPM-0798-122 and an equivalent method for $PM_{2.5}$ EQPM-0308-170 by the U.S. EPA.

A Thermo Fischer Scientific UV Photometric O_3 Analyzer (Model 49*i*, Franklin, MA): The Model 49*i* operates on the principle that ozone (O_3) molecules absorb UV light at a wavelength of 254 nm, has a time resolution of one minute, and costs more than $7,000. The Model 49*i* is designated as an equivalent method for the measurement of ambient concentrations of ozone EQOA-0880-047 by the U.S. EPA.

A Rotronic AG HygroClip2-S3 Temperature/RH probe (Hauppage, NY) was used to measure t h e ambient temperature and relative humidity at the SCAQMD fixed ambient air monitoring Riverside-Rubidoux station (see appendix B for manual reference).

Collocation testing was based on a side-by-side comparison between the ten sensor pods and the FRM/FEM instruments that were measuring the same pollutant(s). A series of performance-related parameters that would affect air quality measurements in the field were evaluated. These parameters included:

- Intra-model variability
- Data recovery
- Linear correlation coefficient (R^2)

A detailed description of the methodology for estimating each evaluation parameter as well as detailed experimental procedures for sensor testing are described in sections 3.1 and 3.2 of the AQ-SPEC Field Setup and Testing Protocol (see appendix B).

1.2. Results

The ten EPA CSAM units were co-located at the RIVR AMS and operated alongside EPA-approved FEM and FRM instruments from October 13, 2016 to January 5, 2017. Due to problems with solar power generation, consistent data recovery for the CSAM units was not obtained until November 9, 2016. As a result, the data obtained for the comparison of the temperature, relative humidity, and ozone levels extended from November 9, 2016 to January 5, 2017. Additionally, because the Grimm 180 EDM was undergoing calibration by Grimm Technologies during the beginning of the study, the particulate matter data comparison period was delayed until December 8, 2016 and extended to January 5, 2017. CSAM units #401, #402, #403, #404, #406, #407, #408, #409 and #410 were included in the co-location analysis. CSAM unit #405 was removed from the analysis due to an error with the time stamp readings. The unit was sent back to EPA for re-configuration and was subsequently included in the field deployment portion of the study.

1.2.1. Ambient $PM_{2.5}$

CSAM PM data validation and recovery
Standard QA/QC procedures were used to validate the data collected from the $PM_{2.5}$ sensors (model OPC-N_2, AlphaSense, UK) in the CSAM units. Obvious outliers, negative values, and invalid data-points were   eliminated from the data-set. Data recovery for the $PM_{2.5}$ sensor from all nine CSAM units was > 99.1%. Descriptive and correlation statistics for the nine units are presented in Tables 1.1a-b below.

3

Table 1.1a. Descriptive statistics for PM$_{2.5}$ sensors in the CSAMs and the FEM GRIMM reference instrument (5-minute average)

PM$_{2.5}$ (µg/m^3)	Unit 401	Unit 402	Unit 403	Unit 404	Unit 406	Unit 407	Unit 408	Unit 409	Unit 410	FEM GRIMM
mean	3.2	41.0	21.2	4.4	20.3	21.7	23.5	20.5	30.8	15.1
median	3.3	17.8	5.7	0.0	5.6	5.7	5.7	5.1	9.1	9.6
STDEV	0.8	52.2	35.4	12.8	33.6	37.0	40.8	36.1	48.5	13.4
Count (#)	7947	7948	7948	7946	7947	7946	7947	7947	7947	7967
Recovery (%)	99.7	99.8	99.8	99.7	99.7	99.7	99.7	99.7	99.7	100

Table 1.1b. Correlation statistics for PM$_{2.5}$ sensors in the CSAMs against the FEM GRIMM reference instrument (5-minute average), [FEM= (slope*sensor reading) + intercept]

	Unit 401	Unit 402	Unit 403	Unit 404	Unit 406	Unit 407	Unit 408	Unit 409	Unit 410
Slope	0.4849	0.1903	0.2715	0.2892	0.2889	0.2573	0.2237	0.2504	0.1974
Intercept	13.595	7.3293	9.3622	8.8361	9.2564	9.5382	9.8765	10.006	9.0523
R^2	0.0008	0.5488	0.5138	0.2356	0.5247	0.5039	0.4644	0.4551	0.5098

CSAM PM intra-model variability

Moderate measurement variations were observed between the nine CSAM units for PM$_{2.5}$ mass concentrations (µg/m^3). Figure 1.3 shows a modest intra-model variability (mean and median values) between seven of the CSAM PM$_{2.5}$ units, excluding units #401 and #404.
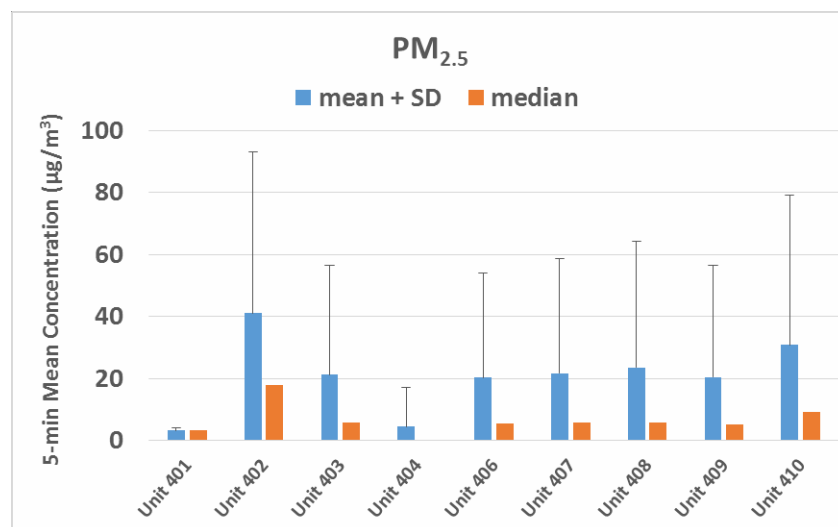
Figure 1.3. Intra-model variability for nine of the ten CSAM PM$_{2.5}$ sensors tested. Vertical bars represent the standard deviation for each mean value

FEM data validation and recovery

Standard QA/QC procedures were used to validate the FEM data collected (i.e., obvious outliers, negative values, and invalid data-points were eliminated from the data-set). PM$_{2.5}$ data recovery was 100% for the GRIMM and 96 % for the BAM reference instruments.

Excellent correlation was observed between the 1-hour average mass concentrations of the two

equivalent methods for PM$_{2.5}$ (R^2: 0.945). The two FEM instruments tracked well with each other throughout the entire co-location test period (see Figures 1.4 and 1.5).
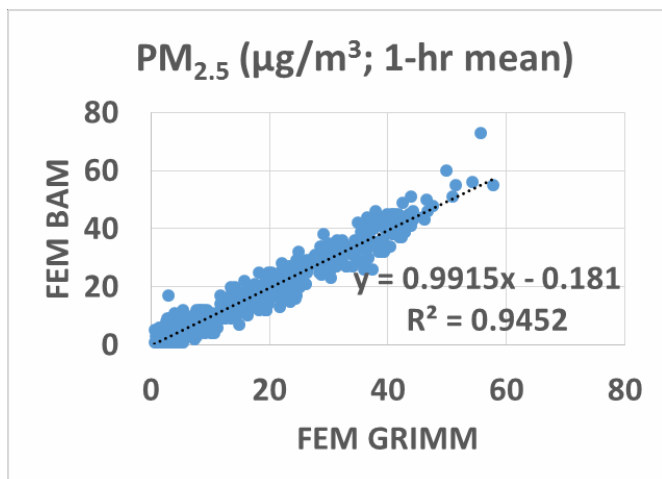
Figure 1.4. Correlation coefficient (R^2) plot for the 1-hour average PM$_{2.5}$ measurements by the FEM GRIMM and FEM BAM units (1-hour average)
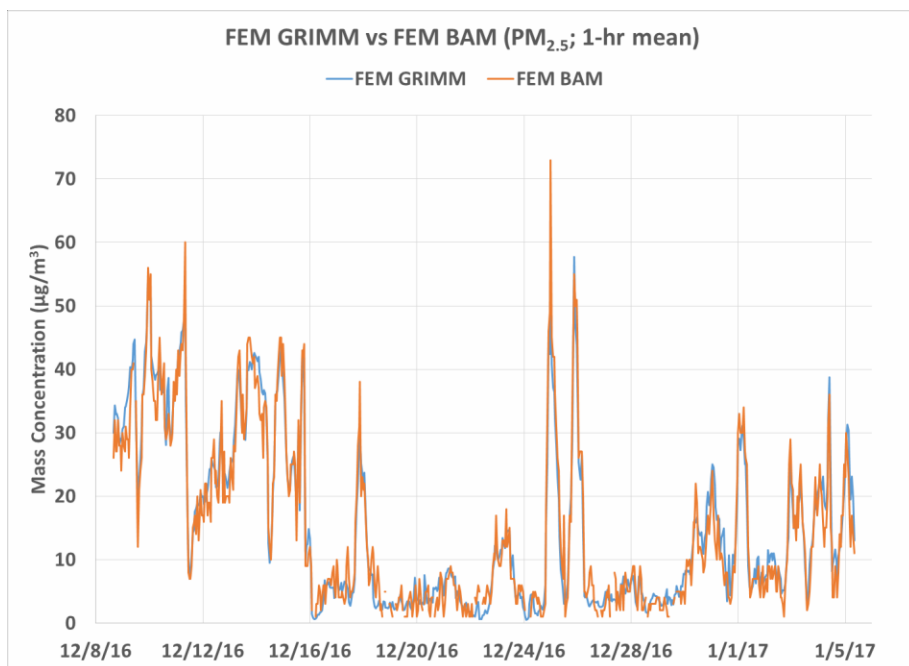
Figure 1.5. Time-series plot of PM$_{2.5}$ measurements from the FEM GRIMM vs FEM BAM units (1-hour average)

*CSAM vs FEM GRIMM (*PM$_{2.5}$ *mass; 5-min mean)*

Most of the 5-minute average CSAM PM$_{2.5}$ mass measurements showed a modest correlation with the corresponding FEM GRIMM data (R^2 > 0.45) (Table 1.2.). The PM$_{2.5}$ from units #401 and #404 did not correlate well with the FEM GRIMM data. The nine sensor units did not appear to track well the diurnal PM variations recorded by the FEM GRIMM instrument (Figures 1.6-1.7).
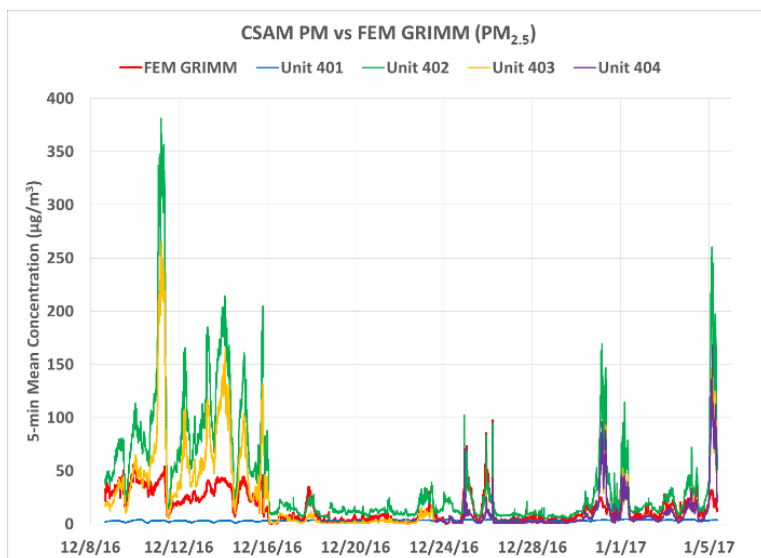
Figure 1.6. Time-series plot of PM$_{2.5}$ measurements from units #401 through #404 and the FEM instrument (5-minute average)
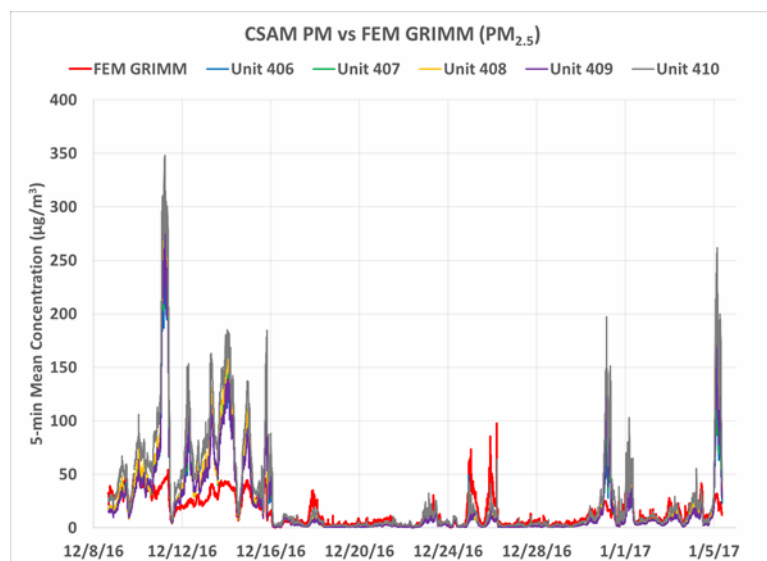
Figure 1.7. Time-series plot of PM$_{2.5}$ measurements from units #406 through #410 and the FEM instrument (5-minute average)

Table 1.2. Correlation Coefficient (R^2) matrix for the 5-minute average PM$_{2.5}$ mass concentrations measured by the FEM and CSAM units.

R^2	FEM GRIMM	Unit 401	Unit 402	Unit 403	Unit 404	Unit 406	Unit 407	Unit 408	Unit 409	Unit 410
FEM GRIMM	1									
Unit 401	0.0008	1								
Unit 402	0.5488	0.0002	1							
Unit 403	0.5138	0.0007	0.9831	1						
Unit 404	0.2356	0.0676	0.9655	0.9815	1					

6

R^2	FEM GRIMM	Unit 401	Unit 402	Unit 403	Unit 404	Unit 406	Unit 407	Unit 408	Unit 409	Unit 410
Unit 406	0.5247	0.0010	0.9775	0.9945	0.9827	1				
Unit 407	0.5039	0.0001	0.9820	0.9931	0.9806	0.994	1			
Unit 408	0.4644	0.0004	0.9736	0.9708	0.9583	0.961	0.972	1		
Unit 409	0.4551	0.0001	0.9739	0.9783	0.9587	0.971	0.979	0.989	1	
Unit 410	0.5098	0.0001	0.9857	0.9762	0.9669	0.968	0.976	0.991	0.989	1

CSAM vs FEM GRIMM (PM$_{2.5}$ ***mass; 1-hour mean)***

Most of the 1-hour average CSAM PM$_{2.5}$ mass measurements showed a modest correlation with the corresponding FEM GRIMM data (R^2 > 0.46) (Table 1.3). The PM$_{2.5}$ measurements from units #401 and #404 did not correlate with the FEM GRIMM data. The nine CSAM units did not appear to track well the diurnal PM variations recorded by the FEM GRIMM instrument (Figures 1.8-1.9).
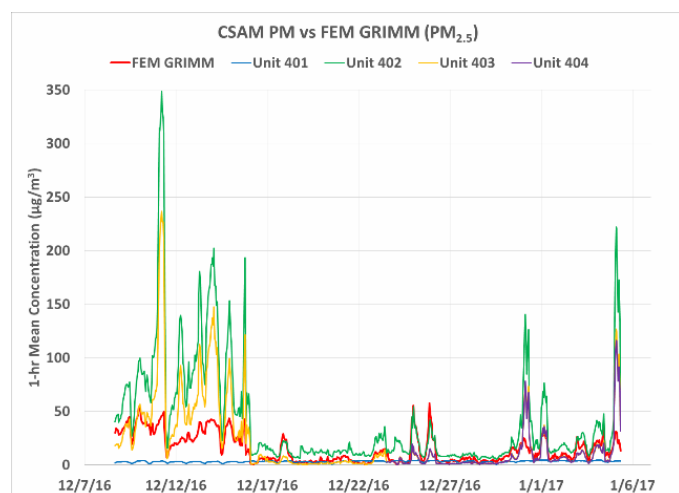
Figure 1.8. Time-series plot of PM$_{2.5}$ measurements from units #401 through #404 and the FEM instrument (1-hour average)
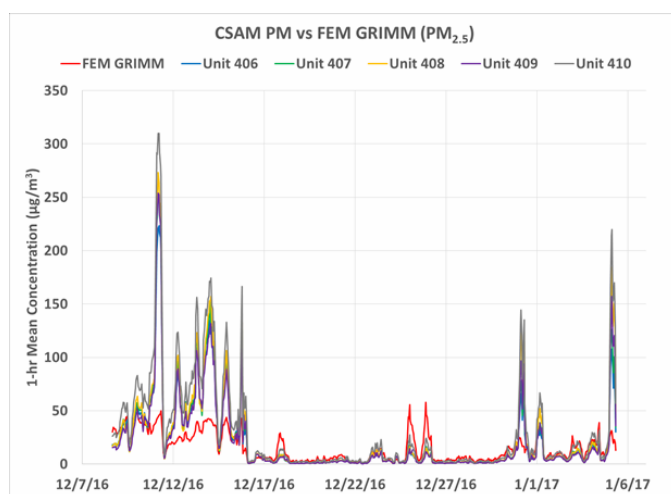
Figure 1.9. Time-series plot of PM$_{2.5}$ measurements from units #406 through #410 and the FEM instrument (1-hour average)

Table 1.3. Correlation Coefficient (R^2) matrix for the 1-hour average PM$_{2.5}$ mass concentrations measured by the FEM and CSAM units

R^2	FEM GRIMM	Unit 401	Unit 402	Unit 403	Unit 404	Unit 406	Unit 407	Unit 408	Unit 409	Unit 410
FEM GRIMM	1									
Unit 401	0.0006	1								
Unit 402	0.5641	0.0001	1							
Unit 403	0.5269	0.0009	0.9885	1						
Unit 404	0.2541	0.0715	0.9880	0.9977	1					
Unit 406	0.5376	0.0011	0.9846	0.9983	0.9971	1				
Unit 407	0.5164	0.0001	0.9874	0.9972	0.9978	0.997	1			
Unit 408	0.4762	0.0003	0.9823	0.9783	0.9832	0.969	0.980	1		
Unit 409	0.4670	0.0001	0.9813	0.9855	0.9831	0.978	0.985	0.992	1	
Unit 410	0.5234	0.0001	0.9921	0.9829	0.9926	0.976	0.981	0.994	0.990	1

CSAM vs FEM GRIMM (PM$_{2.5}$ mass; 24-hour mean)

Most of the 24-hour average CSAM PM$_{2.5}$ mass measurements showed a modest correlation with the corresponding FEM GRIMM data ($R^2 > 0.49$) (Table 1.4). The PM$_{2.5}$ measurements from units #401 and #404 did not correlate with the FEM GRIMM data. The nine CSAM units did not appear to track well the diurnal PM variations recorded by the FEM GRIMM instrument and tended to overestimate the FEM measurements (Figures 1.10-1.11).
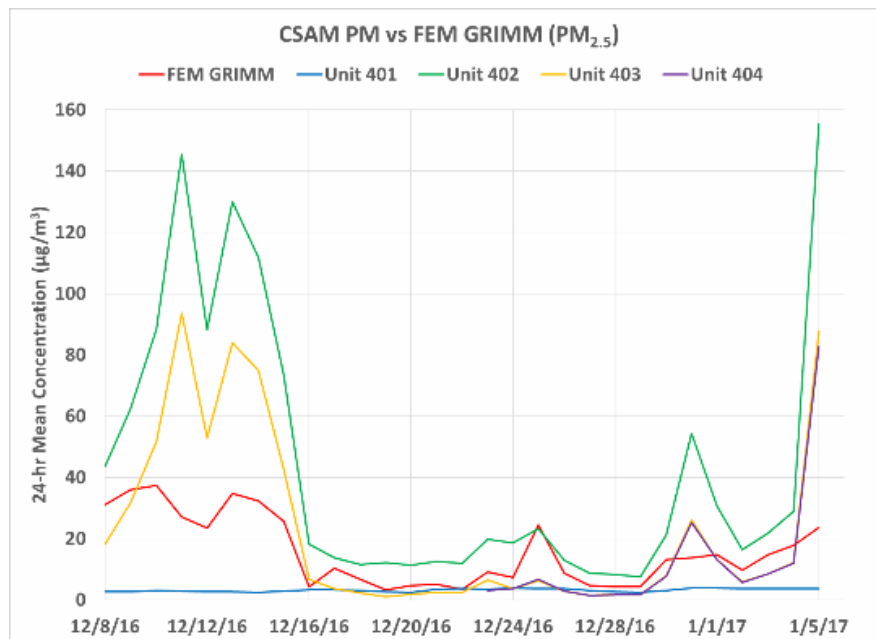
Figure 1.10. Time-series plot of PM$_{2.5}$ measurements from units #401 through #404 and the FEM instrument (24-hour average)
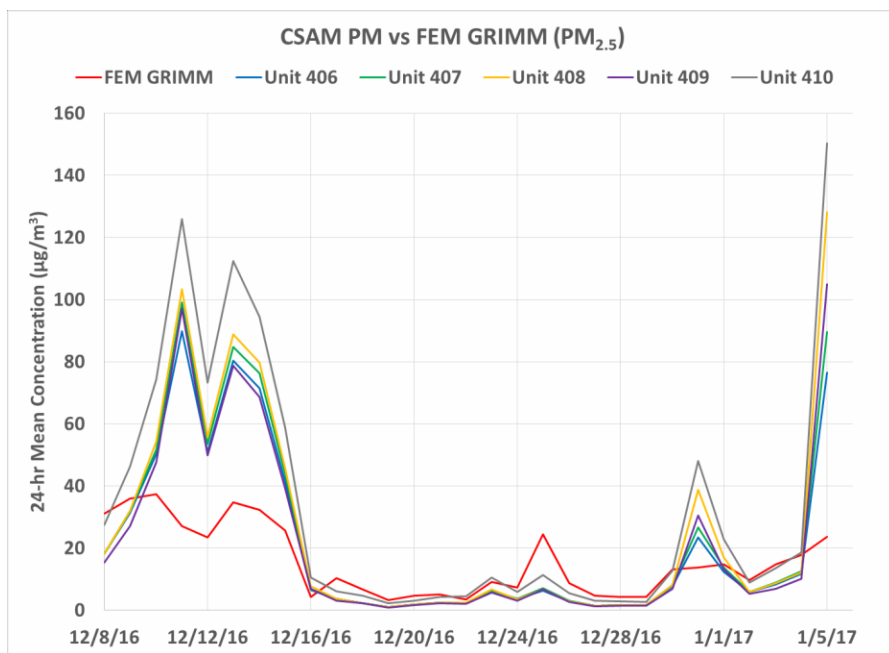
Figure 1.11. Time-series plot of PM$_{2.5}$ measurements from units #406 through #410 and the FEM instrument (24-hour average)

Table 1.4. Correlation Coefficient (R^2) matrix for the 24-hour average PM$_{2.5}$ mass concentrations measured by the FEM and CSAM units

R^2	FEM GRIMM	Unit 401	Unit 402	Unit 403	Unit 404	Unit 406	Unit 407	Unit 408	Unit 409	Unit 410
FEM GRIMM	1									
Unit 401	0.0664	1								
Unit 402	0.5946	0.0365	1							
Unit 403	0.5782	0.0539	0.9900	1						
Unit 404	0.3807	0.1077	0.9947	0.9980	1					
Unit 406	0.5985	0.0639	0.9817	0.9976	0.9982	1				
Unit 407	0.5698	0.0522	0.9888	0.9994	0.9985	0.997	1			
Unit 408	0.4933	0.0214	0.9836	0.9695	0.9961	0.951	0.969	1		
Unit 409	0.5000	0.0287	0.9885	0.9824	0.9960	0.969	0.984	0.995	1	
Unit 410	0.5415	0.0257	0.9935	0.9790	0.9975	0.964	0.978	0.996	0.994	1

CSAM vs FEM BAM (PM$_{2.5}$ mass; 1-hour mean)

Most of the 1-hour average CSAM PM$_{2.5}$ mass measurements showed a modest correlation with the corresponding FEM BAM data ($R^2 > 0.40$) (Table 1.5). The PM$_{2.5}$ measurements from units #401 and #404 did not correlate with the FEM BAM data. The nine sensor units did not appear to track well the diurnal PM variations recorded by the FEM BAM instrument and tended to overestimate the FEM measurements (Figures 1.12-1.13).

9
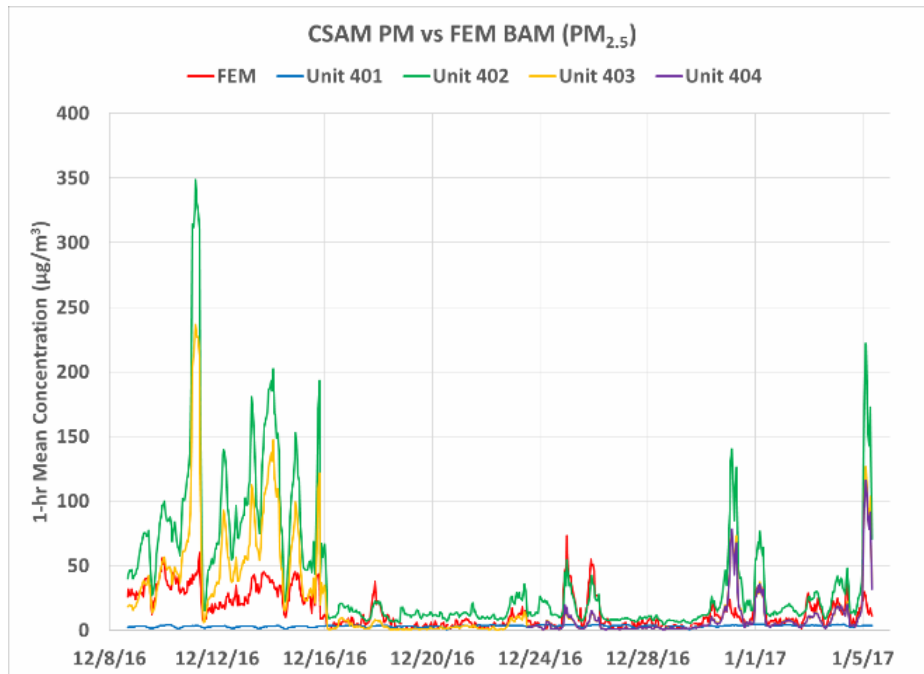
Figure 1.12. Time-series plot of PM$_{2.5}$ measurements from units #401 through #404 and the FEM instrument (1-hour average)
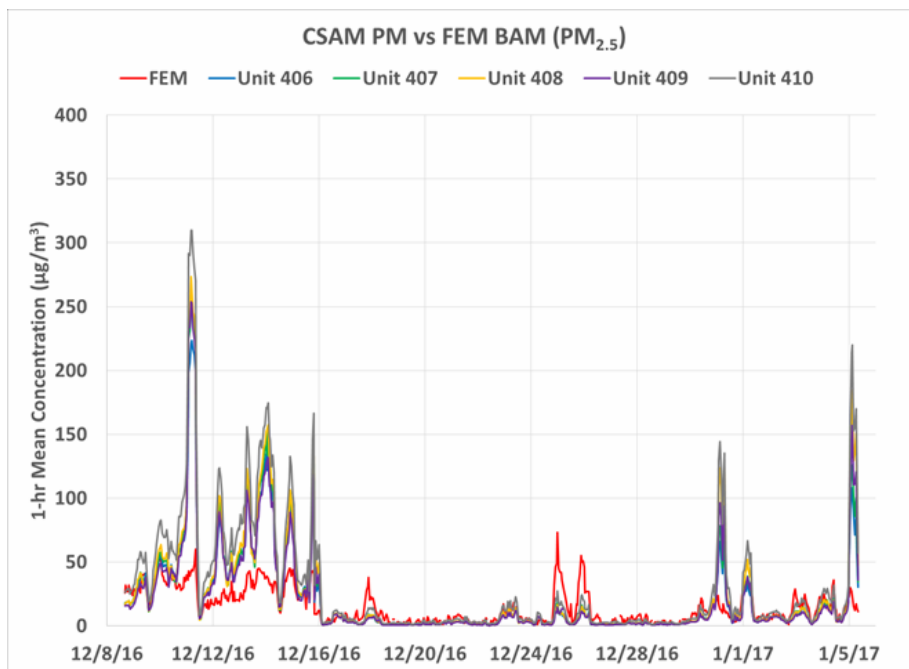
Figure 1.13. Time-series plot of PM$_{2.5}$ measurements from units #406 through #410 and the FEM instrument (1-hour average)

Table 1.5. Correlation Coefficient (R^2) matrix for the 1-hour average PM$_{2.5}$ mass concentrations measured by the FEM and CSAM units

R^2	FEM BAM	Unit 401	Unit 402	Unit 403	Unit 404	Unit 406	Unit 407	Unit 408	Unit 409	Unit 410
FEM BAM	1									
Unit 401	0.0012	1								
Unit 402	0.4941	0.0001	1							
Unit 403	0.4612	0.0009	0.9885	1						
Unit 404	0.1339	0.0715	0.9880	0.9977	1					
Unit 406	0.4730	0.0011	0.9846	0.9983	0.9971	1				
Unit 407	0.4522	0.0001	0.9874	0.9972	0.9978	0.9970	1			
Unit 408	0.4058	0.0003	0.9823	0.9783	0.9832	0.9687	0.9795	1		
Unit 409	0.4027	0.0001	0.9813	0.9855	0.9831	0.9780	0.9853	0.9920	1	
Unit 410	0.4499	0.0001	0.9921	0.9829	0.9926	0.9756	0.9814	0.9942	0.9899	1

***CSAM vs FEM BAM (**PM$_{2.5}$ *mass; 24-hour mean)*

Most of the 24-hour average CSAM PM$_{2.5}$ mass measurements showed a modest correlation with the corresponding FEM BAM data ($R^2 > 0.44$) (Table 1.6). The PM$_{2.5}$ measurements from units #401 and #404 did not correlate with the FEM BAM data. The nine sensor units did not appear to track well with the diurnal PM variations recorded by the FEM BAM instrument and tended to overestimate the FEM measurements (Figures 1.14-1.15).

Figure 1.14. Time-series plot of PM$_{2.5}$ measurements from units #401 through #404 and the FEM instrument (24-hour average)

Figure 1.15. Time-series plot of PM$_{2.5}$ measurements from units #406 through #410 and the FEM instrument (1-hour average)

Table 1.6. Correlation Coefficient (R^2) matrix for the 1-hour average PM$_{2.5}$ mass concentrations measured by the FEM and CSAM units

| R^2	FEM BAM	Unit 401	Unit 402	Unit 403	Unit 404	Unit 406	Unit 407	Unit 408	Unit 409	Unit 410
FEM BAM	1									
Unit 401	0.0546	1								
Unit 402	0.5451	0.0365	1							
Unit 403	0.5377	0.0539	0.9900	1						
Unit 404	0.1676	0.1077	0.9947	0.9980	1					
Unit 406	0.5619	0.0639	0.9817	0.9976	0.9982	1				
Unit 407	0.5307	0.0522	0.9888	0.9994	0.9985	0.9972	1			
Unit 408	0.4407	0.0214	0.9836	0.9695	0.9961	0.9510	0.9692	1		
Unit 409	0.4535	0.0287	0.9885	0.9824	0.9960	0.9687	0.9838	0.9954	1	
Unit 410	0.4881	0.0257	0.9935	0.9790	0.9975	0.9643	0.9777	0.9963	0.9945	1

Pod #405 was removed due to frequent erroneous time stamp readings and returned to the EPA for repair and re-configuration. The initial period of the co-location (October 13, 2016 to November 9, 2016) was littered with errors due to power issues with units #401 through #407. These seven units, which were configured with a solar panel and battery for power generation, did not operate properly. The 3-amp fuse located between the charge controller and the battery was not sufficient to sustain the loads experienced. As a result, fuses failed frequently, which subsequently led to dead batteries and loss of power. The low power situations led to real-time clock errors and an overall data loss. Power adaptors and cords were purchased to remedy the solar power issues, and CSAM units #401 through 407 were configured to 120V power on November 9, 2017. Data recovery improved once 120V power supplies were used for all nine of the CSAM units. As a result, November 9, 2017 was considered the "official" start date for the field co-location study. Another error that occurred for unknown reasons was that the CSAM units would stop logging data and the display would indicate VOC rather than ozone. Due to the Grimm 180 EDM undergoing calibration at the

12

factory, the particulate matter data collocation period for PM was set from December 8, 2016 to January 5, 2017 for data analysis to match the time period that the Grimm data were available.

Overall, the CSAM $PM_{2.5}$ data were very reliable, with data recovery close to 100% for all units tested, and were characterized by modest intra-model variability. The CSAM $PM_{2.5}$ sensor data for seven of the units (#402, #403, #406, #407, #408, #409, and #410) showed a modest correlation (R^2: 0.40 – 0.60) with the corresponding measurements collected using substantially more expensive FEM instruments (i.e., GRIMM, BAM) at 5-minute, 1-hour, and 24-hour time resolutions. The CSAM $PM_{2.5}$ sensors for pods #401 and #404 did not correlate well with the FEM instruments at any time resolution. Overall, the CSAM $PM_{2.5}$ sensors overestimated the mass concentration measurements from the FEM GRIMM and FEM BAM reference instruments.

1.2.2. Ambient Ozone

Data validation and recovery
Standard QA/QC procedures were used to validate the collected data from the ozone sensors (model SM-50, Aeroqual, New Zealand) in the CSAM units. Obvious outliers, negative values, and invalid data-points were eliminated from the data-set. The data recovery for ozone from eight of the CSAM units was 99.3%, for unit #402 was 77.5%, and for the FEM reference instrument was 93.3%, Descriptive and correlation statistics for the nine units and the FRM instrument are presented in Tables 1.7a-b below.

Table 1.7a. Descriptive Statistics for ozone from the CSAMs and the FEM instrument

Ozone (ppb)	FEM	Unit 401	Unit 402	Unit 403	Unit 404	Unit 406	Unit 407	Unit 408	Unit 409	Unit 410
mean	18.9	17.3	15.5	19.6	12.5	18.6	20.8	23.3	12.3	17.2
median	16.9	14.3	14.9	17.6	10.9	15.4	19.2	21.6	9.9	14.9
SD	15.9	14.6	6.9	9.6	9.2	13.5	8.7	10.1	11.6	11.3
Count (#)	15319	16304	12733	16307	16304	16305	16304	16303	16304	16304
Recovery (%)	93.3	99.3	77.5	99.3	99.3	99.3	99.3	99.3	99.3	99.3

Table 1.7b. Correlation statistics for ozone from the CSAMS against the FEM instrument (5- minute average) [FEM = (slope*sensor reading) + intercept]

	#401	#402	#403	#404	#406	#407	#408	#409	#410
Slope	1.0621	2.0249	1.594	1.5779	1.0978	1.7731	1.5367	1.2618	1.3563
Intercept	0.0844	-13.256	-12.845	-1.3013	-1.9282	-18.511	-17.457	3.0019	-4.8449
R2	0.9524	0.8563	0.9394	0.8367	0.877	0.9379	0.9538	0.8549	0.9339

CSAM Ozone; intra-model variability
Low measurement variations were observed between the nine CSAM units for ambient ozone concentrations (ppb). Figure 1.16 shows the intra-model variability (mean and median values) in the nine CSAM ozone sensors.
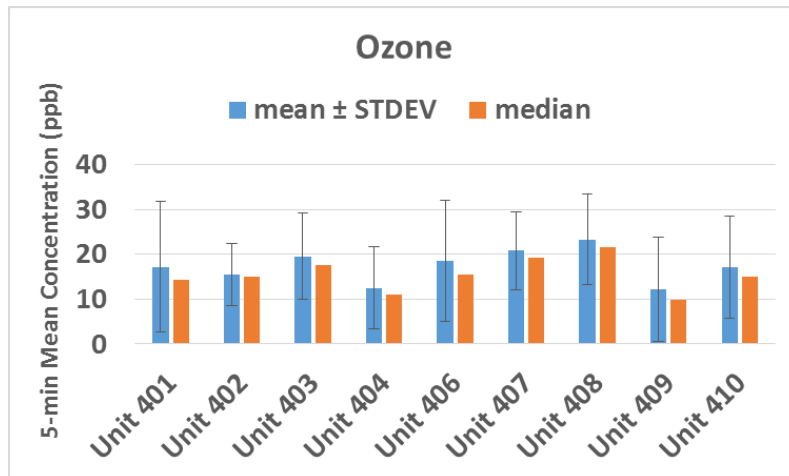
Figure 1.16. Intra-model variability in nine CSAM ozone sensors

CSAM vs FEM (Ozone; 5-minute mean)

All 5-minute average CSAM ozone measurements from the nine sensors correlated very well with the corresponding FEM data ($R^2 > 0.83$) (Table 1.8). The nine CSAM units appeared to track well with the diurnal ozone variations recorded by the FEM instrument but underestimated the 5-minute average ozone concentrations by 10 to 50% as measured by the FEM (Figures 1.17-1.18).
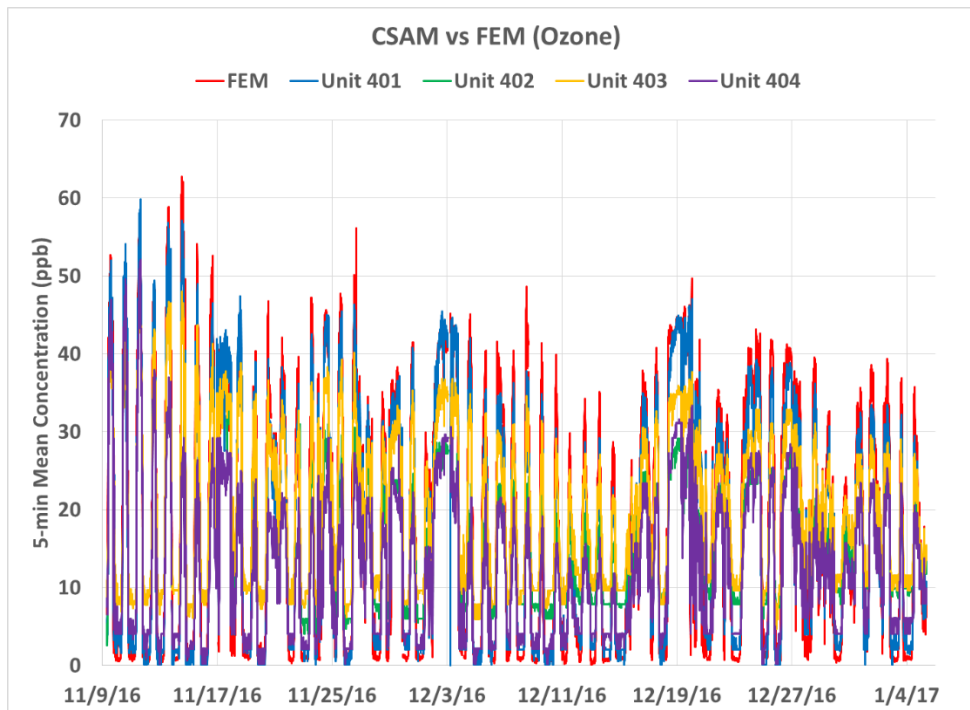
Figure 1.17. Time-series plot of ozone measurements from units #401 through #404 and the FEM instrument (5-minute average)
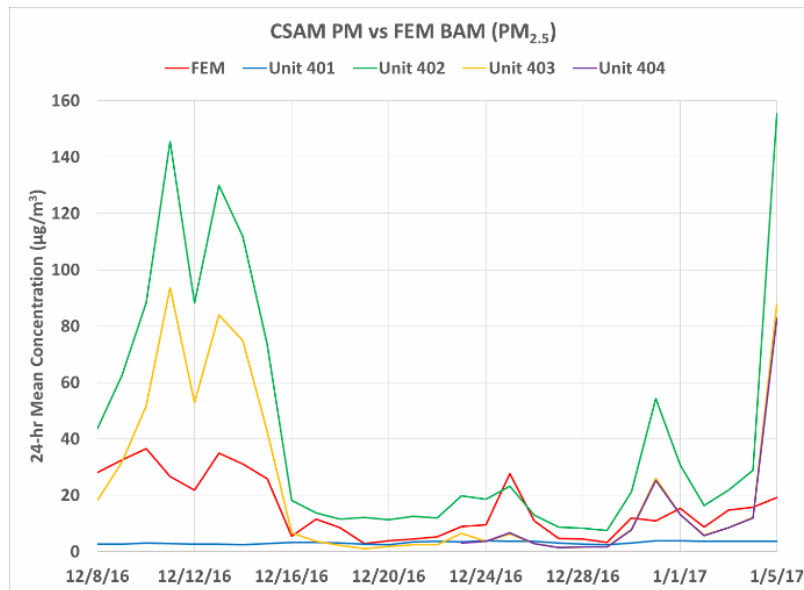
Figure 1.18. Time-series plot of ozone measurements from units #406 through #410 and the FEM instrument (5-minute average)

Table 1.8. Correlation Coefficient (R^2) matrix for the 5-minute average ozone concentrations measured by the FEM and CSAM units
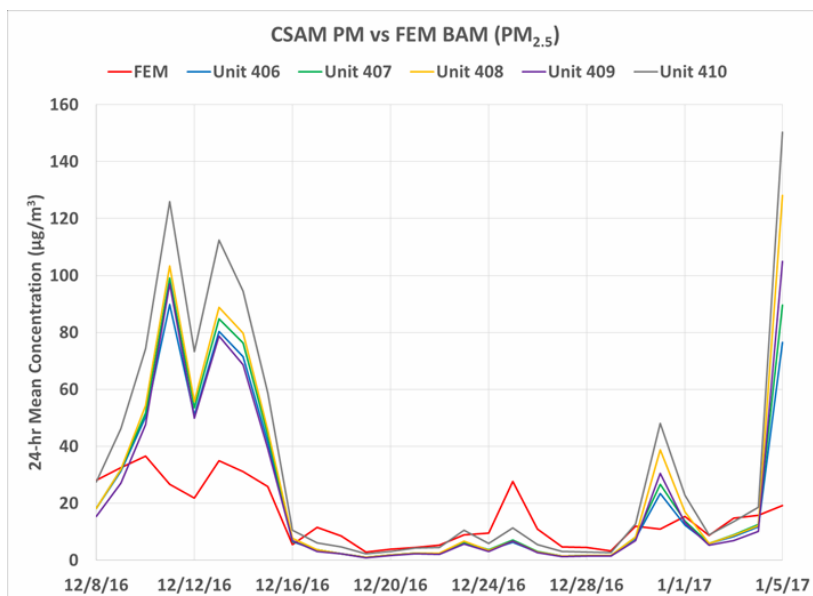
R^2	FEM	Unit 401	Unit 402	Unit 403	Unit 404	Unit 406	Unit 407	Unit 408	Unit 409	Unit 410
FEM	1									
Unit 401	0.9524	1								
Unit 402	0.8563	0.9219	1							
Unit 403	0.9394	0.9780	0.9309	1						
Unit 404	0.8367	0.9091	0.9499	0.8992	1					
Unit 406	0.8770	0.9311	0.9141	0.9468	0.8510	1				
Unit 407	0.9379	0.9796	0.9308	0.9851	0.8920	0.9698	1			
Unit 408	0.9538	0.9881	0.9109	0.9831	0.8830	0.9439	0.9881	1		
Unit 409	0.8549	0.9125	0.9575	0.9314	0.8816	0.9728	0.9520	0.9174	1	
Unit 410	0.9339	0.9860	0.9458	0.9822	0.9291	0.9552	0.9874	0.9819	0.9500	1

CSAM vs FEM (Ozone; 1-hour mean)

All 1-hour average CSAM ozone measurements from the nine sensors correlated very well with the corresponding FEM data ($R^2 > 0.86$) (Table 1.9). The nine sensor units appeared to track well with the diurnal ozone variations recorded by the FEM instrument (Figures 1.19-1.20).

Figure 1.19. Time-series plot of ozone measurements from units #401 through #404 and the FEM instrument (1-hour average)

Figure 1.20. Time-series plot of ozone measurements from units #406 through #410 and the FEM instrument (1-hour average)

Table 1.9. Correlation coefficient (R^2) matrix for the 1-hour average ozone concentrations measured by the FEM and CSAM units

R^2	FEM	Unit 401	Unit 402	Unit 403	Unit 404	Unit 406	Unit 407	Unit 408	Unit 409	Unit 410
FEM	1									
Unit 401	0.9683	1								
Unit 402	0.8891	0.9288	1							
Unit 403	0.9653	0.9825	0.9355	1						
Unit 404	0.8659	0.9121	0.9544	0.9013	1					
Unit 406	0.8999	0.9327	0.9189	0.9496	0.8517	1				
Unit 407	0.9622	0.9830	0.9353	0.9885	0.8936	0.9722	1			
Unit 408	0.9760	0.9905	0.9170	0.9874	0.8853	0.9457	0.9913	1		
Unit 409	0.8796	0.9147	0.9618	0.9336	0.8821	0.9748	0.9538	0.9192	1	
Unit 410	0.9590	0.9894	0.9498	0.9853	0.9309	0.9567	0.9895	0.9846	0.9511	1

CSAM vs FEM (Ozone; 8-hour mean)

All 8-hour average CSAM ozone measurements from the nine sensors correlated very well with the corresponding FEM data (R^2 > 0.85) (Table 1.10). The nine sensor units appeared to track well with the diurnal ozone variations recorded by the FEM instrument (Figures 1.21-1.22).

Figure 1.21. Time-series plot of ozone measurements from units #401 through #404 and the FEM instrument (8-hour average)
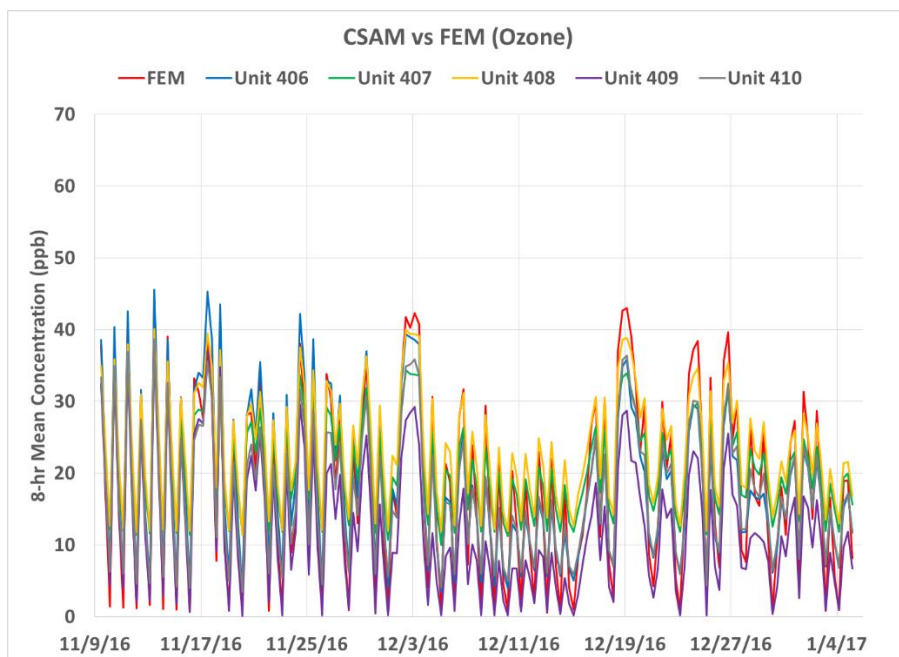
Figure 1.22. Time-series plot of ozone measurements from units #406 through #410 and the FEM instrument (8-hour average)

Table 1.10. Correlation coefficient (R^2) matrix for the 8-hour average ozone concentrations measured by the FEM and CSAM units

R^2	FEM	Unit 401	Unit 402	Unit 403	Unit 404	Unit 406	Unit 407	Unit 408	Unit 409	Unit 410
FEM	1									
Unit 401	0.9742	1								
Unit 402	0.8883	0.9229	1							
Unit 403	0.9684	0.9813	0.9285	1						
Unit 404	0.8556	0.8998	0.9594	0.8878	1					
Unit 406	0.8852	0.9139	0.8901	0.9383	0.8194	1				
Unit 407	0.9617	0.9778	0.9237	0.9884	0.8761	0.9666	1			
Unit 408	0.9775	0.9874	0.9097	0.9879	0.8707	0.9332	0.9897	1		
Unit 409	0.8593	0.8912	0.9376	0.9192	0.8553	0.9698	0.9441	0.8997	1	
Unit 410	0.9603	0.9859	0.9477	0.9856	0.9259	0.9443	0.9869	0.9819	0.9367	1

CSAM vs FEM (Ozone; 24-hour mean)

All 24-hour average ozone measurements from the nine CSAMs correlated very well with the corresponding FEM data ($R^2 > 0.80$) (Table 1.11). The nine CSAMs units appeared to track well with the diurnal ozone variations recorded by the FEM instrument (Figures 1.23-1.24).
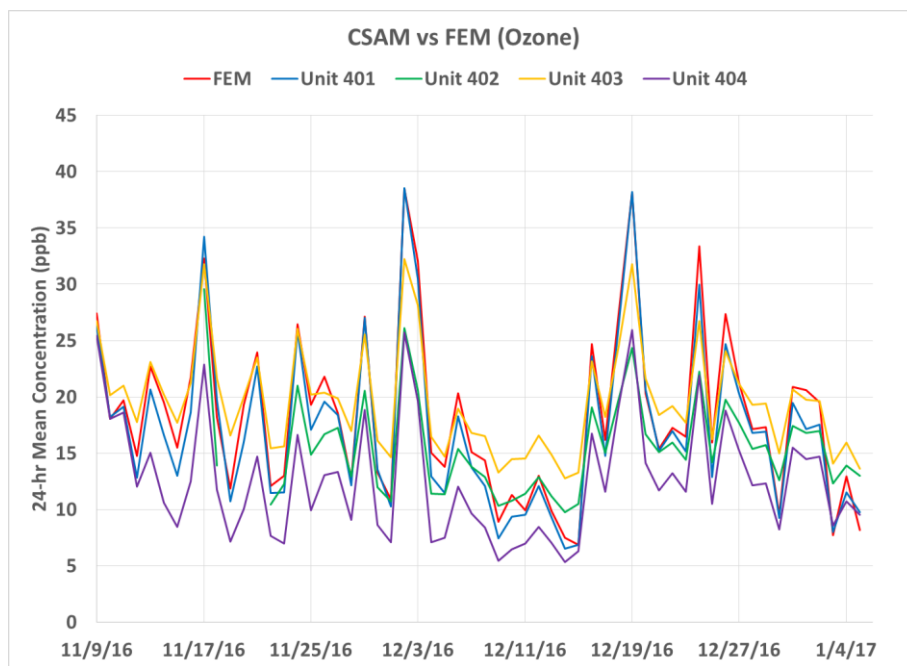
Figure 1.23. Time-series plot of ozone measurements from units #401 through #404 and the FEM instrument (24-hour average)
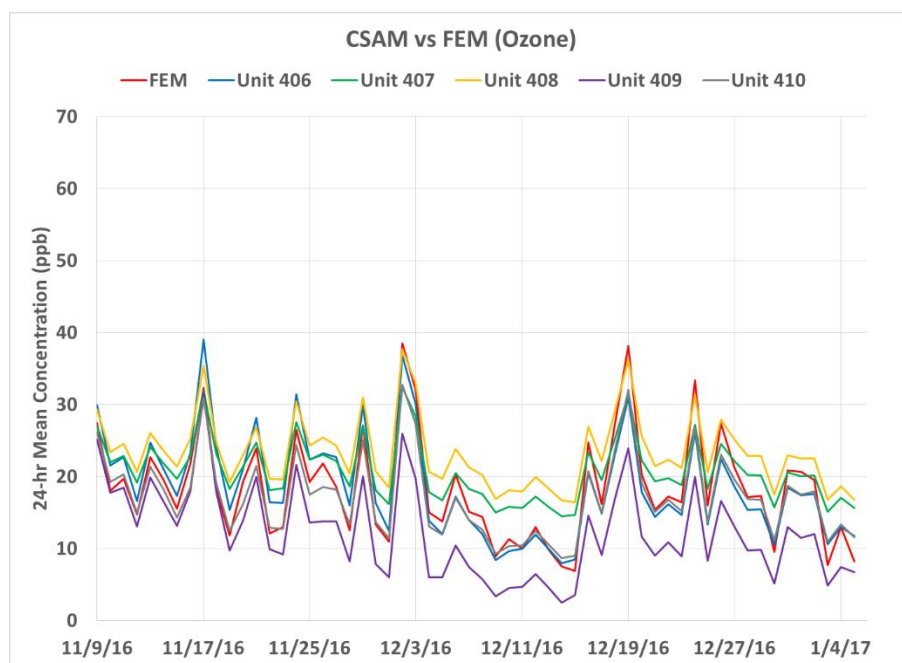
Figure 1.24. Time-series plot of ozone measurements from units #406 through #410 and the FEM instrument (24-hour average)

Table 1.11. Correlation coefficient (R^2) matrix for the 24-hour average ozone concentrations measured by the FEM and CSAM units

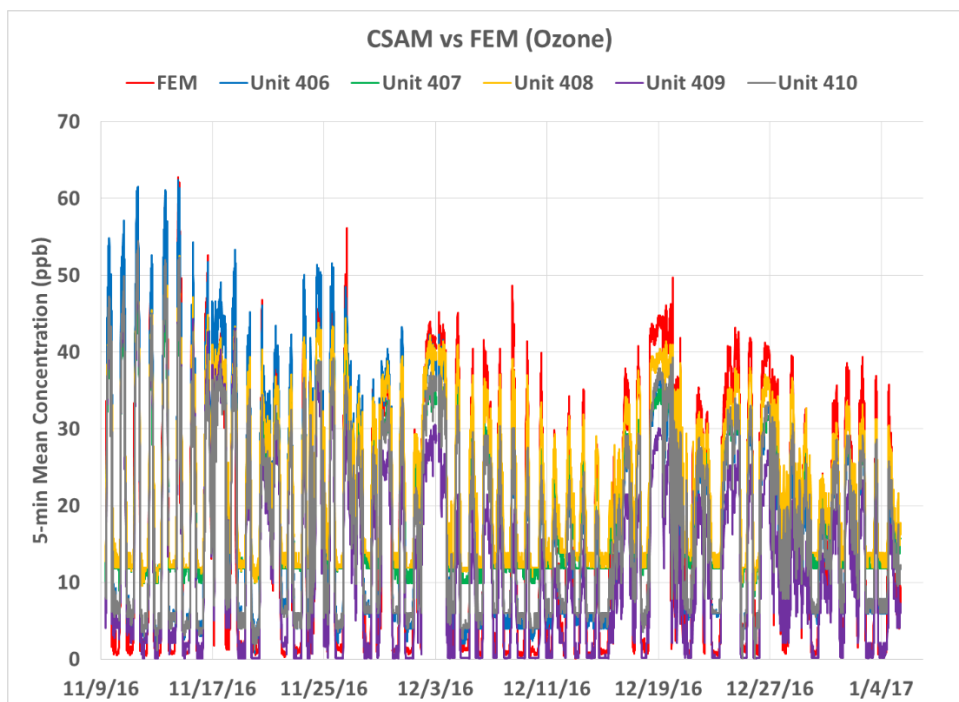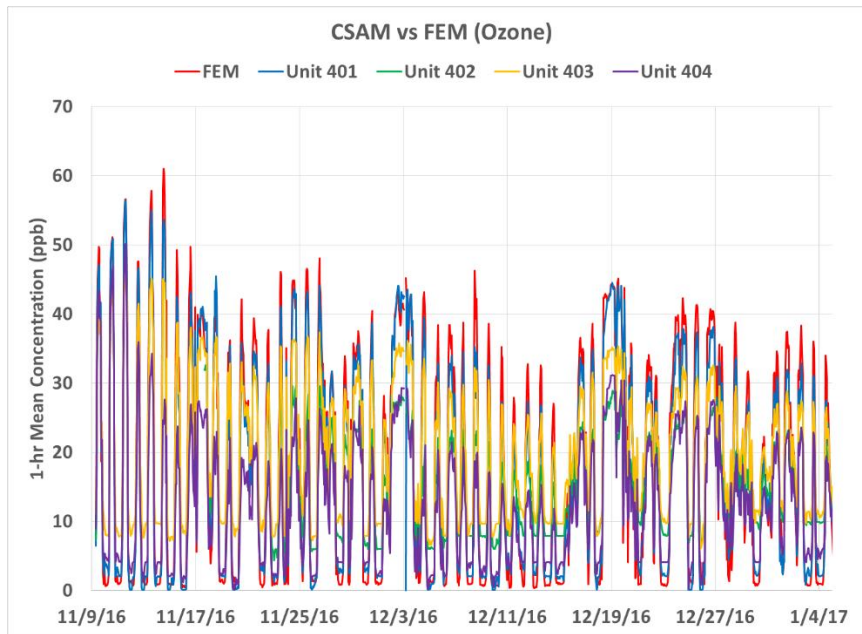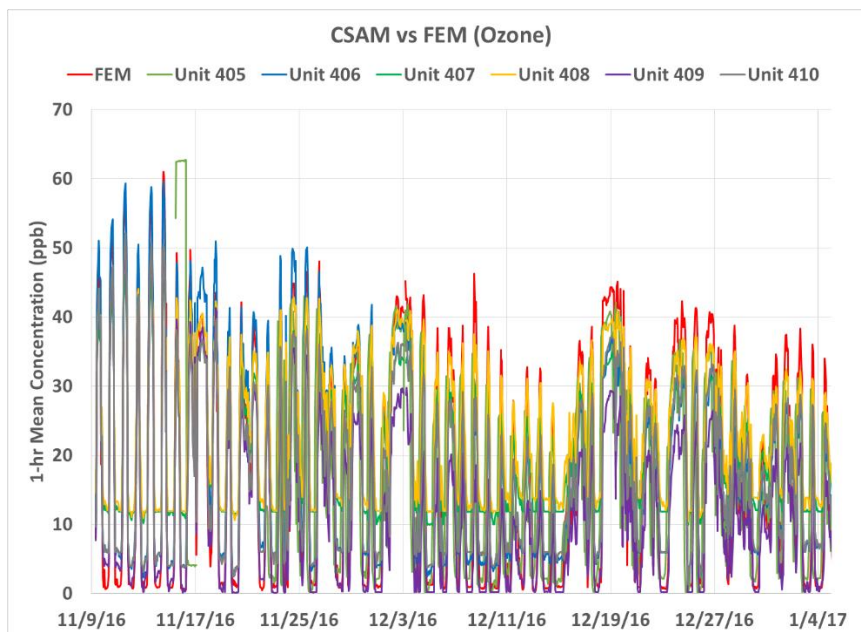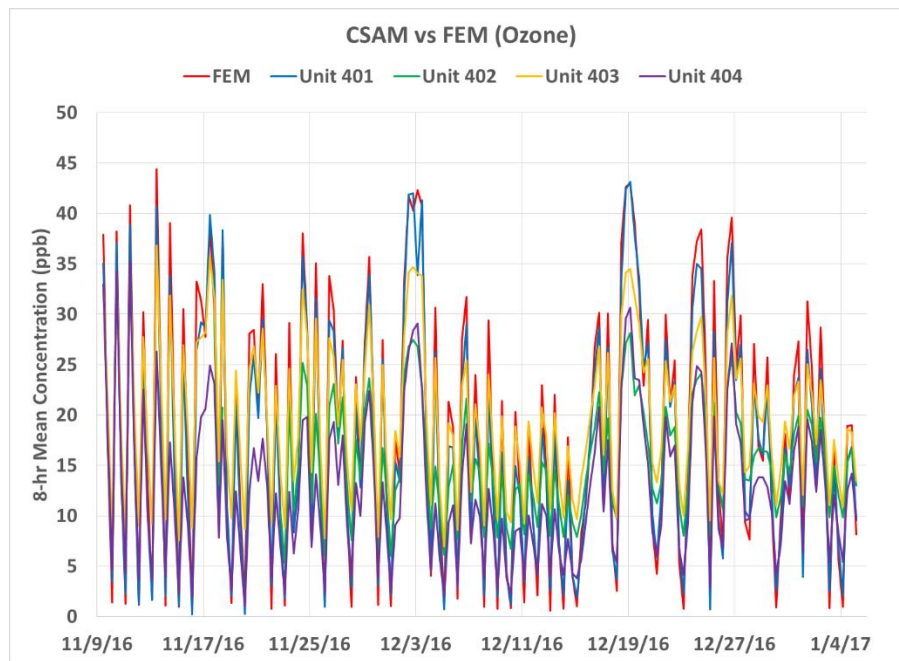| R^2	FEM	Unit 401	Unit 402	Unit 403	Unit 404	Unit 406	Unit 407	Unit 408	Unit 409	Unit 410
FEM	1									
Unit 401	0.9733	1								
Unit 402	0.8260	0.8501	1							
Unit 403	0.9554	0.9783	0.8859	1						
Unit 404	0.8544	0.8862	0.9388	0.8745	1					
Unit 406	0.8312	0.8585	0.8196	0.9024	0.7404	1				
Unit 407	0.9420	0.9620	0.8584	0.9826	0.8385	0.9500	1			
Unit 408	0.9665	0.9848	0.8338	0.9803	0.8382	0.8940	0.9812	1		
Unit 409	0.8042	0.8257	0.8948	0.8877	0.7868	0.9540	0.9206	0.8457	1	
Unit 410	0.9603	0.9847	0.8916	0.9862	0.9170	0.8996	0.9772	0.9747	0.8903	1

As noted above in the discussion section for ambient $PM_{2.5}$ (section 1.3.1), CSAM unit #405 was not included in this comparison due to erroneous time stamp readings.

Overall, the ozone measurements from the nine CSAMs were very reliable, with data recovery close to 100% for eight of the nine units tested, which were characterized by modest intra-model variability. Only CSAM unit #402 had a relatively low data recovery (77.5%). Ozone sensor data for the nine CSAM units (#401, #402, #403, #404, #406, #407, #408, #409, and #410) showed an excellent correlation (R^2: 0.80 – 0.97) with the corresponding reference measurements collected using a substantially more expensive FEM instruments (i.e., Thermo 49i) at 5-minute, 1-hour, 8-hour, and 24-hour time resolutions collectively. The nine CSAM units underestimated the 5-minute average ozone concentrations by 10 to 50% as measured by the FEM instrument.

1.2.3. Ambient Temperature

Data validation and recovery
Standard QA/QC procedures were used to validate the collected data from the temperature sensor (model AM 2315, Adafruit) in the CSAM units. Obvious outliers, negative values, and invalid data-points were eliminated from the data-set. The data recovery for temperature from the nine CSAM temperature sensors was greater than 99.2% with the exception of unit #402 (77.5%). Descriptive statistics for the nine units and the RIVR weather station sensor are presented in table 1.12 below.

Table 1.12. Descriptive statistics for temperature data in the nine CSAMs and RIVR station

T (Celsius)	FRM	Unit 401	Unit 402	Unit 403	Unit 404	Unit 406	Unit 407	Unit 408	Unit 409	Unit 410
mean	14.4	16.5	15.5	16.1	16.2	16.1	15.9	16.1	16.3	16.3
median	13.5	14.8	14.5	14.7	14.9	14.8	14.6	14.3	14.4	14.4
STDEV	5.5	7.1	5.9	6.9	6.7	6.6	6.6	7.6	7.8	7.6
Count	16368	16300	12733	16298	16303	16305	16293	16301	16304	16300
Recovery (%)	99.7	99.3	77.5	99.2	99.3	99.3	99.2	99.3	99.3	99.3

Temperature; intra-model variability

Very low measurement variations were observed among the nine CSAM temperature sensors for ambient temperature (Celsius) measurements. Figure 1.25 shows the intra-model variability (mean and median values) for the nine CSAM temperature sensors.
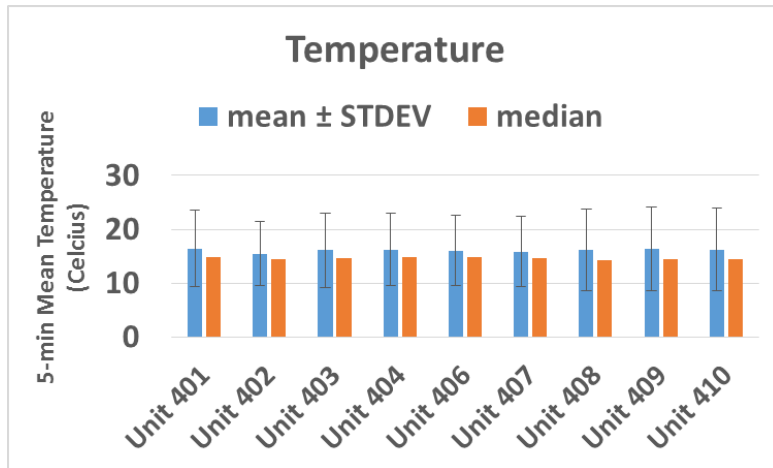
Figure 1.25. Intra-model variability for nine CSAM temperature sensors

CSAM vs RIVR (Temperature; 5-minute mean)

All 5-minute average CSAM temperature measurements from the nine sensors correlated very well with the corresponding RIVR weather station sensor (model HygroClip2-S3, Rotronic AG) data ($R^2 > 0.80$) (Table 1.13). The nine CSAM units appeared to track very well with the diurnal temperature variations recorded by the RIVR weather station sensor (Figures 1.26-1.27).
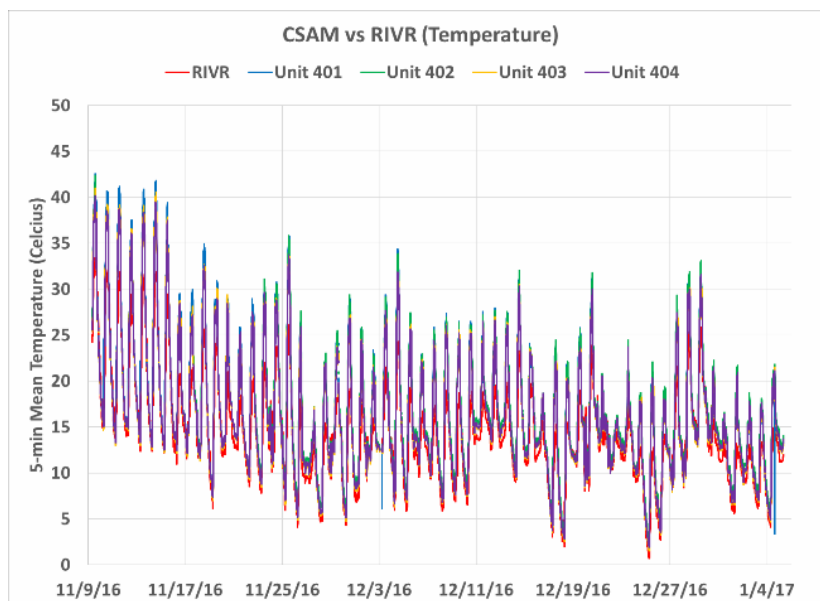
Figure 1.26. Time-series plot of temperature measurements from units #401 through #404 and the weather station sensor (5-minute average)
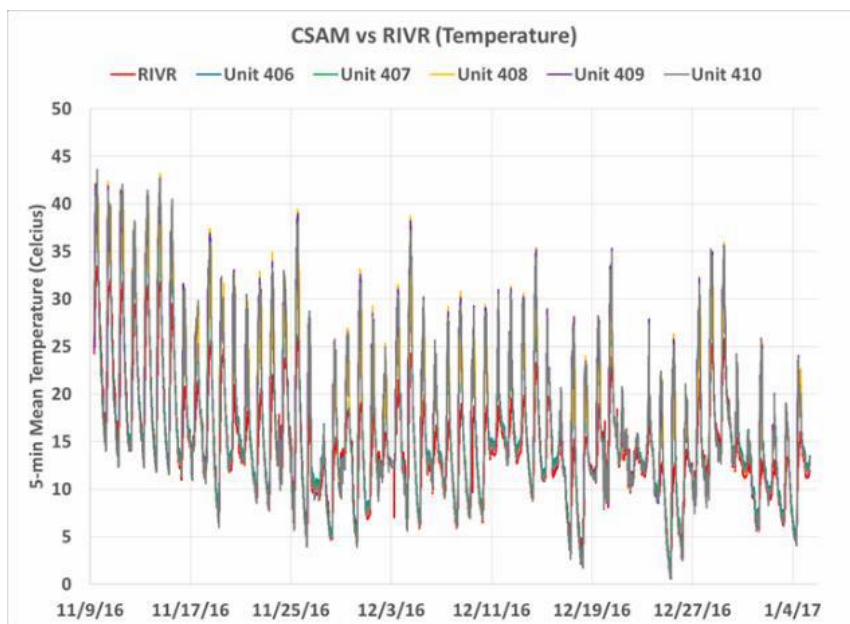
Figure 1.27. Time-series plot of temperature measurements from units #406 through #410 and the weather station sensor (5-minute average)

Table 1.13. Correlation coefficient (R^2) matrix for the 5-minute average temperature values measured by the weather station sensor and CSAM units

	RIVR	Unit 401	Unit 402	Unit 403	Unit 404	Unit 406	Unit 407	Unit 408	Unit 409	Unit 410
RIVR	1									
Unit 401	0.8993	1								
Unit 402	0.8827	0.9964	1							
Unit 403	0.9095	0.9959	0.9959	1						
Unit 404	0.9152	0.9953	0.9970	0.9989	1					
Unit 406	0.9199	0.9922	0.9918	0.9977	0.9975	1				
Unit 407	0.9145	0.9903	0.9907	0.9955	0.9960	0.9982	1			
Unit 408	0.8312	0.9599	0.9560	0.9581	0.9572	0.9596	0.9612	1		
Unit 409	0.8034	0.9506	0.9389	0.9487	0.9451	0.9497	0.9572	0.9771	1	
Unit 410	0.8192	0.9635	0.9524	0.9589	0.9570	0.9589	0.9652	0.9662	0.9842	1

CSAM vs RIVR (Temperature; 1-hour mean)

All 1-hour average temperature measurements from the nine CSAMs correlated very well with the corresponding RIVR weather station data ($R^2 > 0.81$) (Table 1.14). The nine sensor units appeared to track very well with the diurnal temperature variations recorded by the RIVR weather station (Figures 1.28-1.29).

Figure 1.28. Time-series plot of temperature measurements from units #401 through #406 and the weather station sensor (1-hour average)

Figure 1.29. Time-series plot of temperature measurements from units #406 through #410 and the weather station sensor (1-hour average)

Table 1.14. Correlation coefficient (R^2) matrix for the 1-hour average temperature values measured by the RIVR weather station sensor and CSAM units

R^2	RIVR	Unit 401	Unit 402	Unit 403	Unit 404	Unit 406	Unit 407	Unit 408	Unit 409	Unit 410
RIVR	1									
Unit 401	0.9047	1								
Unit 402	0.8902	0.9982	1							
Unit 403	0.9148	0.9971	0.9969	1						
Unit 404	0.9200	0.9967	0.9976	0.9993	1					
Unit 406	0.9246	0.9935	0.9929	0.9981	0.9979	1				
Unit 407	0.9192	0.9921	0.9917	0.9963	0.9965	0.9986	1			
Unit 408	0.8428	0.9692	0.9657	0.9673	0.9654	0.9680	0.9690	1		
Unit 409	0.8129	0.9566	0.9449	0.9544	0.9508	0.9551	0.9617	0.9820	1	
Unit 410	0.8297	0.9702	0.9599	0.9654	0.9631	0.9655	0.9717	0.9753	0.9892	1

CSAM vs RIVR (Temperature; 24-hour mean)

All 24-hour average CSAM temperature measurements from the nine sensors correlated very well with the corresponding RIVR weather station data ($R^2 > 0.88$) (Table 1.15). The nine sensor units appeared to track very well with the diurnal temperature variations recorded by the RIVR weather station sensor and also to be quite accurate (Figures 1.30-1.31).

Figure 1.30. Time-series plot of temperature measurements from units #401 through #404 and the R I V R weather station sensor (24-hour average)

Figure 1.31. Time-series plot of temperature measurements from units #406 through #410 and the R I V R weather station sensor (24-hour average)

Table 1.15. Correlation coefficient (R^2) matrix for the 24-hour average temperature measurements taken by the RIVR weather station sensor and CSAM units

R^2	RIVR	Unit 401	Unit 402	Unit 403	Unit 404	Unit 406	Unit 407	Unit 408	Unit 409	Unit 410
RIVR	1									
Unit 401	0.9790	1								
Unit 402	0.8842	0.9044	1							
Unit 403	0.9818	0.9982	0.9110	1						
Unit 404	0.9828	0.9979	0.9110	0.9998	1					
Unit 406	0.9842	0.9970	0.9109	0.9996	0.9997	1				
Unit 407	0.9837	0.9966	0.9104	0.9994	0.9996	0.9998	1			
Unit 408	0.9764	0.9950	0.8969	0.9928	0.9930	0.9913	0.9916	1		
Unit 409	0.9713	0.9919	0.8910	0.9894	0.9897	0.9878	0.9887	0.9991	1	
Unit 410	0.9781	0.9954	0.8985	0.9937	0.9940	0.9927	0.9931	0.9993	0.9989	1

1.2.4. Ambient Relative Humidity

Data validation and recovery

Standard QA/QC procedures were used to validate the collected data from the relative humidity sensor (model AM 2315, Adafruit) in the CSAM units. Obvious outliers, negative values, and invalid data-points were eliminated from the data-set. The data recovery for relative humidity from the nine of the CSAM relative humidity sensors was greater than 99.2%, whereas it was 77.5% for unit #402. Descriptive statistics for the nine units and the RIVR weather station sensor are presented in Table 1.16 below.

Table 1.16. Descriptive statistics for the Relative Humidity sensors for the CSAM units and the RIVR station

RH (%)	RIVR	Unit 401	Unit 402	Unit 403	Unit 404	Unit 406	Unit 407	Unit 408	Unit 409	Unit 410
mean	54.3	44.5	44.5	40.8	46.8	45.8	42.3	45.4	38.8	49.3
median	54.9	42.8	46.4	38.0	44.1	44.6	39.0	43.0	36.4	43.8
STDEV	28.7	25.8	22.5	23.8	27.8	25.5	24.5	27.2	26.6	30.2
count (#)	16369	16300	12733	16296	16303	16305	16296	16300	16304	16298
recovery	99.7	99.3	77.5	99.2	99.3	99.3	99.2	99.3	99.3	99.2

Relative Humidity; intra-model variability

Very low measurement variations were observed among the nine CSAM sensor units for relative humidity (%) measurements (Figure 1.32).
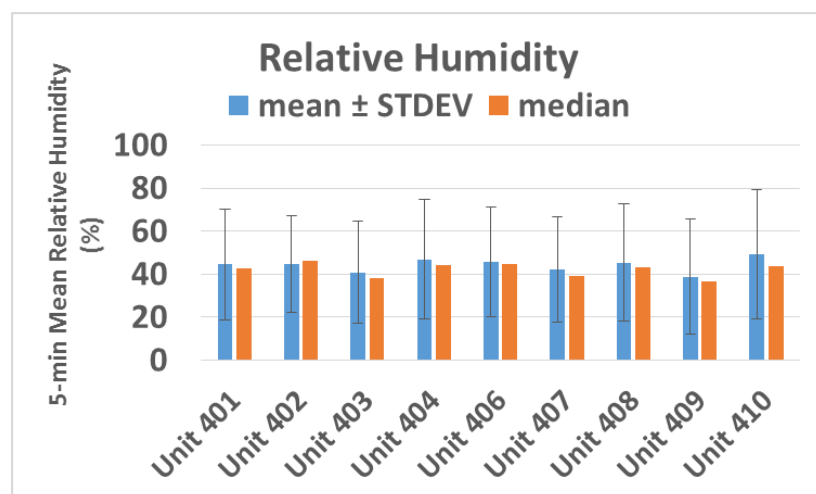
Figure 1.32. Intra-model variability for the nine CSAM RH sensors evaluated in this study

CSAM vs RIVR (RH; 5-minute mean)

All 5-minute average relative humidity measurements from the nine CSAMs correlated very well with the corresponding RIVR weather station data ($R^2 > 0.91$) (Table 1.17). The nine sensor units appeared to track very well with the diurnal relative humidity variations recorded by the RIVR weather station sensor (Figures 1.33-1.34).
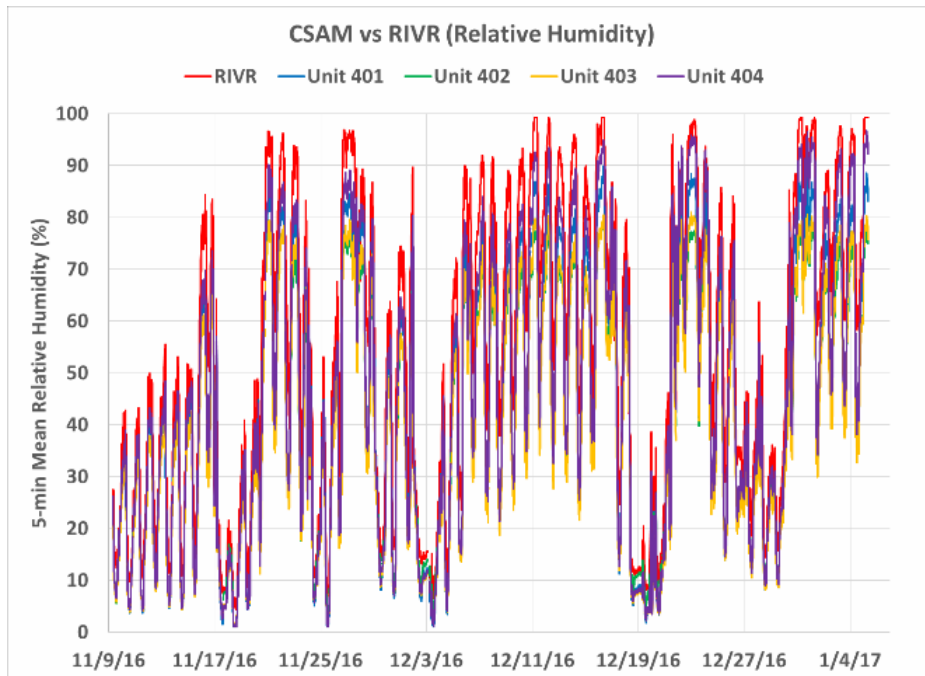
Figure 1.33. Time-series plot of RH measurements from units #401 through #404 and the R I V R weather station sensor (5-minute average)
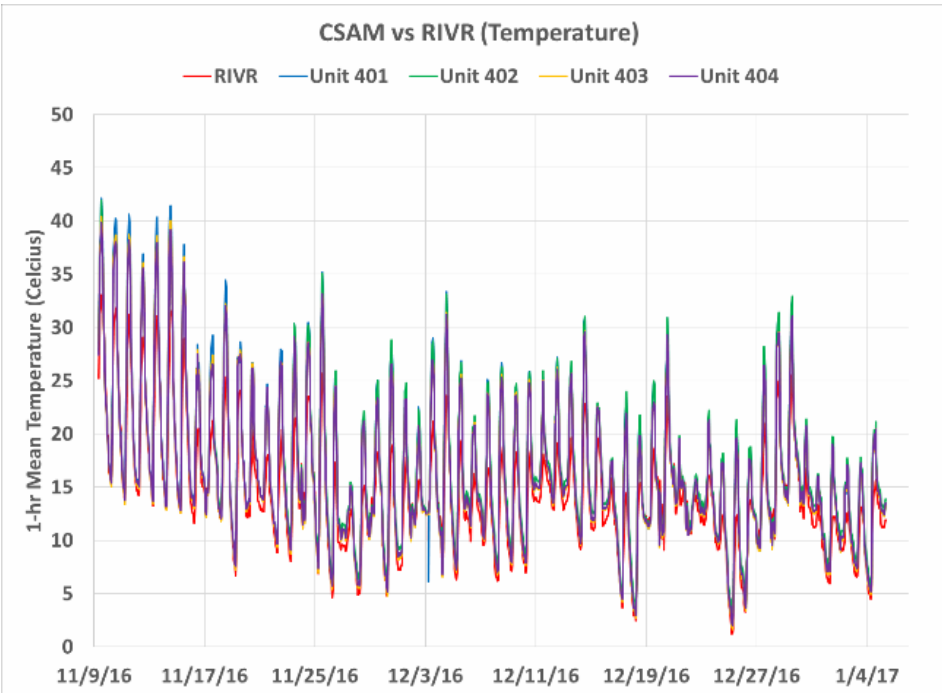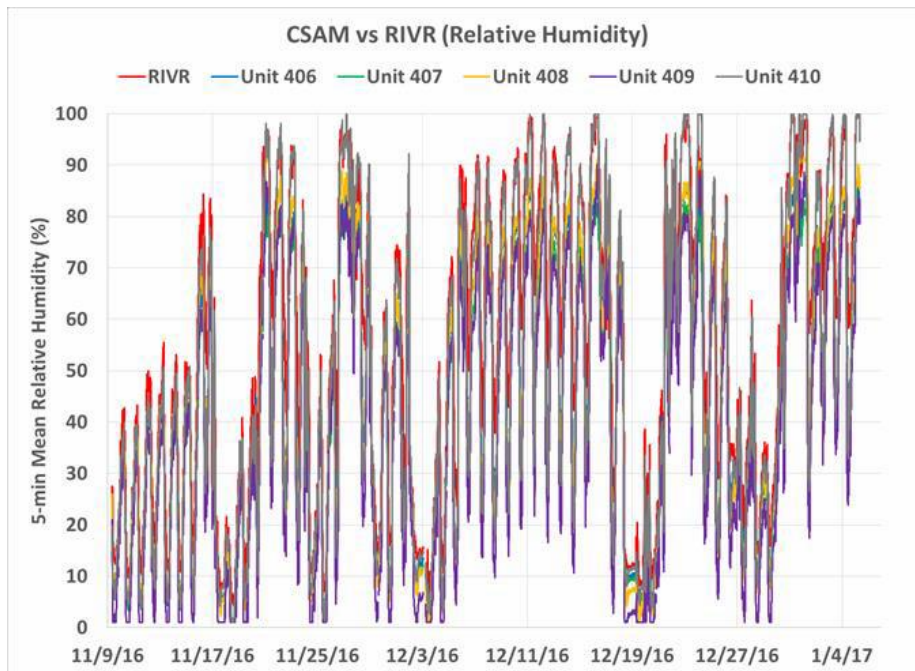

Figure 1.34. Time-series plot of RH measurements from units #406 through #410 and the RIVR weather station sensor (5-minute average)

Table 1.17. Correlation Coefficient (R^2) matrix for the 5-minute average relative humidity values measured by the weather station sensor and CSAM units
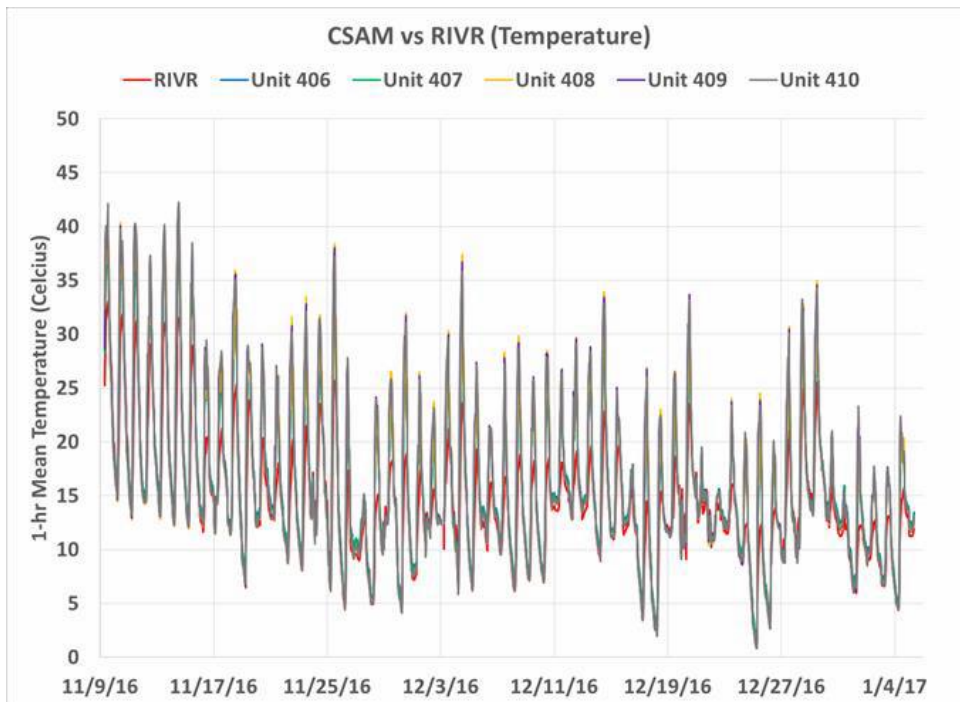
R^2	RIVR	Unit 401	Unit 402	Unit 403	Unit 404	Unit 406	Unit 407	Unit 408	Unit 409	Unit 410
RIVR	1									
Unit 401	0.9623	1								
Unit 402	0.9559	0.9973	1							
Unit 403	0.9598	0.9977	0.9974	1						
Unit 404	0.9619	0.9969	0.9957	0.9975	1					
Unit 406	0.9628	0.9970	0.9959	0.9959	0.9947	1				
Unit 407	0.9610	0.9963	0.9968	0.9979	0.9970	0.9965	1			
Unit 408	0.9398	0.9868	0.9852	0.9877	0.9857	0.9866	0.9856	1		
Unit 409	0.9192	0.9798	0.9796	0.9821	0.9789	0.9794	0.9801	0.9908	1	
Unit 410	0.9270	0.9839	0.9828	0.9868	0.9855	0.9828	0.9870	0.9856	0.9902	1

CSAM vs RIVR (RH; 1-hour mean)

All 1-hour average relative humidity measurements from the nine CSAMs correlated very well with the corresponding RIVR weather station data ($R^2 > 0.92$) (Table 1.18). The nine CSAM units appeared to track very well with the diurnal relative humidity variations recorded by the RIVR weather station sensor (Figures 1.35-1.36).

Figure 1.35. Time-series plot of RH measurements from units #401 through #404 and the weather station sensor (1-hour average)

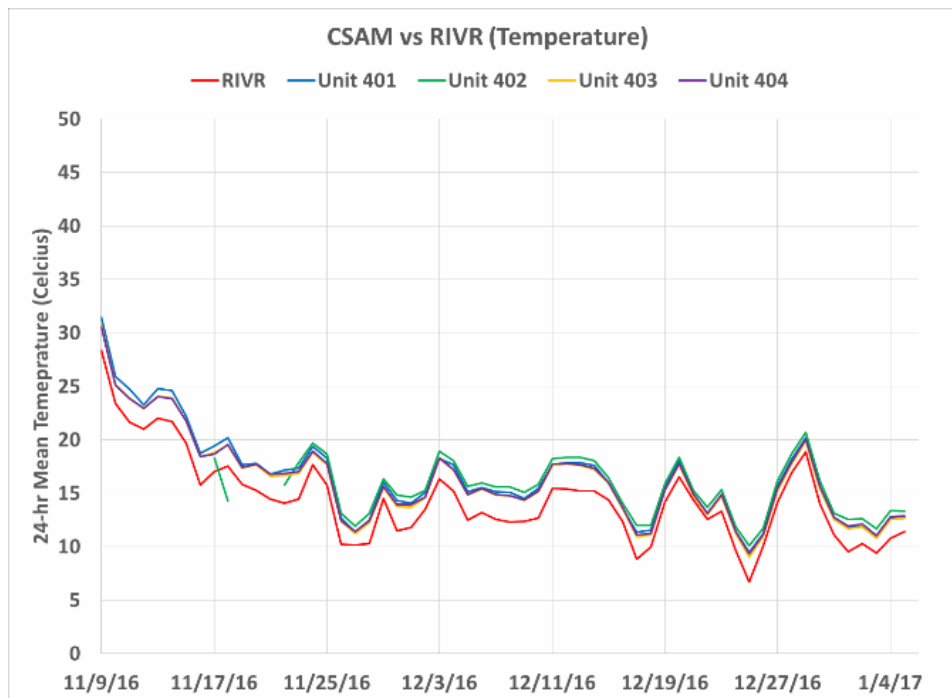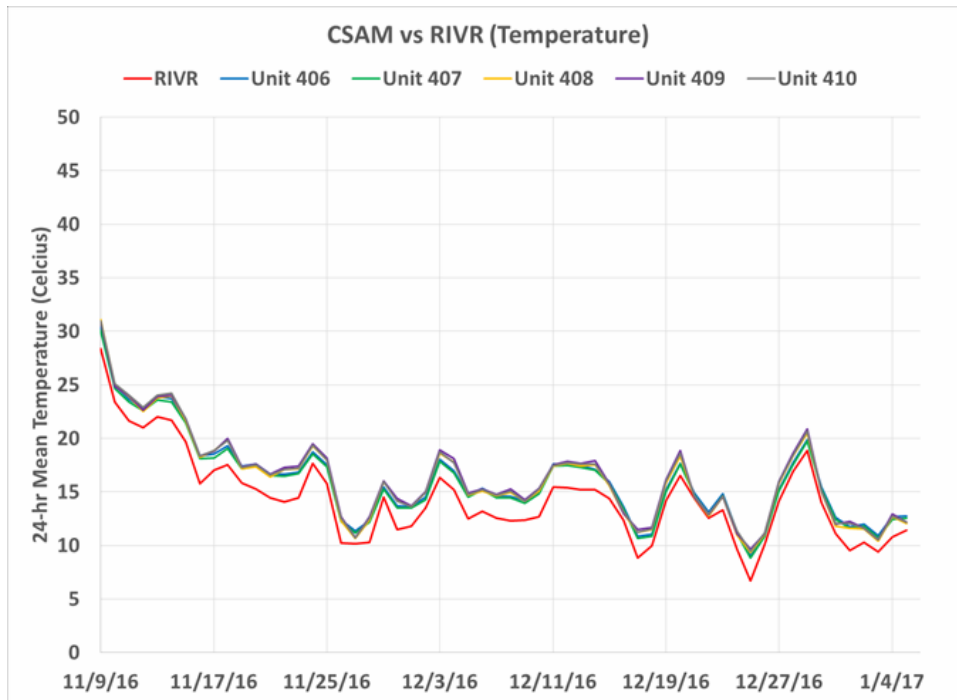**Figure 1.36. Time-series plot of RH measurements from units #406 through #410 and the weather station sensor (1-hour average)**

Table 1.18. Correlation Coefficient (R^2) matrix for the 1-hour average RH values measured by the RIVR weather station sensor and CSAM units

R^2	RIVR	Unit 401	Unit 402	Unit 403	Unit 404	Unit 406	Unit 407	Unit 408	Unit 409	Unit 410
RIVR	1									
Unit 401	0.9671	1								
Unit 402	0.9621	0.9981	1							
Unit 403	0.9653	0.9981	0.9977	1						
Unit 404	0.9671	0.9972	0.9961	0.9977	1					
Unit 406	0.9679	0.9973	0.9966	0.9961	0.9948	1				
Unit 407	0.9663	0.9967	0.9972	0.9980	0.9972	0.9967	1			
Unit 408	0.9462	0.9884	0.9875	0.9894	0.9873	0.9880	0.9871	1		
Unit 409	0.9258	0.9813	0.9813	0.9835	0.9803	0.9807	0.9813	0.9918	1	
Unit 410	0.9336	0.9853	0.9847	0.9881	0.9867	0.9841	0.9884	0.9873	0.9918	1

CSAM vs RIVR (RH; 24-hour mean)

All 24-hour average relative humidity measurements from the nine CSAMs correlated very well with the corresponding RIVR weather station data ($R^2 > 0.98$) (Table 1.19). The nine CSAMs units appeared to track very well with the diurnal relative humidity variations recorded by the RIVR weather station sensor (Figures 1.37-1.38).

Figure 1.37. Time-series plot of RH measurements from units #401 through #404 and the RIVR weather station sensor (24-hour average)

Figure 1.38. Time-series plot of RH measurements from units #406 through #410 and the RIVR weather station sensor (24-hour average)

Table 1.19. Correlation coefficient (R^2) matrix for the 24-hour average RH values measured by the RIVR weather station sensor and CSAM units

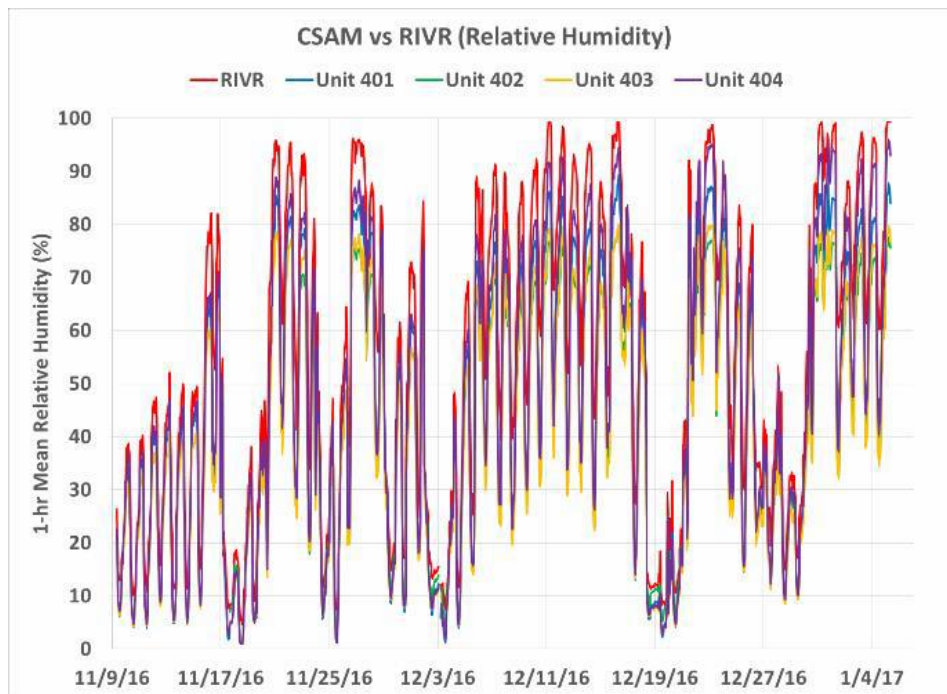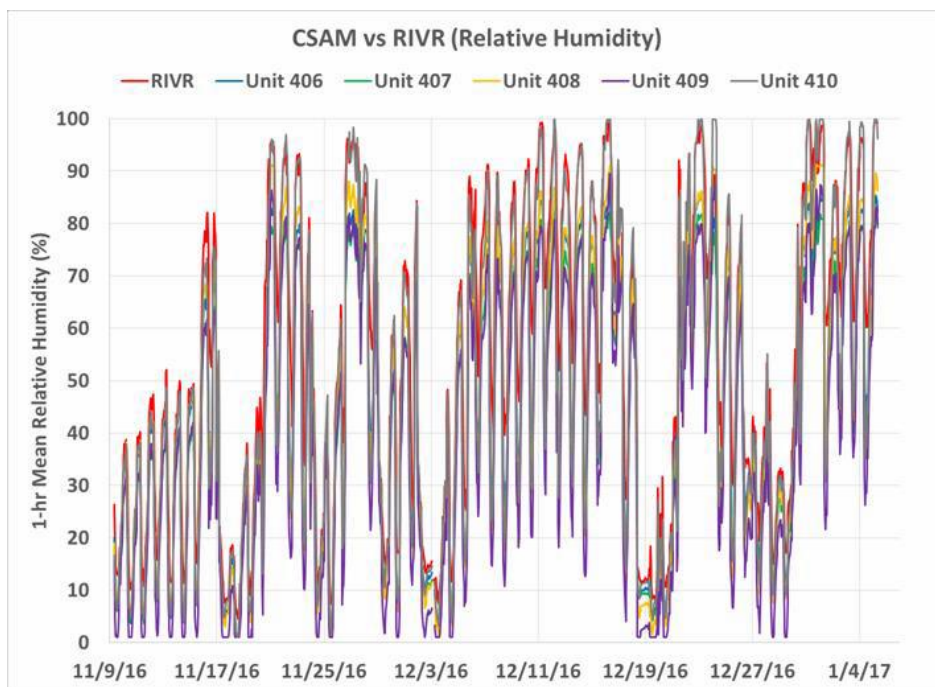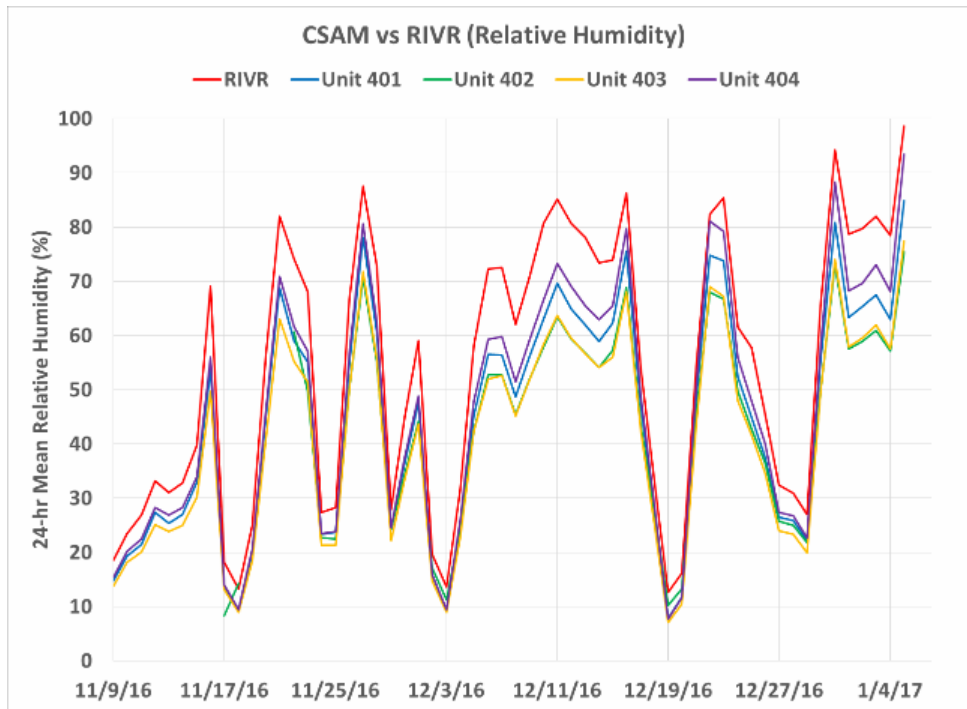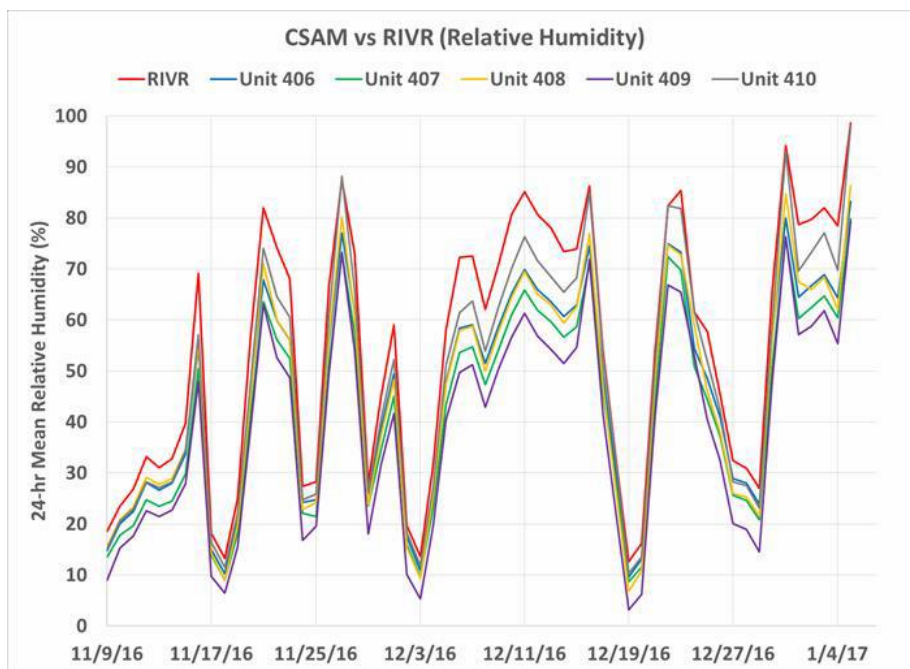| R^2	RIVR	Unit 401	Unit 402	Unit 403	Unit 404	Unit 406	Unit 407	Unit 408	Unit 409	Unit 410
RIVR	1									
Unit 401	0.9899	1								
Unit 402	0.9849	0.9926	1							
Unit 403	0.9916	0.9994	0.9928	1						
Unit 404	0.9881	0.9983	0.9900	0.9979	1					
Unit 406	0.9930	0.9978	0.9925	0.9977	0.9962	1				
Unit 407	0.9906	0.9980	0.9923	0.9982	0.9976	0.9985	1			
Unit 408	0.9878	0.9965	0.9893	0.9968	0.9954	0.9946	0.9940	1		
Unit 409	0.9837	0.9952	0.9887	0.9953	0.9944	0.9926	0.9934	0.9979	1	
Unit 410	0.9854	0.9963	0.9897	0.9961	0.9973	0.9948	0.9974	0.9942	0.9963	1

1.3. QA Summary for Co-location Testing

Throughout the CSAM co-location evaluation period in the field, the ozone and particle instrumentation at the monitoring station was maintained and operated according to standard operating procedures (SOPs) by the Atmospheric Measurements Branch (AM) at SCAQMD. The Thermo 49i FEM ozone instrument underwent routine weekly maintenance checks by the station operator to ensure that the instrument was operating according to specifications. The ozone instrument was challenged with daily precision and weekly span checks to verify that the instrument was operating within 7% of the expected value during the challenge. During the co-location testing, the ozone instrument's precision and span checks were all within 7% of their expected values. The ozone instrument at Rubidoux AMS was calibrated on April 21, 2016 and then again on November 4, 2016. The calibration on November 4, 2016 was an "as-is" equals "final" calibration, which indicates that the slope and intercept remained the same on the instrument. The level of routine maintenance, regular calibrations, and daily precision checks assured that the instrument was collecting quality data that could be submitted to the EPA for regulatory NAAQS attainment determinations.

The Metone FEM $PM_{2.5}$ BAM 1020 received monthly maintenance, service, and verification of the flow, temperature, pressure, and whether there were leaks. Throughout the course of the co-location, the flow, temperature, pressure, and leak checks were all found to be within acceptable limits. The Metone BAM automatically performed a span check each hour with a reference membrane to ensure that the instrument was not drifting over time. The calibration on the BAM was performed on June 24, 2016.

The Grimm 180 EDM underwent monthly verifications during the study that involved verifying the instrument's flow, temperature, and RH values against the reference grade flow and temperature meter. The unit was calibrated by the manufacturer on November 29, 2016. The combined maintenance, calibrations, verifications, and checks on the FEM equipment provided assurance that the instrumentation was operating in good condition and producing quality data.

The CSAM units were checked weekly to ensure proper data logging and reasonability of values. Having ten CSAM units in one area provided the opportunity to visibly spot check the units for reasonability with each other in regard to $PM_{2.5}$ and ozone concentrations. No flow checks were performed during the study on the Alphasense OPC sensors. Notice was given to spot check the date and time stamp of the CSAM units weekly

to compare them with the station time to ensure that the two data sources could be time aligned properly in the data analysis phases of the project.

2. Laboratory Chamber Evaluation

2.1. Methods

A characterization chamber system, designed by the AQ-SPEC team and developed and integrated in collaboration with AmbiLabs (Warren, RI), was used for the laboratory testing of two representative CSAM sensor pods (Units #406 and #409). The chamber system (Figure 2.1) and the methods developed to evaluate sensor performance under controlled conditions are described in detail in the paper "Development of an environmental chamber for evaluating the performance of low-cost air quality sensors under controlled conditions" (Papapostolou et al., 2017). Specifically, the following chamber system components were used for testing the CSAM sensor pods under controlled environmental conditions.

- A T/RH controlled rectangular-shaped stainless-steel enclosure [38" (width) x 38" (height) x 54" (depth)] (referred to as the "outer chamber"), used to conduct aerosol sensors testing experiments
- A T/RH controlled cylindrical-shaped Teflon-coated stainless-steel enclosure [12" (base radius) x 15" (height)] (referred to as the "inner chamber"), used to conduct gaseous sensors' testing experiments
- A dry, gas- and particle-free air ("zero-air") generation system
- A dust monitor by GRIMM (model EDM180, Ainring, Germany): The EDM 180 spectrometer provides high-resolution real-time aerodynamic measurements of PM_{10}, $PM_{2.5}$, $PM_{1.0}$, TSP, and PM_{coarse} particles. The EDM 180 measures light-scattering and is designated as a class III equivalent method EQPM-0311-195 for ambient $PM_{2.5}$ mass concentration by the U.S. EPA.
- An aerodynamic particle sizer (APS) by TSI (Model 3321): The APS 3321 spectrometer provides high-resolution, real-time aerodynamic measurements of particles from 0.5 to 20 μm in diameter. The APS measures light-scattering intensity in the equivalent optical size range of 0.37 to 20 μm (BAT for measuring particle size distribution above 0.5 μm in aerodynamic diameter)
- An aerosol generator made by PALAS (model AGK 2000; Karlsruhe, Germany), used to produce ultrafine and fine particles from various solutions and suspensions
- An O_3 analyzer by American Ecotech (model Serinus 10, Warren, RI). The Serinus 10 is designated as an equivalent method EQOA-0809-187 by the U.S. EPA (40 CFR Part 53).
- A dynamic dilution calibrator with an internal ozone generator by Teledyne API (model T700U, San Diego, CA)
- A certified 48.6 ppm nitric oxide cylinder (Air Liquide, Santa Fe Springs, CA)
- An American Ecotech Serinus 40 oxides of nitrogen analyzer (FRM for ambient NO_2 concentration)
- An HMM100 humidity module by Vaisala to measure temperature and relative humidity

A custom-developed software was used to automatically and remotely control and operate the chamber and all reference instruments. This software allows for the design of extensive sensor testing experiments using programmed sequences.
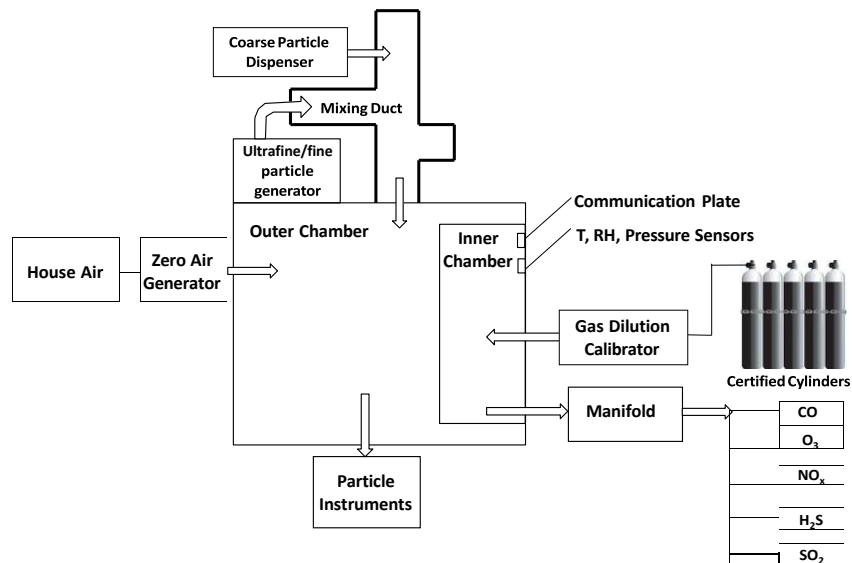
Figure 2.1. Schematic of AQ-SPEC's environmental chamber

Both the outer and inner chambers are capable of maintaining a wide range of temperature and relative humidity conditions. The HVAC heating/cooling system is used to control the temperature, and a humidifier/de-humidifier is used to control varying relative humidity. A set of two fans, installed in the rear wall of the outer chamber and behind the upper wall perforations, generates a circular airflow in the outer chamber, with the air flowing in from the bottom first through the cooling and dehumidifying coils and then passing through the heating elements. This air movement mechanism provides for uniform mixing inside the outer chamber. To achieve target T/RH conditions in the inner chamber, a pump draws the conditioned air from the outer chamber at a set flow (approximately 10 LPM). This relatively high flow is also used to mix the air in the inner chamber, creating a homogenous atmosphere. The pump flow is controlled by a mass flow controller.

Due to their size and the inner chamber volume of 110 L, only two CSAM sensor pods (as opposed to three units per the standard AQ-SPEC laboratory testing protocol) could be installed inside the inner chamber for ozone testing. Thus, it was decided to use only two representative units (#406 and #409) for chamber evaluation for both the PM and gas sensors testing.

Figure 2.2 shows the CSAM $PM_{2.5}$ and ozone sampling ports as well as those of the reference instruments. For $PM_{2.5}$ testing, the rectangular-shaped stainless-steel "outer" chamber was used. For ozone testing, the CSAM pods were placed inside a smaller cylindrical-shaped Teflon coated stainless-steel unit installed within the "outer" chamber.
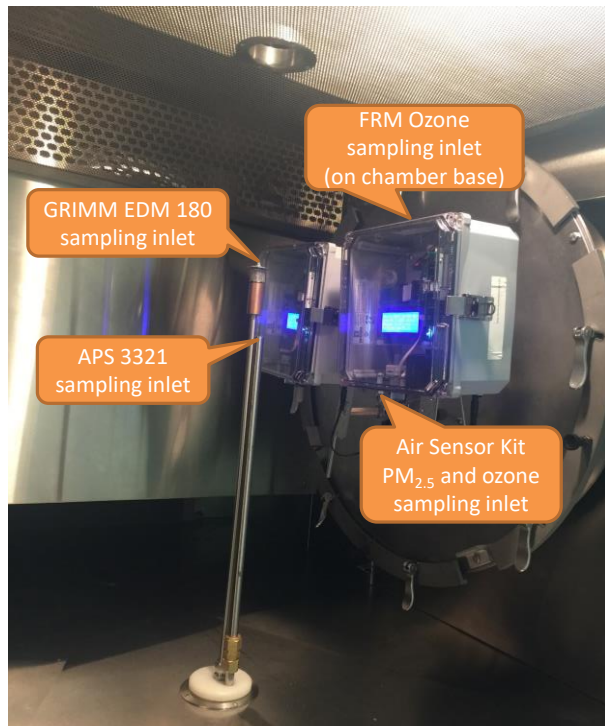
Figure 2.2. Two CSAM units installed on the inner chamber base

The CSAM sensor pod reports data at a 5-minute time resolution. The AQ-SPEC testing procedures were modified accordingly to ensure a representative number of data points were collected for statistical analysis. A detailed description of the procedures used for testing the PM$_{2.5}$ and ozone sensors of the CSAM pods is discussed below.

2.1.1. PM$_{2.5}$ testing procedure

As noted above, the chamber equipment used to conduct PM$_{2.5}$ sensor testing in the CSAM sensor pod consisted of an "outer" chamber, a PALAS particle generator, a FEM GRIMM EDM 180 dust monitor, and an TSI APS 3321 for measuring aerosol size distribution.

Before beginning an experiment, the chamber wall surfaces were cleaned with Kimwipes dampened in deionized water. The two CSAM units that were selected for the chamber evaluation, #406 and #409, had been used previously in the field co-location studies with the other CSAM units. Units #406 and #409 were mounted on a customized aluminum shelf (Figure 2.2). The sensors' inlets were located approximately three inches from the reference instrument sampling inlets to ensure that all FRM/FEM monitors were sampling from approximately the same location inside the chamber. Subsequently, the chamber door was closed, and the chamber was flushed with dry, particle- and gas-free air. Particle mass and number concentrations were monitored using the chamber PM reference instruments (GRIMM and APS) to confirm that the PM mass and count concentration levels inside the chamber were negligible.

The CSAM units logged data locally on an internal SD memory card, and the data were downloaded to a computer at the conclusion of an experiment. The procedure for evaluating the CSAM pod's ability to measure PM$_{2.5}$ involved several concentration ramping experiments under (1) "average ambient" T/RH and (2) extreme T/RH combinations.

<u>Phase 1</u>: Concentration ramping experiments under "average ambient" T and RH conditions

Once the chamber had reached the desired average ambient conditions of 20 °C and 40% relative humidity, a concentration ramping experiment was initiated. Per the *AQ-SPEC Sensors Lab Testing Protocol*, a total of 5 concentration steps were selected to mimic a diverse pollutant profile from very low (0-10 µg/m^3) to very high (300 µg/m^3) PM mass concentrations of ultrafine/fine particles. Each concentration ramping step was maintained for 210 minutes to allow for at least a steady-state period of 60 minutes. The test aerosol was created using a 21.9% potassium chloride (KCl) aqueous solution in the PALAS system. Experimental parameters, such as frequency and duration of aerosol injection into the chamber, were pre-determined and programmed in the software sequence scheduler. The chamber fans that were used to create uniform mixing inside the outer chamber were maintained at a constant speed (e.g., frequency of 25 Hz).

Information derived from this experiment was used to evaluate the sensors' performance parameters, such as linear correlation coefficient, accuracy, and intra-model variability.

<u>Phase 2</u>: Concentration ramping experiments under extreme T and RH conditions

Four T-RH combinations were used to test the PM$_{2.5}$ sensor in the CSAM units. For each condition, a 3-step concentration ramping experiment was conducted. The concentrations were selected to represent low, medium, and high ambient PM concentrations.

The information derived from these experiments was used to evaluate parameters such as the precision and effect of T and RH.

Table 2.1. Four representative T-RH combinations

Condition	Temperature (°C)	Relative Humidity (%)	Environment
1	5	15	cold, dry
2	5	65	cold, humid
3	35	15	hot, dry
4	35	65	hot, humid

2.1.2. Ozone testing procedure

The equipment used to test the ozone sensor in the CSAM units consisted of the cylindrical-shaped Teflon coated stainless-steel inner chamber, a Teledyne T700U gas dilution calibrator and ozone generator, a certified 48.6 ppm NO cylinder, a Serinus 10 ozone monitor, and a Serinus 40 oxides of nitrogen analyzer.

The procedure for evaluating the CSAM ozone sensor's performance included the following steps: (1) ozone concentration ramping experiment under "average ambient" T and RH; (2) concentration ramping experiment at more extreme T and RH; and, (3) an evaluation of potential interferences due to the presence of NO$_2$.

<u>Phase I</u>: Concentration ramping experiments under ambient T and RH conditions

Once the inner chamber reached the "average ambient" conditions of 20 °C and 40% RH, an ozone concentration ramping experiment was initiated. A total of 5 concentration steps were selected to mimic a diverse pollutant profile from very low (0-30 ppb) to very high (300 ppb) ground-level ambient ozone

concentrations. Each concentration ramping step was maintained for 150 minutes to allow for a steady-state period of at least 60 minutes. Ozone was generated using the T700U's internal ozone generator, which was then introduced to the inner chamber and mixed with conditioned zero air to achieve the desired target ozone concentration inside the inner chamber. Dilution factors and the expected ozone loss rate had been taken into account prior to the experiments and were pre-determined and programmed in a sequence. The information derived from this experiment was used to evaluate parameters such as linear correlation coefficient, accuracy, and intra-model variability.

Phase II: Concentration ramping experiments under "extreme" T and RH conditions

The same four T-RH combinations that were used for the PM testing were also used for testing the CSAM ozone sensor's performance (see Table 2.1 above). For each condition, a 3-step concentration ramping experiment was conducted. The concentrations were selected to represent low, medium, and high ground-level ambient ozone concentrations. The information derived from these experiments was used to evaluate parameters such as precision and the effects of T and RH.

Phase III: Potential interference due to the presence of NO_2

The effect of an NO_2 interferent was evaluated by exposing the two CSAM units to an increasing concentration of NO_2. NO_2 was formed by mixing nitric oxide (NO) from a certified cylinder with the ozone generated in the T700 internal ozone generator inside the T700 dilution calibrator at a ratio of 1.3:1. The NO_2 and O_3 concentrations were monitored with the reference instruments and the two CSAM units.

2.1.3. CSAM Evaluation Parameters

The following parameters were established for evaluating the CSAM's ability to measure $PM_{2.5}$ and ozone: (1) linear correlation coefficient, (2) accuracy, (3) precision, (4) lower detection limit, (5) effect of T/RH, (6) intra-model variability, (7) data recovery, and (8) effect of interferents (where applicable).

Linear correlation coefficient
This parameter expresses the strength of the linear relationship between the average measurements from the units tested and the corresponding reference instrument values. The linear correlation coefficient (R^2) was determined in a 5-step pollutant ($PM_{2.5}$ or ozone) concentration ramping experiment from a very low to a very high concentration at "average ambient" conditions of 20 °C and 40% relative humidity. Paired reference instrument and averaged sensor data were entered in an excel spreadsheet, and a linear correlation coefficient was calculated and reported along with slope and intercept values. An R^2 approaching the value of 1 reflects a nearly perfect agreement between the sensors and the reference instrument readings, whereas a value of 0 indicates a complete lack of correlation.

Accuracy
Accuracy (*A*) is the degree of closeness between the sensors' measured values and the reference instrument's value. For the purpose of these chamber tests, accuracy was estimated from the five steady state periods of the concentration ramping experiment at 20 °C and 40% relative humidity. At each steady state, accuracy w a s calculated by:

$$A(\%) = 100 - \frac{|\bar{X} - R|}{R} * 100 \qquad (1)$$

Where,

X is the average concentration measured by the sensors throughout the steady state period and,

R is the reference instrument average concentration during the same steady state period.

An accuracy value close to 100% implied that the sensors measured exactly what the reference instrument measured at a specific pollutant concentration. In cases in which sensors overestimated the reference instrument by more than 100%, the sensor's accuracy was reported as a negative value as defined in equation (1).

Precision
Precision (P) represents the variation around the mean of repeated measurements of the same pollutant concentration. This parameter was evaluated at the steady state period of each tested condition. Four T-RH combinations were used for testing (listed in Table 2.1). In each T/RH combination, a concentration ramping experiment with low, medium, and high pollutant concentration was performed.

Precision was calculated by data acquired from each steady state concentration ramping step:

$$P(\%) = 100 - \frac{\overline{SE_{sensor}}}{\bar{X}} * 100 \qquad (2)$$

Where,

$\overline{SE_{sensor}}$ is the standard error of the averaged concentrations of the sensors during the steady state period considered.

X the average concentration measured by the sensors throughout the same steady state period.

Effect of T and RH
The effect of T and RH on sensor's performance are for four the T/RH conditions of "cold, dry", "cold, humid", "hot, dry", and "hot, humid," as listed in Table 2-1.

Intra-model Variability
Intra-model variability is related to how close the measurements agree among the CSAM units. The intra-model variability was evaluated through a set of descriptive statistical parameters, such as mean, median, and standard deviation (each calculated at low, medium, and high pollutant concentrations). These values were derived from the concentration ramping experiment at 20 °C and 40% RH. For both the aerosol and ozone experiments, the 5-minute average data from each steady state period were used. For the two CSAM pod units tested in the environmental chamber, their difference is presented as a percentage and calculated as follows:

$$\text{Intra-model variability (\%)} = \frac{\text{Mean}_{high} - \text{Mean}_{low}}{\text{Mean}_{average}} * 100 \ (3)$$

Where,
Mean$_{high}$ is the higher value of the two CSAM Pods average concentration at the steady state, Mean$_{low}$ is the lower value of the two CSAM Pods average concentration at the steady state, Mean$_{average}$ is the average of the two CSAM Pods average concentration at the steady state.

Data recovery

Data recovery is calculated using a percentage ratio of the number of valid sensor data points over the total number of data points collected during the testing period (e.g., 10 hours of testing at a 5-minute time resolution results in a total of 120 data points). Data recovery is reported as a percentage and calculated as follows:

$$\text{Data recovery (\%)} = \frac{N_{valid\ data}}{N_{test\ period}} * 100 \ (4)$$

Where,

$N_{valid\ data}$ is the number of valid sensor data points during the testing period and $N_{test\ period}$ is the total number of data points for the testing period

Effect of interferents

Metal oxide ozone sensors may be susceptible to nitrogen dioxide cross-sensitivity. In the laboratory, the effect of NO_2 interferent was evaluated by exposing the CSAM units to a ramping experiment of known NO_2 concentration. If CSAM responded to the interferent, a quantitative relationship of units' response and NO_2 concentration was determined.

2.2. Results

2.2.1. Laboratory PM$_{2.5}$

Linear correlation coefficient: The linear correlation coefficient between the two CSAMs and FEM GRIMM was determined from the following concentration ramping experiment (Figure 2.3) at 20 °C and 40% RH. As shown in the figures below, both units #406 and #409 correlated well with the FEM instrument ($R^2 > 0.99$). Unit 406 recorded higher PM$_{2.5}$ mass concentrations than unit 409. As a secondary reference, APS 3321 measured similar PM$_{2.5}$ mass concentrations to those reported by the FEM GRIMM ($R^2 > 0.99$, slope = 1.01, and intercept = 3.81).

	R²	Slope	Intercept
Unit 406 vs GRIMM	0.9931	1.40	13.03
Unit 409 vs GRIMM	0.9942	1.30	10.08
APS vs GRIMM	0.9978	1.01	3.81
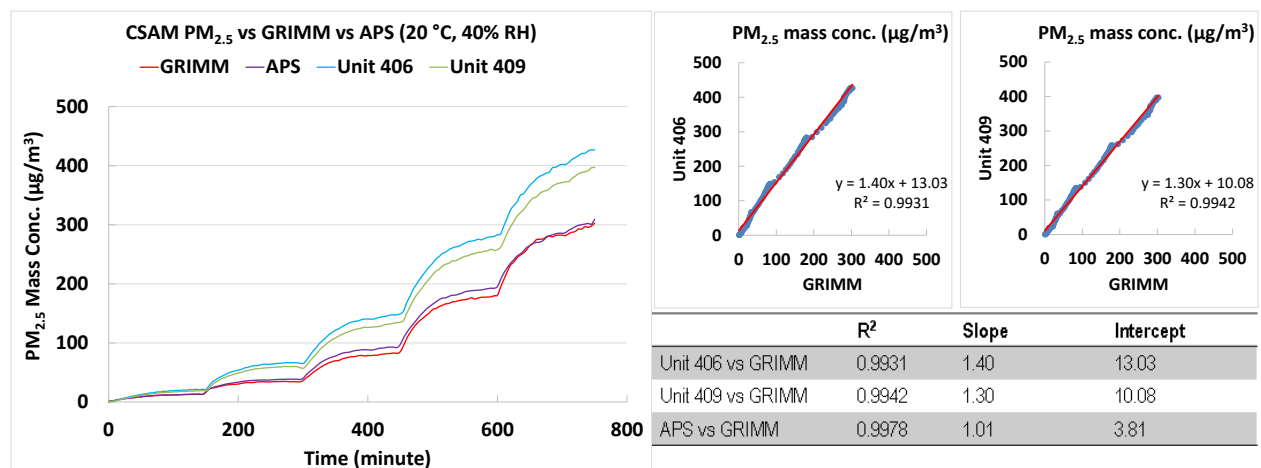
Figure 2.3. PM$_{2.5}$ mass concentrations as measured by the CSAM and the reference instruments used for these tests (FEM GRIMM and APS)

Accuracy: The CSAM PM$_{2.5}$ data showed low to moderate accuracy compared to the FEM GRIMM PM$_{2.5}$ during the concentration ramping experiment between 0-300 µg/m³. With accuracy ranging between 17.1% and 62.6%. Overall, the two CSAMs overestimated the PM$_{2.5}$ mass concentrations as measured by the FEM GRIMM (Table 2.2).

Table 2.2. CSAM PM$_{2.5}$ Accuracy

Steady State (#)	CSAM mean (µg/m³)	FEM GRIMM (µg/m³)	Accuracy (%)
1	19.8	13.0	47.6
2	63.1	34.5	17.1
3	138.9	81.8	30.2
4	267.6	178.5	50.1
5	407.2	296.4	62.6

Precision: The CSAMs demonstrated excellent precision (97-99%) in measuring PM$_{2.5}$ under most of the conditions tested (Table 2.3), except at 5 °C and 65% relative humidity. The precision of both units was affected by the low temperature and high humidity (and high humidity variation). The precision was between 74 and 91% for low to high PM$_{2.5}$ mass concentrations at 5 °C and 65% RH. At 35 °C and 15% RH, and also at 35 °C and 65% RH, precision was very high when ranging between low and high PM$_{2.5}$ mass concentrations, indicating the two CSAMs demonstrated similar performance under most environmental conditions.

Table 2.3. CSAM PM$_{2.5}$ precision under extreme T and RH conditions

		5 °C		35 °C	
Low		CSAM	GRIMM	CSAM	GRIMM
PM$_{2.5}$	15%	98.9	99.2	99.3	99.7
(µg/m³)	65%	74.0	93.0	98.8	97.1

		5 °C		35 °C	
Medium		CSAM	GRIMM	CSAM	GRIMM
PM$_{2.5}$	15%	99.6	99.7	99.7	99.8
(µg/m³)	65%	86.2	96.7	99.4	99.5

		5 °C		35 °C	
High		CSAM	GRIMM	CSAM	GRIMM
PM$_{2.5}$	15%	99.6	99.7	99.7	99.5
(µg/m³)	65%	90.5	97.9	99.7	99.7

Effect of T and RH: The CSAM's ability to measure low to high PM$_{2.5}$ concentrations was evaluated under four T-RH conditions (Figure 2.4). At 5 °C and 65% RH, both units #406 and #409 reported spiked PM$_{2.5}$ mass concentrations, whereas the FEM GRIMM and APS reported stable concentrations with very low variability. It is possible that this CSAM response might be associated with the sensor's limitation in measuring PM$_{2.5}$ under low temperature and high humidity (also humidity variation).
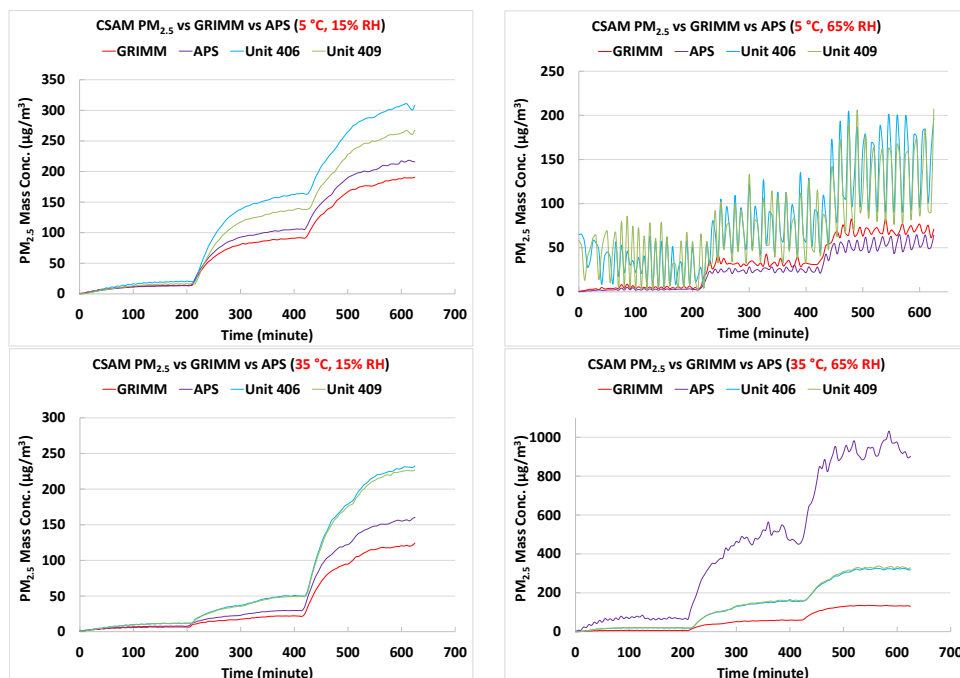
Figure 2.4. Effect of T-RH on CSAM PM$_{2.5}$ Performance

Data Recovery: Both CSAMs had excellent data recovery (nearly 100%) for PM$_{2.5}$.

Intra-model Variability: At 20 °C and 40% RH, units #406 and #409 correlated well with each other (R^2 > 0.99, slope = 1.08, intercept = 2.06). Low measurement variations were observed at low, medium, and high PM$_{2.5}$ mass concentrations (Figure 2.5).
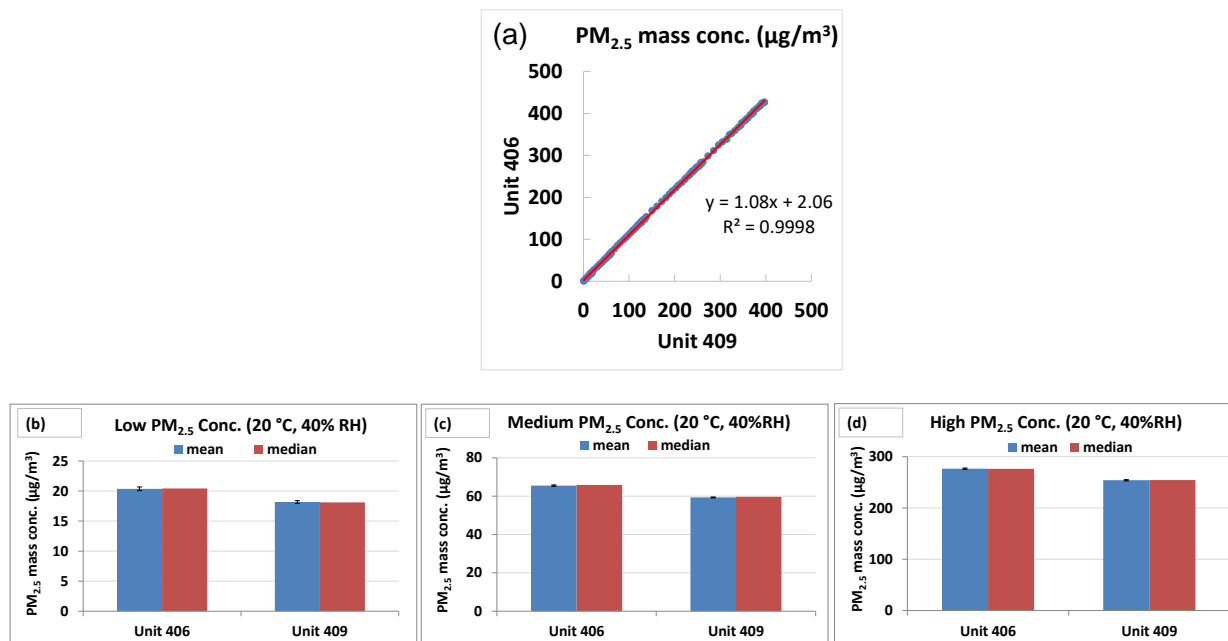
Figure 2.5. (a) Unit #406 vs unit #409; (b-d) intra-model variability at low, medium, and high PM$_{2.5}$ conc.

2.2.2. Laboratory Ozone

Linear correlation coefficient: The linear correlation coefficient between the two CSAM sensor pods and the FEM ozone was determined from the following concentration ramping experiment (Figure 2.6) at 20 °C and 40% RH. As shown in Figure 2.6 below, the CSAM units followed the ozone concentration changes, as measured by the FEM ozone monitor. Both units #406 and #409 correlated well with the FEM instrument ($R^2 > 0.95$). However, the two CSAM units had a high baseline value of 20 ppb (intercept: ~ 20 ppb). At high ozone concentrations, the two CSAM units significantly underestimated the FEM ozone concentration (slope: 0.12-0.13).

Figure 2.6. CSAM vs FEM ozone concentration ramping experiment (20 °C, 40% RH)

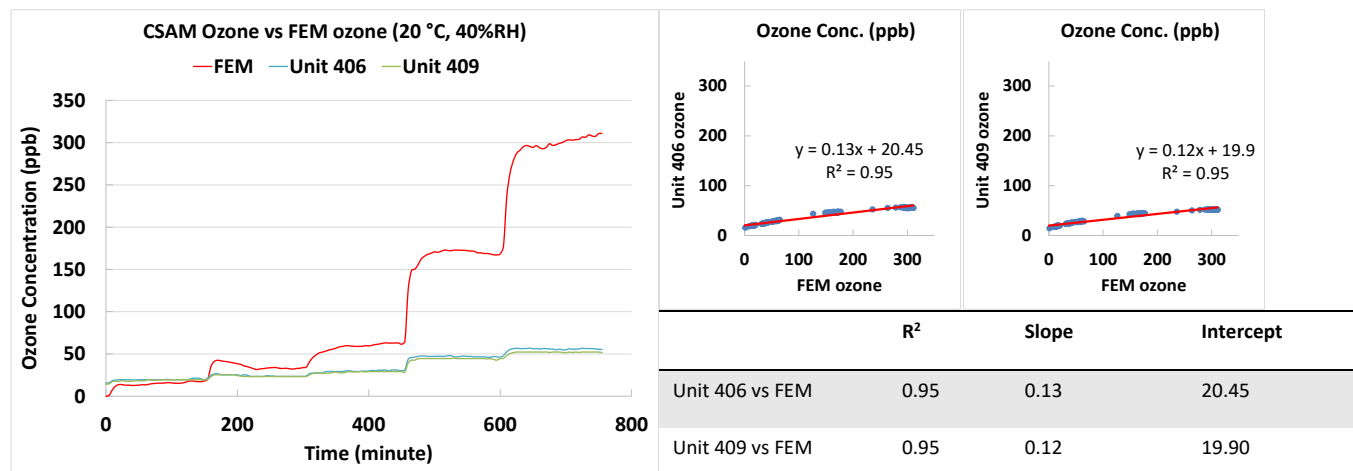|	R^2	Slope	Intercept
Unit 406 vs FEM	0.95	0.13	20.45
Unit 409 vs FEM	0.95	0.12	19.90

Accuracy: The CSAMs' accuracy in measuring ozone decreases as the ozone concentration increases, and ranges from 86.4% to 17.5% (Table 2.4). The CSAM units had baseline reading of approximately 20 ppb and the highest concentration reported was around 55 ppb, whereas the FEM's measured ozone concentration was between 0 to 310 ppb. The CSAMs in most cases underestimated the ozone concentrations as measured by the FEM instrument.

Table 2.4. CSAM Ozone Accuracy

Steady State (#)	CSAM mean (ppb)	FEM (ppb)	Accuracy (%)
1	20.0	17.6	86.4
2	23.3	32.9	71.0
3	29.9	62.7	47.6
4	45.2	168.1	26.9
5	54.0	308.8	17.5

Precision: The CSAMs demonstrated good precision under most of the environmental conditions tested for this evaluation (Table 2.5). At 5 °C and 15% RH, CSAM unit #406 reached its maximum reading of 500 ppb when the FEM ozone changed from 100 ppb to 300 ppb. Precision under this condition could not be evaluated because unit #406 appeared to be showing abnormal measurements. At 5 °C and 65% RH, unit #406 reported unusually high ozone concentrations when the FEM was recording a stable ozone concentration around 350 ppb. At 35 °C and 15% and 65% RH, the two CSAMs showed a similar high precision compared to the ambient conditions.

Table 2.5. CSAM Ozone Precision under extreme T and RH conditions

		5 °C		35 °C	
Low		CSAM	FEM	CSAM	FEM
Ozone	15%	99.0	97.6	99.6	99.7
(ppb)	65%	99.7	100.0	99.3	99.5

		5 °C		35 °C	
Medium		CSAM	FEM	CSAM	FEM
Ozone	15%	99.4	99.1	99.6	99.6
(ppb)	65%	99.8	100.0	99.7	99.7

		5 °C		35 °C	
High		CSAM	FEM	CSAM	FEM
Ozone	15%	N/A	99.7	99.7	99.9
(ppb)	65%	92.9	100.0	99.6	99.9

Effect of T and RH: The CSAMs' ability to measure low to high ozone concentrations was evaluated at the four T-RH conditions (see table 2.1 above). Unit #409 was consistent with its performance as it was exposed to ambient T-RH. However, at high ozone concentrations, unit #406 reported unusually high values and a maximum reading of 500 ppb at 5 °C and 15% and 65% (Figure 2.7).
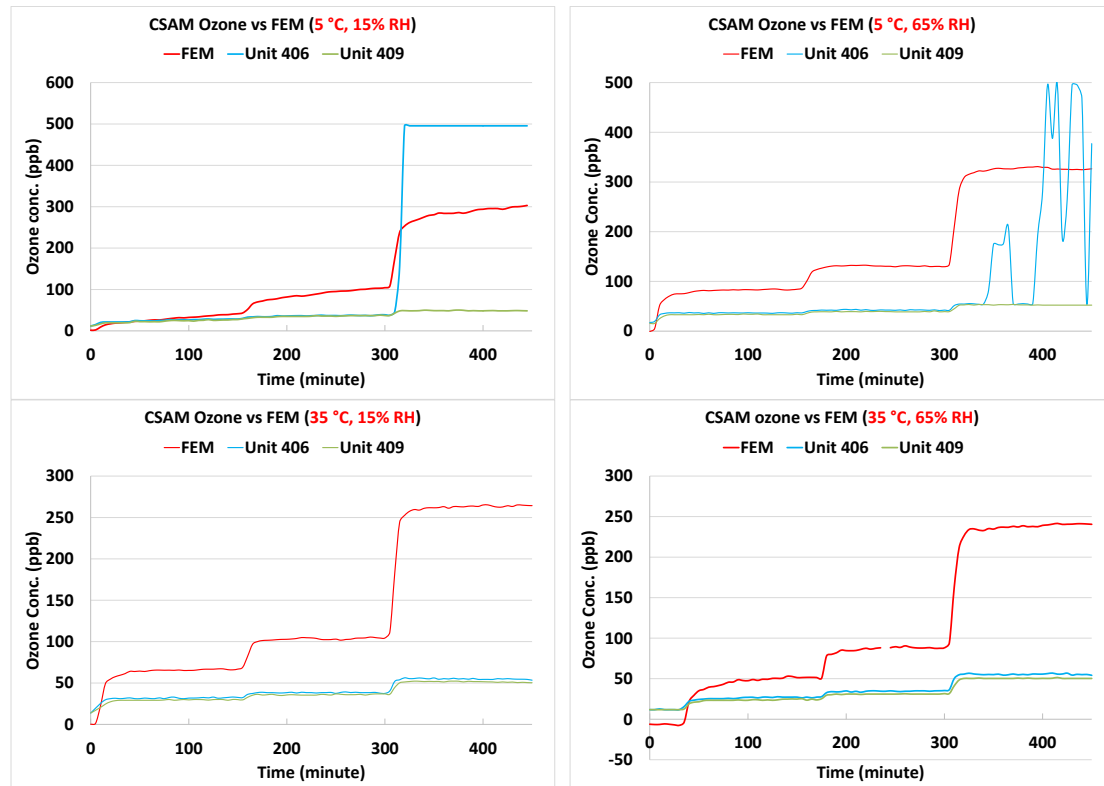
Figure 2.7. Effect of T-RH on CSAM ozone performance

Data Recovery: Both CSAMs had excellent data recovery (close to 100%) for ozone.

Intra-model Variability: At 20 °C and 40% RH, units #406 and #409 had very high linear correlation between

each other ($R^2 > 0.99$, slope = 1.41, and intercept = - 1.41). Low ozone measurement variations were observed at low, medium, and high ozone concentrations. However, it is notable that at 5 °C and 15% and 65% RH and at high ozone concentrations, unit # 406's performance was significantly different than that of unit #409, reporting spiked values and a very high concentration of nearly 500 ppb (Figure 2.8).

a.
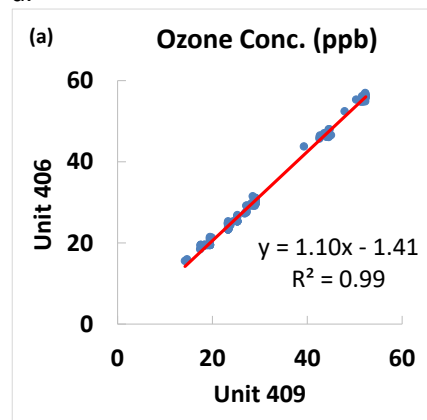
b.
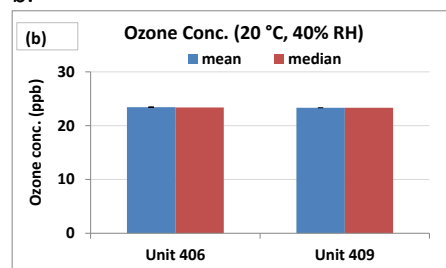
c.
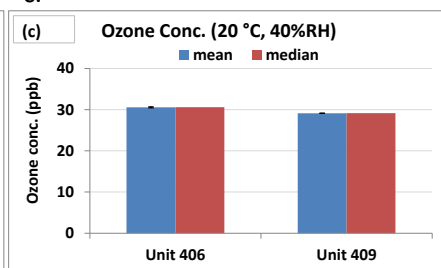
d.
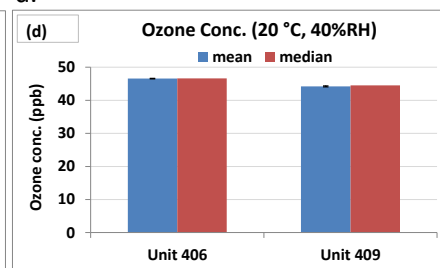
Figure 2.8. (a) Unit #406 vs unit #409; (b-d) intra-model variability at low, medium, and high ozone concentrations

Effect of NO_2 Interferent:

At 20° C and 40% RH, units #406 and #409 were evaluated for their responses to NO_2 concentrations. In the inner chamber, the NO_2 concentration was increased from 0 to 250 ppb, while the O_3 concentration was maintained at 0 ppb. As shown in Figure 2.9, units #406 and #409 did not respond to the increasing concentration of NO_2 and maintained their baseline concentrations of 15 ppb and 13 ppb, respectively.
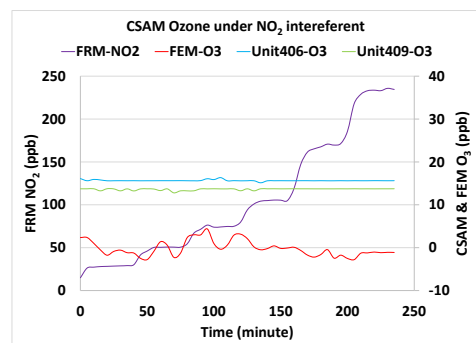
Figure 2.9. Effect of NO_2 interferent

2.3. QA summary for laboratory testing

The GRIMM monitor is serviced and calibrated by the manufacturer annually. The most recent service and calibration procedures are valid until January 2018. The CSAM evaluation experiments using the GRIMM were conducted between January 12 and January 27, 2017. The APS is serviced and calibrated every three years. As the instrument was first used on August 25, 2016, its calibration is valid until August 2019. The Serinus 10 ozone monitor is calibrated every six months (or more often). The most recent calibration was performed on February 1, 2017. The ozone evaluation experiments performed on the CSAM units were conducted between February 8 and February 16, 2017. The Serinus 40 oxides of nitrogen monitor is calibrated every six months (or more often). Its most recent calibration was performed on October 27, 2016. The NO_x interferent experiment was conducted on April 27, 2017.

Prior to the CSAM's laboratory testing, routine cleaning procedures were followed on the chamber's mixing duct. The mixing duct, shown in Figure 2.1, was fully disassembled and the various parts were flushed with clean air to remove deposited particles from the wall surfaces.

One deviation from the AQ-SPEC laboratory testing protocol methods was the period of time maintained each steady state. The AQ-SPEC testing procedures were developed for testing sensors with data averaged at 1 minute intervals. However, the CSAM unit was designed to report data at a 5-miuten time resolution. Therefore, the experiments were modified accordingly to ensure that a representative number of data points were collected for the CSAM PM and ozone sensors' evaluations. The concentration steady-state period in these experiments was maintained for a longer time period than was typically maintained with other sensor applications. For example, in the CSAM PM test, the steady-state period was increased from 150 min to 210 min, and in the CSAM ozone test, the steady-state period was increased from 40 to 150 minutes. A detailed description of the testing procedures used for testing the $PM_{2.5}$ and ozone sensors in the CSAM units is discussed in section 2.1.1. and section 2.1.2.

Due to the increased length of each experiment and demanding testing schedule, the sensor's climate susceptibility was evaluated using four representative weather (T and RH) combinations based on our objective judgement (Table 2.1.). Although the chamber has the potential to generate much lower or higher T and RH, we could not afford to conduct exhaustive testing of additional weather combinations. The four T/RH combinations were evaluated at low, medium, and high pollutant concentrations for a total of 12 experiments. In routine AQ-SPEC sensor testing, 27 experiments are conducted for variations in T/RH/pollutant concentrations.

Additionally, as discussed in the previous section, due to the chamber's size limitation, only two CSAM pods were evaluated rather than the three described in the original AQ-SPEC laboratory testing protocol.

In this study, the CSAM's response time was not tested because of the chamber's system design. After units #406 and #409 were installed inside the chamber, the chamber door was closed. The pollutant concentration was then gradually increased over 30 minutes (gas) or 90 minutes (aerosol) to the steady-state set-points. Therefore, the sensor's response time was not evaluated.

Finally, with respect to the PALAS artificial aerosol generation system, it is possible to approximate a broad range of PM mass concentrations. However, the chemical nature, the pre-defined size distribution, and the physical properties of the generated artificial aerosol cannot replicate the diverse profile of an urban ambient aerosol chemical composition.

3. Field Deployment

After the field and laboratory (chamber) testing activities were completed, ten CSAM pods were deployed throughout the South Coast Air Basin (SCAB) and the Salton Sea Air Basin (SSAB) in Southern California. The rolling deployment extended for three months, from January 11, 2017 to April 21, 2017. The pods were clustered in the three distinct geographical areas of Long Beach, Jurupa Valley, and Coachella Valley. In each of these areas, three locations were chosen as deployment sites. Each of these three distinct geographical areas exhibits its own unique air quality challenges. Specifically, the Long Beach area included a near-roadway location and two environmental justice locations that are affected by their proximity to localized sources that include refineries, railyards, roadways, and other industrial facilities. The close proximity to these sources in the Long Beach area causes a number of environmental justice problems in the region. Due to the common occurrence of daytime on-shore winds pushing ozone pre-cursors inland, ozone is not typically a significant concern for communities located near the shore.

The Jurupa Valley and Coachella Valley are both inland locations that are impacted by elevated ozone and particulate matter concentrations. In regard to the National Ambient Air Quality Standard (NAAQS) attainment, the SCAB was designated with a nonattainment ("extreme") status for its 2008 8-hour ozone standard (0.075 ppm) and designated with a nonattainment ("serious") status for the 2006 24-hour $PM_{2.5}$ standard (35 μg/m^3). The only two SCAQMD's stations with designated values over the 24-hour $PM_{2.5}$ NAAQS within the SCAB in the most recent three-year period (2013-2015) were the Riverside/Rubidoux and the Mira Loma Air Monitoring stations. In Riverside County in 2015, 76 days exceeded the 2015 8-jhur ozone standard (0.070 ppm).

The SSAB was designated with as nonattainment ("Severe-15") status for the 2008 8-hour ozone standard (0.075 ppm) and was designated as unclassifiable/attainment for the 2006 24-hour $PM_{2.5}$ standard (35 μg/m^3). The area was previously in non-attainment status for PM_{10} due to mechanically generated dust from agricultural activities, but it is expected to meet the current PM_{10} standard pending documentation submittal and subsequent U.S EPA approval. The Coachella Valley region had 58 days in 2015 that exceeded the 2015 8-hour ozone National Ambient Air Quality Standard (NAAQS) at 0.070 ppm (2016 SCAQMD AQMP). For these reasons, these locations were selected as deployment sites for the CSAM pods.

The field deployment from January 11 to April 21, 2017 experienced varied weather conditions among the three locations. The deployment period coincided with a record-setting rainy season in southern California. Long Beach experienced 23 rain days and 8 fog days for the duration of the study. The 23 rain days accounted for a total of 12.8 inches of rain. The temperature ranged from 3.9 to 30 °C with a mean of 15.6 °C. RH ranged from 6-100% with an average of 64% RH. The Jurupa Valley experienced 22 rain days and 4 fog days. The 22 rain days accounted for a total of 5.2 inches of rain. The temperature ranged from 0 to 33 °C with an average temperature of 15.6 °C. The RH ranged from 11-100% with an average RH of 63%. The Coachella Valle experienced 12 rain days and 1 fog day. The 12 rain days accounted for a total of 1.25 inches of rain. The temperature ranged from 1.1 to 37.8 °C with an average temperature of 18.3 °C. The RH ranged from 3-100% with an average of 46.6%. (Source: Weather Underground https://www.wunderground.com/history/).

3.1. Methods

The CSAM units were deployed in a rolling fashion at nine different locations. Seven of the pods were placed at existing SCAQMD air monitoring stations (AMS) including a duplicate unit at the Rubidoux AMS.

The three remaining CSAM pods were deployed at Ventura Transfer Company, Valley View Elementary School, and the Jurupa Area Recreation and Parks District (JARPD). Table 3.1 describes the nine field deployment locations, geographical coordinates (latitude and longitude), and the rationale for the site selection. Figure 3.1 shows the location of the sensors (colored dots) within the South Coast Air Basin (outlined in blue).

Table 3.1. CSAM Deployment Locations

Site Name	Pod #	Latitude/ Longitude	Address	Rationale
Hudson AMS	401	33°48'8.82"N 118°13'11.78"W	2425 Webster St. Long Beach, CA 90806	Near-road/High Concentration/EJ Area
710 NR AMS	402	33°51'34.73"N 118°12'2.64"W	5895 Long Beach Blvd. Long Beach, CA 90810	Near-road/High Concentration/EJ Area
Ventura Transfer Company	404	33°48'57.62"N 118°13'57.87"W	2418 E 223rd St. Carson, CA 90810	Near-source/High Concentration/EJ Area
Rubidoux AMS (Primary)	403	33°59'58.57"N 117°24'57.88"W	5888 Mission Blvd. Riverside, CA 92509	High Concentration
Rubidoux AMS (Collocated)	405	33°59'58.57"N 117°24'57.88"W	5888 Mission Blvd. Riverside, CA 92509	High Concentration
Jurupa Area Recreation and Parks District	407	34° 0'5.89"N 117°28'26.35"W	4810 Pedley Rd. Jurupa Valley, CA 92509	High Concentration
Mira Loma AMS	408	33°59'46.98"N 117°29'32.67"W	5130 Poinsettia Pl. Riverside, CA 92509	High Concentration
Saul Martinez AMS	406	33°34'19.27"N 116° 3'49.86"W	65705 Johnson St. Mecca, CA 92254	High Concentration/ EJ Area
Valley View Elementary School	409	33°40'1.08"N 116°10'39.07"W	85-270 Valley Rd. Coachella, CA 92236	High Concentration/ EJ Area
Indio AMS	410	33°42'30.70"N 116°12'55.57"W	46990 Jackson St. Indio, CA 92201	High Concentration
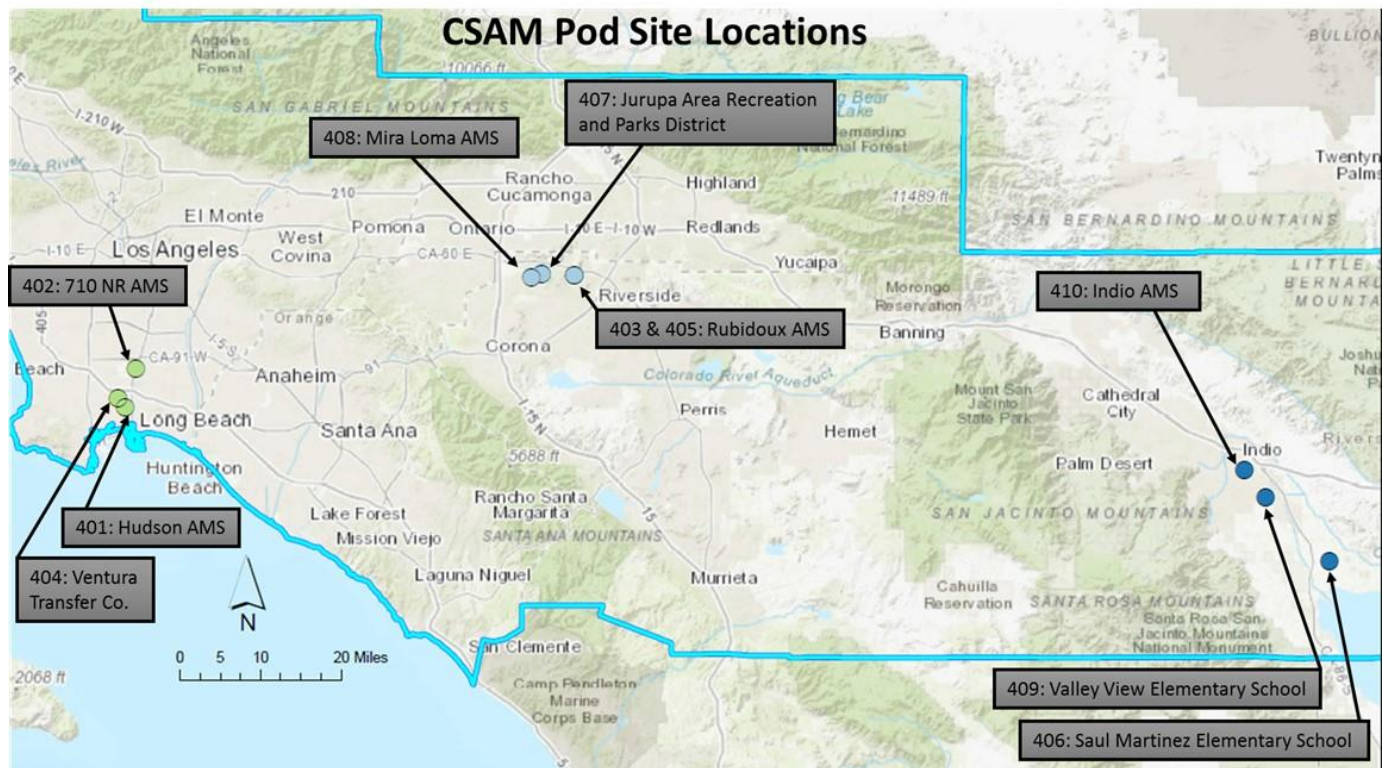
Figure 3.1. Sensor Pod Placement in the South Coast Air Basin

The rolling deployment was staggered to accommodate access to both the sites and the sensor pods. Table 3.2 shows the deployment dates and the total number of days and weeks each CSAM pod was deployed. CSAM PODs #406 and #409 were delayed in their initial deployment because they were undergoing AQ-SPEC laboratory evaluations. Unit #404 at Ventura Transfer Company experienced date and time stamp issues that resulted in an invalidation of all data collected after March 17, 2017.

Table 3.2 Deployment Location and Dates

Pod #	Site Name	Start Date	End Date	# of Days	# of Weeks
401	Hudson AMS	1/13/2017	4/19/2017	96	13.7
402	710 NR AMS	1/13/2017	4/15/2017	92	13.1
403	Rubidoux AMS (Primary)	1/11/2017	4/15/2017	94	13.4
404	Ventura Transfer Company*	1/17/2017	3/17/2017	59	8.4
405	Rubidoux AMS (Collocated)	1/11/2017	4/15/2017	94	13.4
406	Saul Martinez AMS**	2/22/2017	4/19/2017	56	8.0
407	Jurupa Area Rec and Parks District	1/20/2017	4/21/2017	91	13.0
408	Mira Loma AMS	1/11/2017	4/15/2017	94	13.4
409	Valley View Elementary**	2/22/2017	4/19/2017	56	8.0
410	Indio AMS	1/17/2017	4/19/2017	92	13.1

* Date/time issues starting March 27, 2017
** Delay for laboratory testing

After initial deployment of the CSAM pods, bi-weekly to monthly site visits were conducted to ensure proper operation, record the date/time, and copy the data from the SD card. Information on all site visits along with repairs and pod issues were recorded in the electronic CSAM Field Deployment log book. Figures 3.2– 3.9 below show the locations of CSAM pods #401, #402, #404, #406, #407, #408, #409, and #410.

Figure 3.2. CSAM Pod #401 at Hudson AMS

Figures 3.3. CSAM Pod #402 at 710 NR

Figures 3.4. CSAM Pod #404 at Ventura Transfer Company

Figures 3.5. CSAM Pod #406 at Saul Martinez Elementary School

Figures 3.6. CSAM Pod #407 at Jurupa Area Recreation and Parks District

Figures 3.7. CSAM Pod #408 at Mira Loma AMS

Figures 3.8. CSAM Pod #409 at Valley View Elementary School

Figure 3.9. CSAM Pod #410 at Indio AMS

3.2. Results

Overall, the CSAM units performed well for data recovery with the exception of the particulate matter data (Table 3.3). Several documented events accounted for reduced data recovery. CSAM #401 at Hudson AMS experienced a power outage due to a blown ground fault interrupter (GFI). The unit was without power for approximately three days (January 22, 2017 at 13:35 to January 25, 2017 at 12:40). CSAM #402 at the 710 NR AMS also stopped working for approximately 13 days (March 8, 2017 at 17:20 to March 21, 2017 at 9:20), during which time the unit displayed VOC rather than ozone concentrations and did not record any data. The unit resumed collecting valid data after a site visit and a manually powered on/off cycle. CSAM unit #405 did not display T and RH readings consistently during the co-location testing period and was designated to

the duplicate CSAM unit at Rubidoux AMS. CSAM unit #408 at Mira Loma AMS experienced a power failure due to heavy rains penetrating the sealed tote containing the power cord and 12V adaptor. The 12V adaptor shorted out internally and the unit was without power for approximately eight days (January 24, 2017 at 20:15 to February 1, 2017 at 16:40) while a new power adaptor was sourced and installed.

Table 3.3. Percent Data Recovery

Unit	Location	PM$_{2.5}$	Ozone	Temp	RH
401	Hudson AMS	92.6%	96.5%	94.0%	94.1%
402	710 NR AMS	85.9%	85.9%	85.9%	85.9%
403	Rubidoux AMS (Primary)	56.2%	99.6%	99.2%	99.2%
404	Ventura Transfer Company	43.9%	99.6%	99.6%	99.6%
405	Rubidoux AMS (Collocated)	66.4%	99.6%	43.1%	43.1%
406	Saul Martinez AMS	0.7%	99.6%	99.6%	99.6%
407	JARPD	80.0%	99.6%	97.3%	97.9%
408	Mira Loma AMS	20.9%	91.2%	91.1%	91.0%
409	Valley View Elementary	5.4%	99.6%	99.1%	99.1%
410	Indio AMS	58.9%	99.6%	99.1%	99.2%

The data recovery for T and RH exceeded 97% for all pods except for units #401, #402, #405, and #408. Data recovery for ozone was greater than 96% for all CSAM except units #402 and #408. The data recovery for PM$_{2.5}$ varied from 0.7% to 92%. The reduced data recovery for PM$_{2.5}$ was caused by a known error with the Alphasense OPC-N2. The OPC-N2 initiates a fault error after experiencing high RH. Once the error is initiated, the device reads 0.00 µg/m^3 or near zero until the device is manually powered on/off. The error is not consistent between devices, or even for the same device, and occurs randomly during high RH conditions. Unfortunately, this error could not be remedied with the software generated reset on the CSAM unit each night. The unit did not recover from this error unless it was manually powered off/on during a site visit. Thus, all values less than 1 µg/m^3 were considered invalid and removed from the data set. Both units that were tested in the chamber (#406 and #409) had extremely low data recovery after being deployed in the field (0.7 and 5.4%, respectively). The next lowest PM$_{2.5}$ data recovery (20%) was recorded for unit #408 at the Mira Loma AMS site. This drastic reduction in data recovery for the two units that underwent laboratory testing was likely to have been caused by the high PM loadings experienced during chamber testing, which negatively affected the operation of the optic system, thereby resulting in a substantial number of 5-minute PM$_{2.5}$ readings less than 1 µg/m^3.

3.2.1. Ambient PM$_{2.5}$

The CSAM pods utilize an Alphasense Ltd. OPC-N$_2$ particulate matter optical sensor. Overall, the sensors correlated well with one another during the co-location period with the exception of unit #401 (Table 3.4). As a result, the differences noted between among most of the sensors during this field deployment should be indicative of quantitate differences in PM$_{2.5}$ levels between different locations. The complexity of inter-comparing descriptive statistics is increased when there are issues with data recovery and reliable sensor performance. For example, CSAM pods #406 and #409 (deployed in the Coachella Valley) were characterized by extremely low data recovery (<10%) for PM$_{2.5}$ and, therefore, summary statistics from this pod were not included in our analysis. Because CSAM pod #401 did not correlate well with the reference instrumentation during the co-location testing, its data are also suspect in regard to providing reliable

ambient PM$_{2.5}$ data during this deployment.

**Table 3.4. CSAM PM$_{2.5}$ Summary Statistics**

PM$_{2.5}$ (µg/m^3)	Long Beach			Jurupa Valley				Coachella Valley		
	401	402	404	403	405	407	408	406	409	410
Min	1	2.55	1	1	1	1	1	1.4	1	1
Max	451.1	488.5	279.9	124.9	165.1	456.5	470.6	4.6	7.2	209.0
Median	5.1	15.9	5.0	4.4	7.9	5.2	10.3	1.9	1.7	3.6
Mean	14.6	24.3	7.4	9.2	14.5	11.5	20.2	2.3	2.3	6.5
SE	0.2	0.2	0.2	0.1	0.1	0.2	0.4	0.1	0.0	0.1
STDEV	36.6	29.8	14.8	13.7	19.3	22.7	31.4	0.8	1.3	12.8
Recovery (%)	96.2	85.9	43.9	56.2	66.4	80.0	20.9	0.7	5.4	58.9

Table 3.5. FEM Metone BAM PM$_{2.5}$ Summary Statistics

FEM PM (µg/m^3)	Rubidoux	MLVB
Min	0.0	0.0
Max	47	61
Median	9	11
Mean	10.6	12.6
STDEV	8.0	7.9
SE	0.17	0.17
Recovery (%)	93.2	92.7

Long Beach

The three units deployed in Long Beach included CSAM pods #401, #402, and #404. The time series for these three units is shown in Figure 3.10. Unit #402 at the 710 NR AMS measured the highest mean concentration of PM$_{2.5}$ among all nine locations. In regard to the other two Long Beach sites, the mean concentration at the 710 NR AMS (24.2 µg/m^3) was more than three times the mean concentration of that observed at the Ventura Transfer Company (unit #404, 7.4 µg/m^3) and 1.5 times the mean concentration at Hudson AMS (unit #401, 14.6 µg/m^3). The 710 NR AMS is located in close proximity (~15 miles) to interstate 710, which is one of the primary goods movement corridor routes going inland from the marine ports.
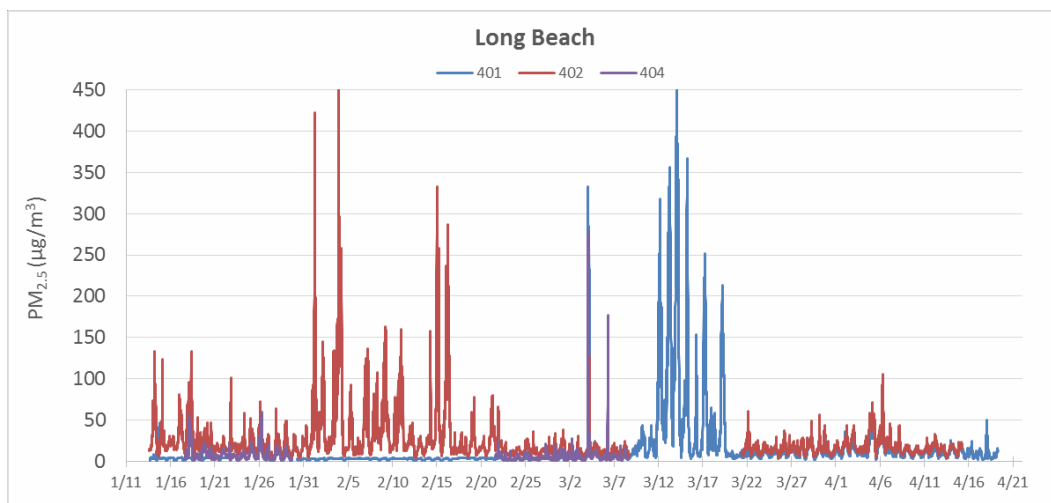
Figure 3.10 Long Beach PM$_{2.5}$

The measurements from unit #401 at Hudson AMS provide a good example of how to manage questionable sensor data. First, unit #401 did not perform well during the co-location period. Moreover, the time series for the Hudson AMS unit included time periods when sensor response was characterized by different levels of data quality, as illustrated in Figure 3.11 using a colored scaled from green (trustworthy-normal response) to orange (suspect-high readings) to red (not-trustworthy-no response/flat line). From January 13, 2017 to March 2, 2017, the sensor reported PM$_{2.5}$ that were consistently at around 3 μg/m^3, which is interesting for its closeness to the mean of the co-location period (3.2 μg/m^3; see co-location testing in Chapter 1 above). Between March 2, 2017 and March 21, 2017, the same sensor reported high PM concentrations. Unfortunately, due to data recovery issues with the other two sensors in the Long Beach region during this specific period, the results cannot be confirmed to be representative of the Long Beach area. From March 22, 2017 to April 19, 2017, the sensor indicated changes in PM and tracked very closely to unit #402 at the 710 NR AMS (see the time series in Figure 3.12). This is a good example of how data from one sensor can be validated by using that from another unit when the two devices are within a reasonable proximity from each another. Building this type of logic and capability into a real-time cloud-based application to validate and display sensor data is important in the evolution of low-cost air quality sensor technology and applications.
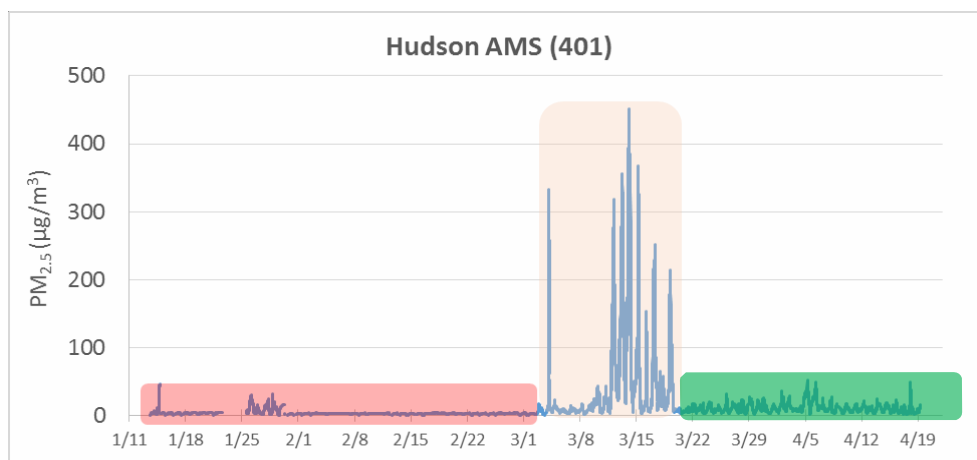

Figure 3.11. Hudson AMS time series
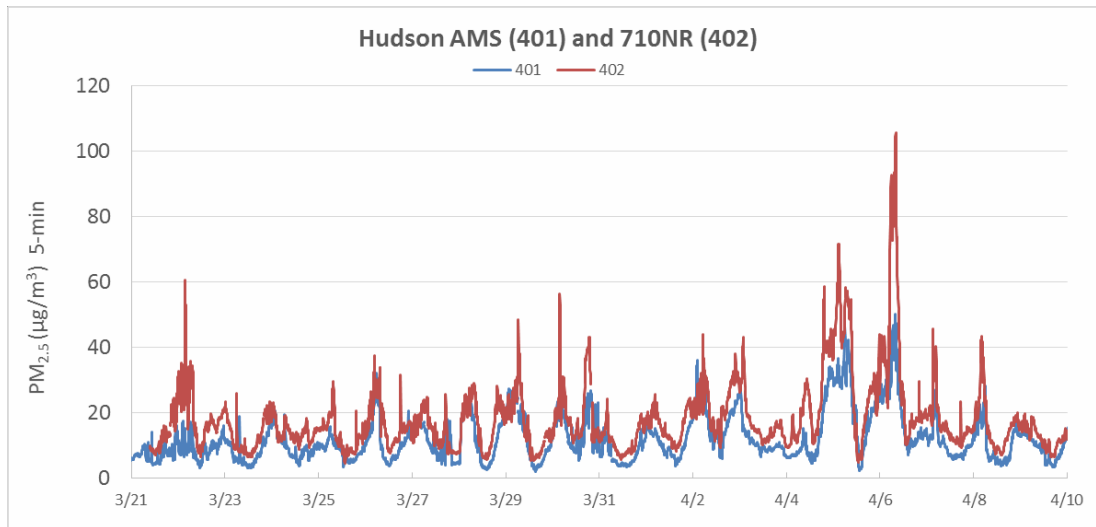
**Figure 3.12. Hudson AMS and 710 NR AMS**

Jurupa Valley

Four CSAM units were deployed in the Rubidoux area south of State Route (SR) 60 and west of Interstate 15. The three locations included the Rubidoux AMS, where unit #403 and #405 (co-located units) were deployed, Mira Loma AMS, where unit #408 was installed, and Jurupa Area Recreation and Parks District (JARPD,) where unit #407 was operated. The three locations in the Jurupa Valley are relatively close to one another, with a maximum distance of 5.4 miles separating the Rubidoux and Mira Loma AMS. The Mira Loma AMS and JARPD are 1.3 miles apart, with a railway and a four-lane roadway between them. These two-lane sources could have a direct impact on either location dependent of wind direction. The 24-ouhr mean concentrations at these four locations are shown in Figure 3.13.
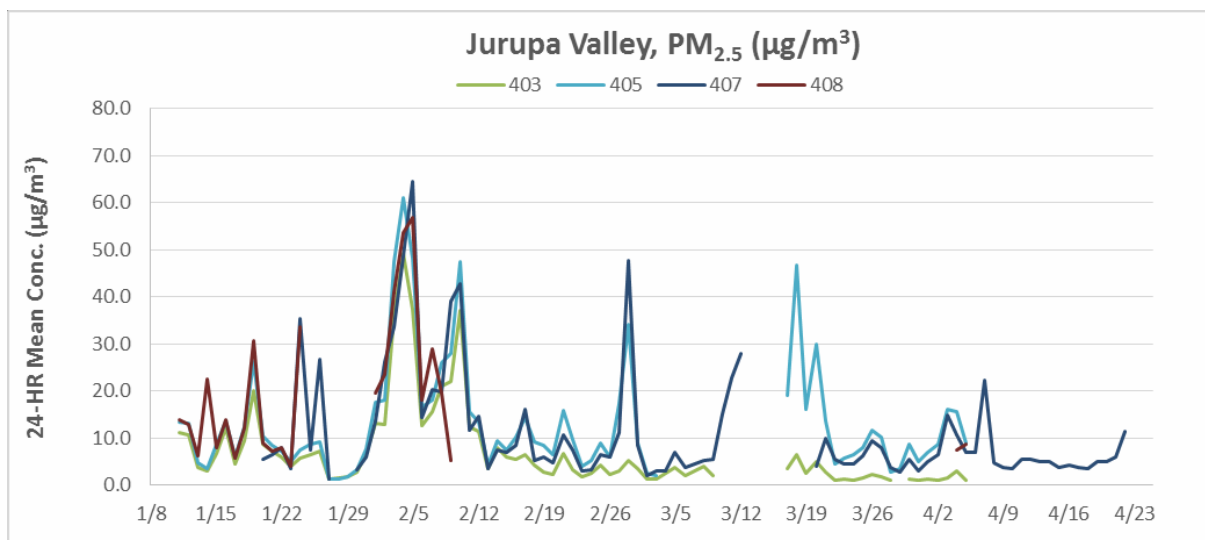
Figure 3.13. Jurupa Valley PM$_{2.5}$ 24-hour time series

Considering the 24-hour averages for the Jurupa Valley, the CSAM units show multiple days with 24-hour PM$_{2.5}$ concentrations above the NAAQS of 35 µg/m^3. These high particulate 24-hr average concentrations that exceed the NAAQS requirements warrant additional scrutiny with higher-cost FEM instrumentation. Both the Rubidoux and Mira Loma AMS are equipped with FEM BAM PM$_{2.5}$ instruments. The FEM BAM at Rubidoux does not indicate a single 24-hour average that exceeds the NAAQS of 35 µg/m^3 (Figure 3.14).

The overestimation of PM concentrations in a community deployment setting may raise unfounded concerns over exposure levels in the region.
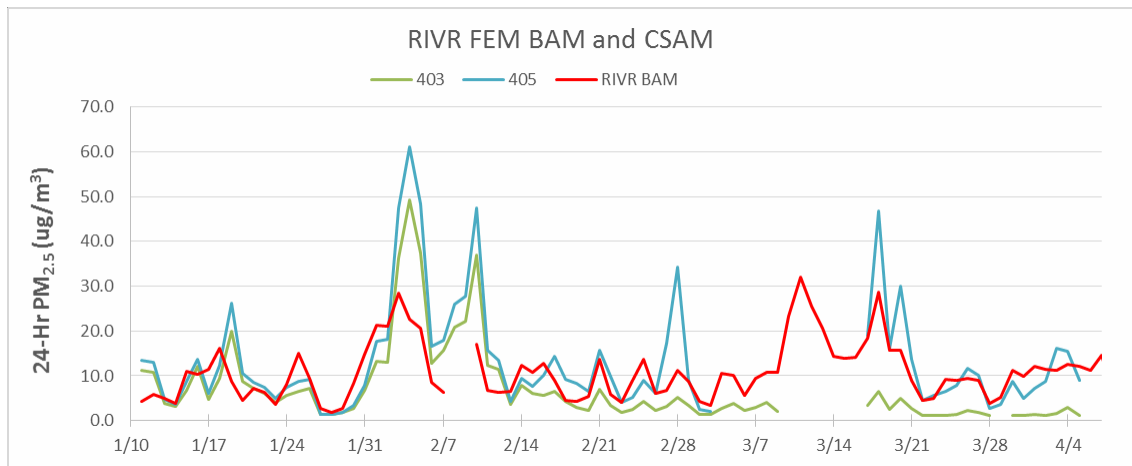

Figure 3.14. Rubidoux FEM BAM and CSAM PM$_{2.5}$ time series

The Mira Loma AMS is within 1.3 miles of the JARPD location, where unit #407 indicated several days that exceeded the NAAQS for PM$_{2.5}$, whereas the FEM BAM unit at the Mira Loma AMS did not indicate any exceedances throughout the study, as shown in Figure 3.15.
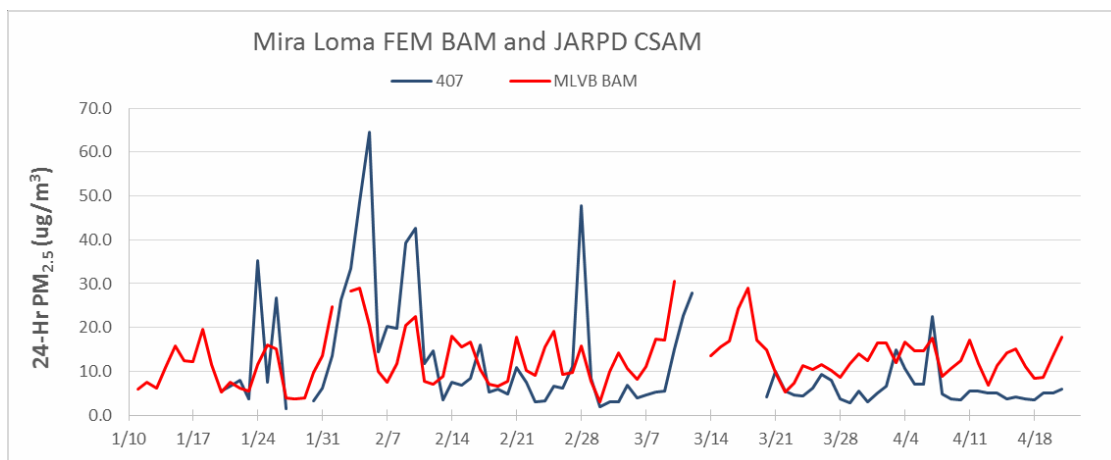

Figure 3. 15. Mira Loma FEM BAM and JARPD CSAM 24-hour PM$_{2.5}$ Data

The two units co-located at the Rubidoux AMS tracked well with one another and showed a correlation (R^2) value of 0.62. The mean PM$_{2.5}$ concentration for unit #403 was 9.2 μg/m^3, whereas the mean for #405 was higher, at 14.5 μg/m^3. The regressions, shown in Figure 3.17, between units #403 and #405 demonstrate linearity between the two sensors, with a notable time period during which #405 recorded higher concentrations than #403. Upon further examination of the time series data, it appeared that unit #403 had begun to underestimate #405 after February 26, 2017. Upon filtering the data to include only values recorded before February 26, 2017, the R^2 between the two units increased from 0.64 to 0.97. It is likely that the OPC-N2 in the CSAM #403 pod was losing sensitivity to changes in PM concentrations over time.
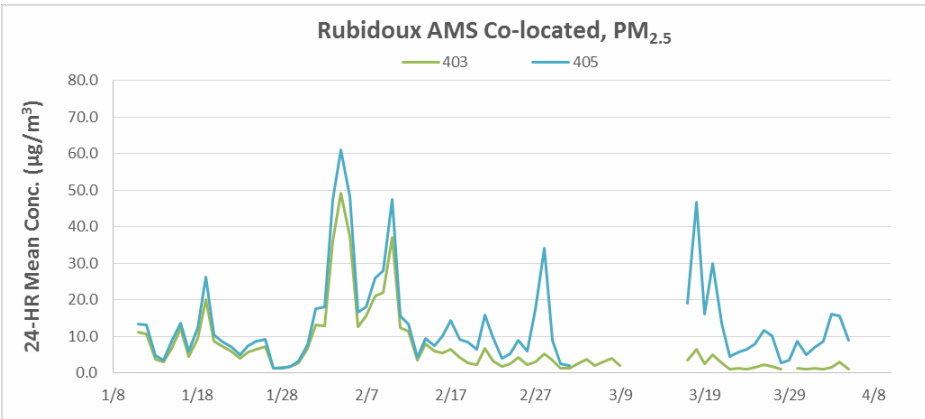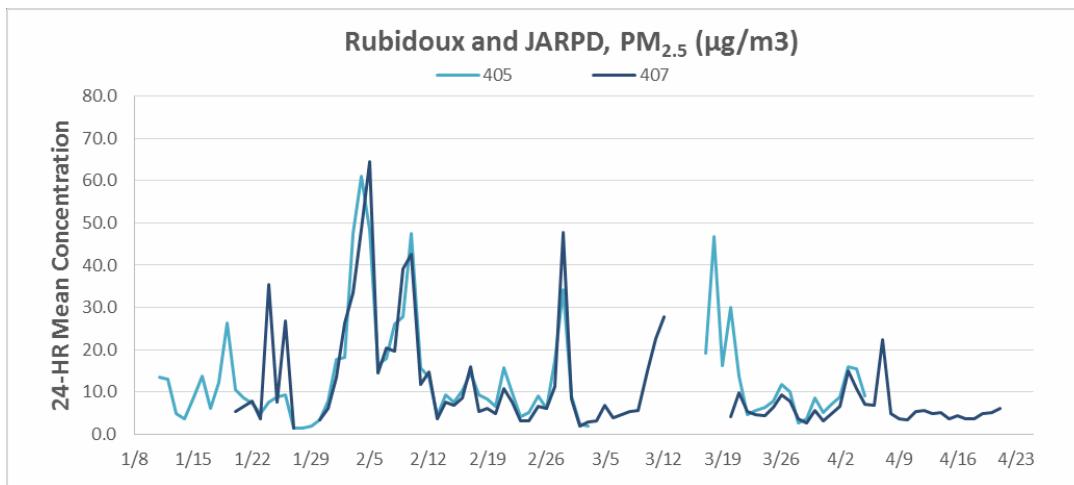
Figure 3.16. Rubidoux Co-located CSAM time series
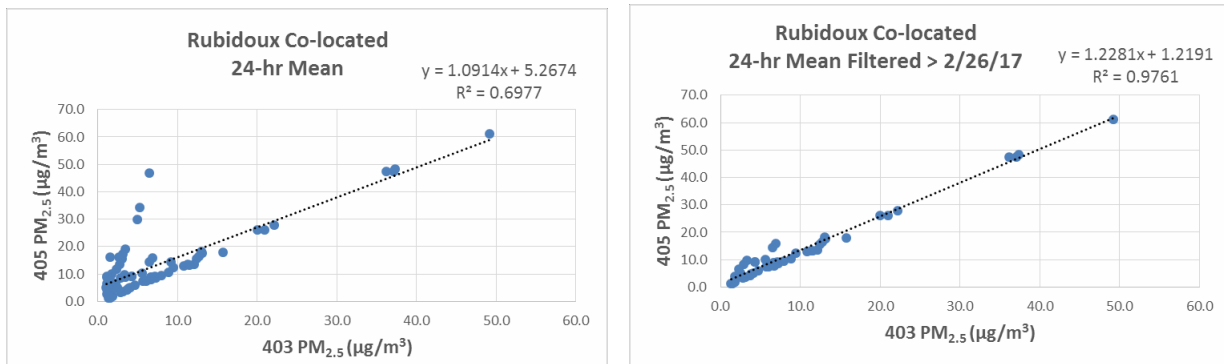
Figure 3.17. Rubidoux Co-Location Scatterplots Full Time Period (left) and Filtered for January 11, 2017 to February 11, 2017 (right)

CSAM unit #408 at the Mira Loma AMS had the highest mean concentration among all the Jurupa Valley locations. However, the data recovery for this device was low at 20.9%. A meaningful inter-comparison among unit #408 and the units at other locations in Jurupa Valley is difficult to attain due to the low data recovery. CSAM #405 (Rubidoux) and #407 (JARPD) do track closely with each other, indicating that the two locations are probably impacted by similar PM$_{2.5}$ sources (Figure 3.18). The two locations are separated by residential areas, open space, and some light industrial complexes.

Figure 3.18. Time series of Rubidoux Co-located CSAM Pods #405 and #407

Coachella Valley

The three units deployed in the Coachella Valley include CSAM #406 at Saul Martinez AMS, CSAM #409 at Valley View Elementary School, and CSAM #410 at the Indio AMS. The deployment date for units #406 and #409 was delayed until February 22, 2017 due to unfinished laboratory testing activities, and the Indio AMS was deployed earlier, on January 17, 2017. The data recovery for CSAMs #406 and #409 for $PM_{2.5}$ was low, at 0.7% and 5.4%, respectively (the Alphasense OPC-N_2 sensor readings were consistently below 1 $\mu g/m^3$). The time series for the Coachella Valley region is represented by the measurements provided by the CSAM #410, deployed at the Indio AMS (Figure 3.19).
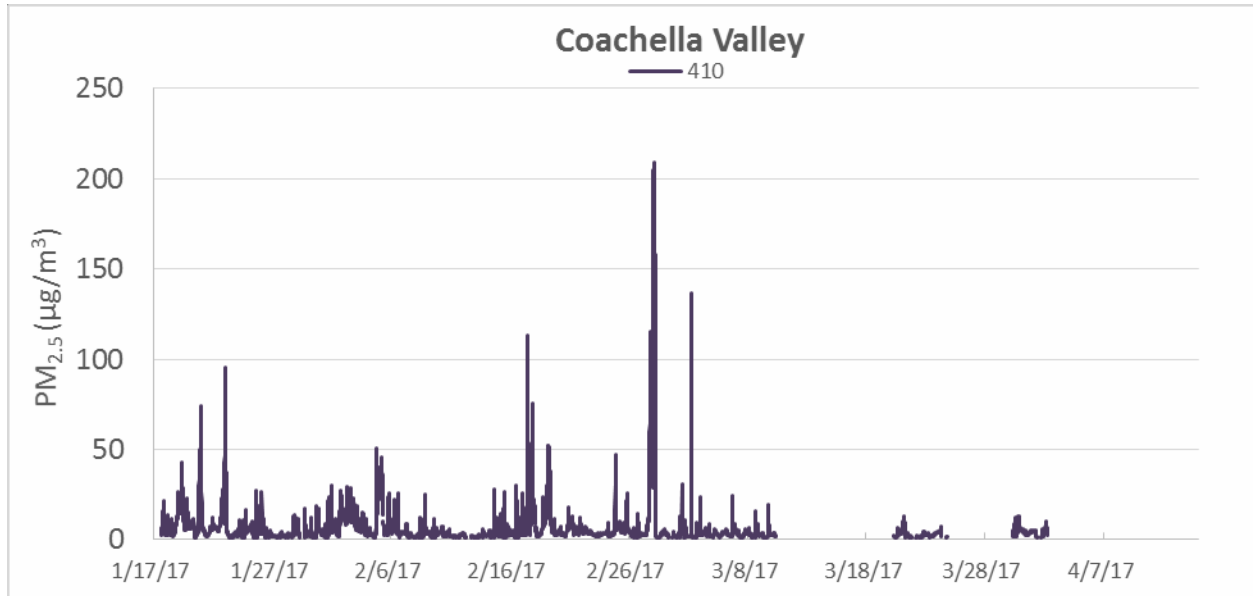
Figure 3.19. Time series of CSAM Pod #410 in Coachella Valley

3.2.2. Ambient Ozone
The CSAM pods utilize an Aeroqual metal oxide ozone sensor. During the co-location testing at the Rubidoux AMS, the ozone sensors correlated well with the reference instrumentation, with low intra- model variability. As a result, differences among the sensors should be indicative of the quantitative differences among the various locations. The Data recovery for the CSAM ozone sensor was high (>85%) during the field deployment. Table 3.6 shows the summary statistics for ozone from the ten CSAM units.

Table 3.6. CSAM Ozone Summary Statistics

Ozone (ppb)	Long Beach			Jurupa Valley				Coachella Valley		
	401	**402**	**404**	**403**	**405**	**407**	**408**	**406**	**409**	**410**
Min	0.1	6.0	0.2	5.4	0.2	7.9	2.6	13.3	9.9	5.1
Max	80.3	36.0	45.9	50.8	63.2	50.1	82.5	38.8	36.9	57.3
Median	25.6	14.7	17.3	17.5	22.4	23.5	27.4	27.3	23.7	33.0
Mean	23.8	15.2	17.8	20.2	21.4	23.7	27.0	26.9	23.6	30.4
STDEV	14.16	4.32	9.08	7.69	14.36	8.19	9.98	4.78	5.80	10.82
SE	0.09	0.03	0.07	0.05	0.09	0.05	0.06	0.04	0.05	0.07
Recovery (%)	96.5	85.9	99.6	99.6	99.6	99.6	99.6	91.2	99.6	99.6

The CSAM pods that were located at SCAQMD air monitoring stations equipped with ozone analyzers are the pods at Hudson, Mira Loma, Rubidoux, and Indio. The summary statistics for the FEM ozone analyzers can be found in Table 3.7.

Table 3.7. FEM Air Monitoring Station Ozone Summary Statistics

FEM Ozone (ppb)	Hudson	MLVB	Rubidoux	Indio
Min	0.0	0.2	0.0	0.1
Max	94.8	102.0	101.6	133.0
Median	25.5	26.5	27.9	40.9
Mean	23.8	27.3	27.6	38.8
STDEV	16.0	20.6	20.4	18.5
SE	0.10	0.13	0.12	0.11
Recovery (%)	91.7	93.8	94.5	98.5

The overall results are unsurprising, as they indicate a well-known diurnal variation of O_3 in the air basin related to the photochemical production of O_3. The diurnal variability is characterized by high concentrations during daytime hours and lower concentrations at nighttime and early in the morning. Throughout the study, the mean concentration for the Long Beach sites was 18.9 ppb. The mean values in Jurupa Valley and Coachella Valley were 23.1 and 27.0 ppb, respectively. Although the mean O_3 concentration in the Coachella Valley was higher than that measured in the Jurupa Valley, the maximum 5-minute average readings were recorded at the Jurupa Valley site.
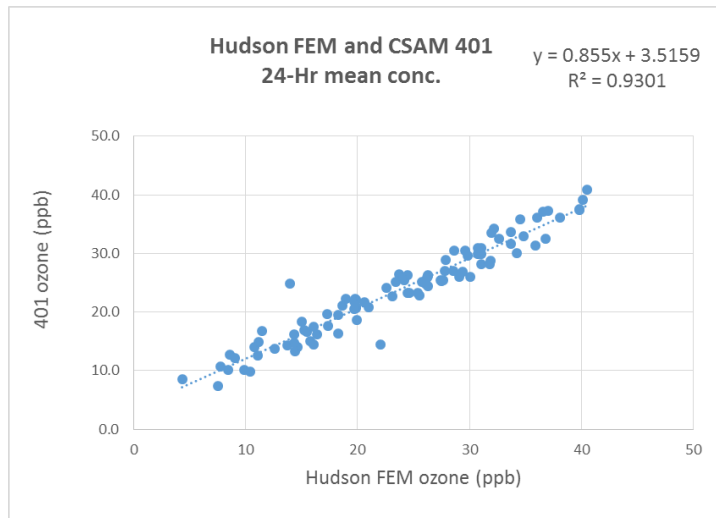
Long Beach
The lowest mean concentration for ozone among the Long Beach locations was at the near roadway site along the I-710. The I-710 near-roadway location is considered an ozone sink, with localized emissions of NO scavenging O_3. The time series for the three Long Beach locations are shown in Figure 3.22. The highest readings in this region were recorded by unit #401 at the Hudson AMS, with a mean concentration of 23.8 ppb. The summary statistics for unit #401 match well with the FEM ozone analyzer at Hudson AMS. When comparing the 24-hour mean concentrations between CSAM 401 and the FEM at Hudson, the sensor tracked the FEM ozone analyzer well, as shown in Figure 3.20.
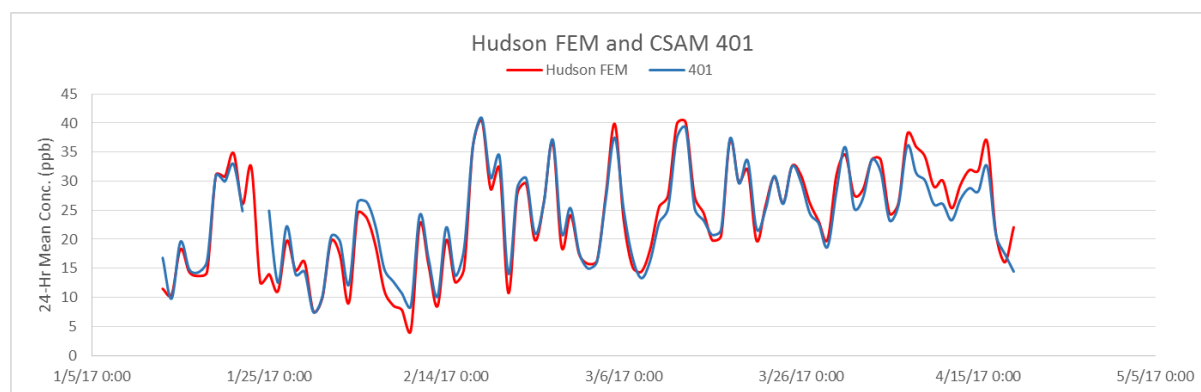

Figure 3.20. Hudson FEM and CSAM #401 time series

The scatterplot shown in Figure 3.21 between the FEM at Hudson and CSAM 401 indicates that the sensor performed well throughout the field deployment stage. The R^2 value was found to be 0.93 with a slope of 0.85.
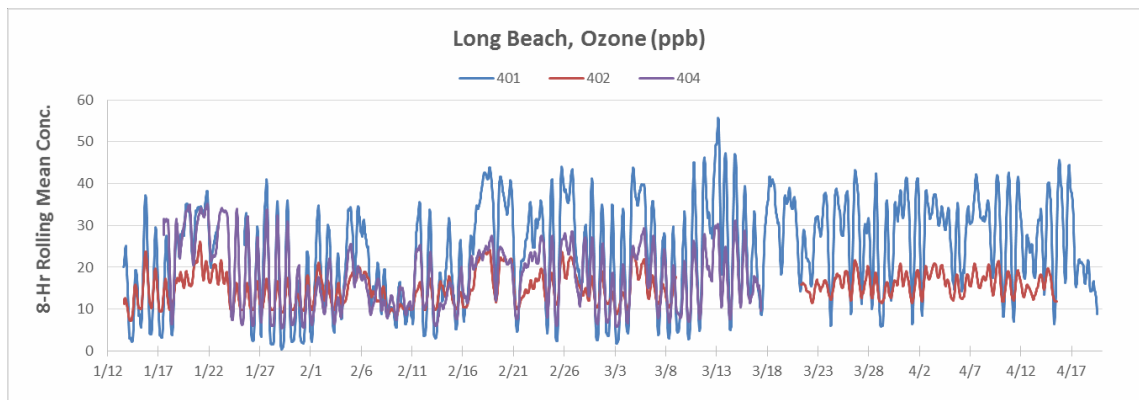
Figure 3.21. Hudson FEM and CSAM #401 scatterplot

For the entire duration of the study, the 8-hour ozone average level never exceeded the NAAQS (70 ppb) in the Long Beach area, as shown in Figure 3.23.
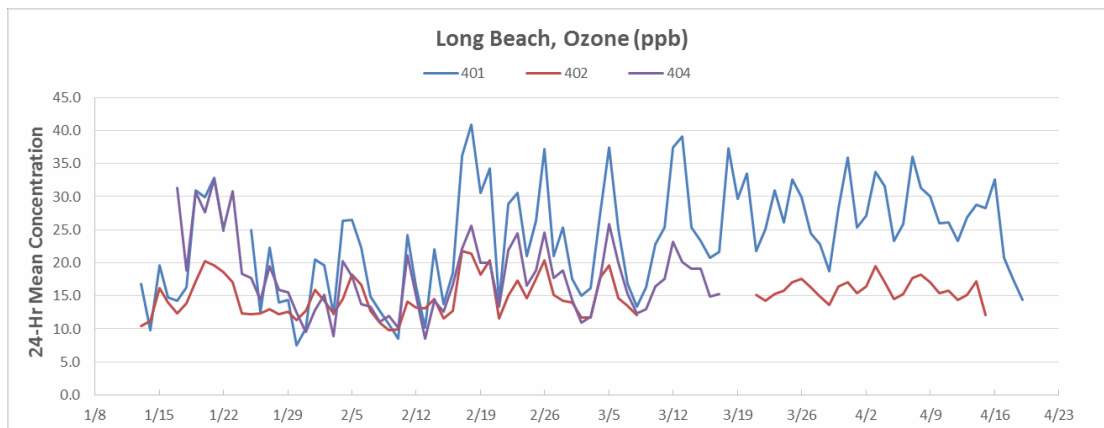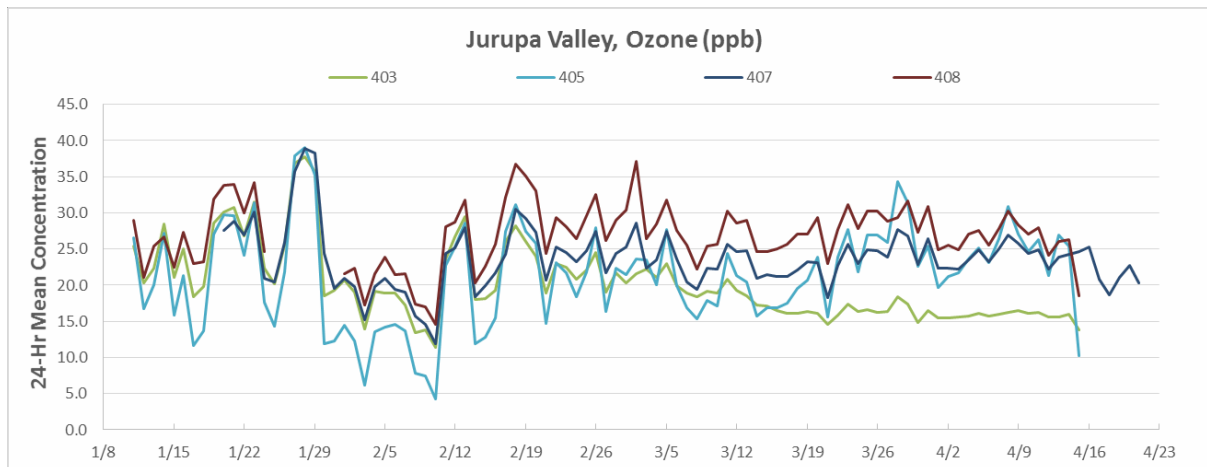

Figure 3.22. Long Beach Ozone 24-hour time series

**Figure 3.23. Long Beach Ozone 8-hour time series**

Jurupa Valley

The four CSAM pods (#403, #405, #407 and #408) deployed in the Jurupa Valley tracked well with one another when considering their 24-hour averages (Figure 3.24). The unit deployed at the Mira Loma AMS recorded the highest mean concentrations for the Jurupa Valley.

Figure 3.24. Jurupa Valley Ozone Concentrations, 24-hour Mean

For the duration of the study, the 8-hour average ozone level in the Jurupa Valley area did not exceed the NAAQS (70 ppb) as shown in Figure 3.25.
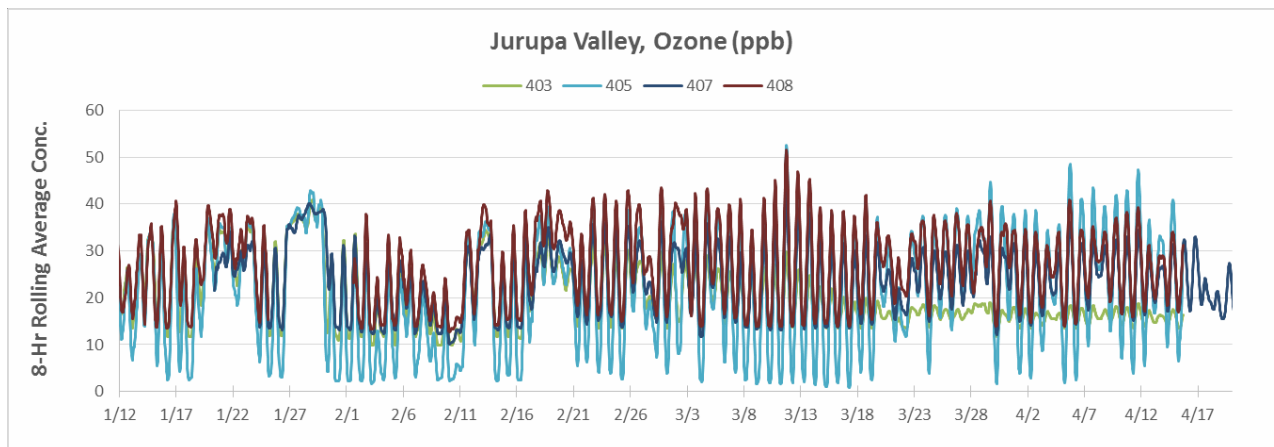
Figure 3.25. Jurupa Valley Ozone Time series, 8-hour average

CSAM units #403 and #405 were co-located at the Rubidoux AMS. As the study progressed, the CSAM #403 ozone sensor appeared to gradually lose sensitivity to changes in ozone concentrations. This gradual trend was observed as the study progressed and became more apparent beginning around February 26, 2017. Figure 3.26 displays the time series data of the two co-located ozone sensors and the changes over time. When comparing the two sensors, the R^2 value improved from 0.53 to 0.96, as shown in Figure 3.27.a-b, when filtering the data prior to February 26, 2017. The co-location time series and scatterplot for $PM_{2.5}$ (Figures 3.25 and 3.28) indicates a similar result, with an increase in R^2 values after filtering out data generated after February 26, 2017. The lessened performance of both the PM and O_3 sensors in CSAM #403 around the same time (February 26, 2017) indicates a potential systematic problem (i.e., a power supply or board issue) rather than an individual sensor problem.

61
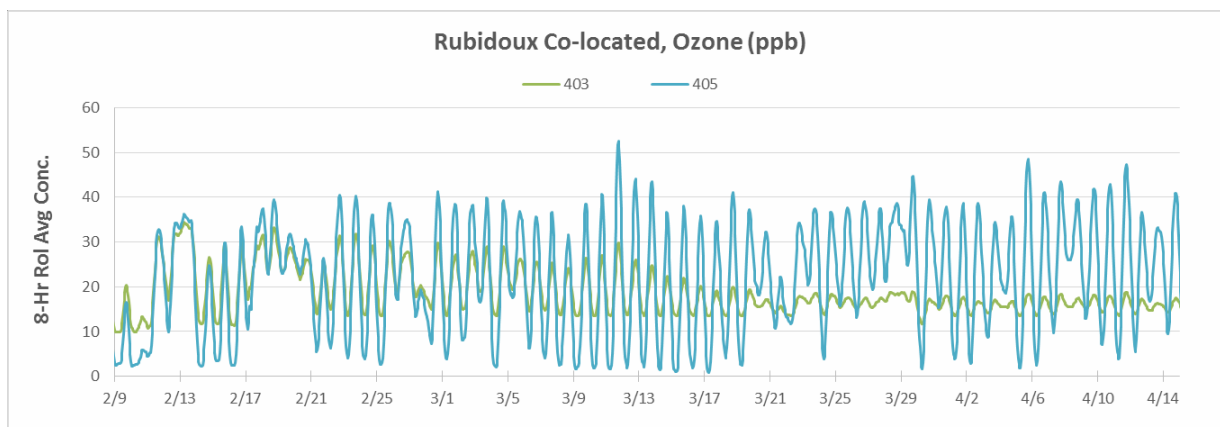
Figure 3.26. Rubidoux Co-Location Ozone time series, 8-hour average

a.

b.
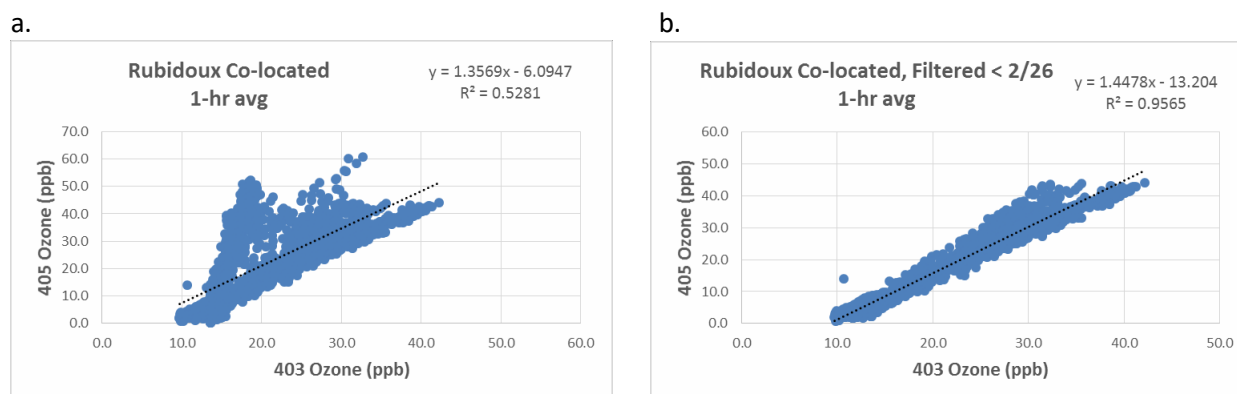
Figure 3.27. Rubidoux Co-Location Correlation Plots: a. Full time period, b. Filtered time to include January 1, 2017 to February 26, 2017

The FRM ozone instrument at the Rubidoux station was found to correlate well with CSAM #405, with an $R^2 = 0.94$, and not to correlate well with CSAM #403 ($R^2=0.35$), as shown in Figure 3.28.
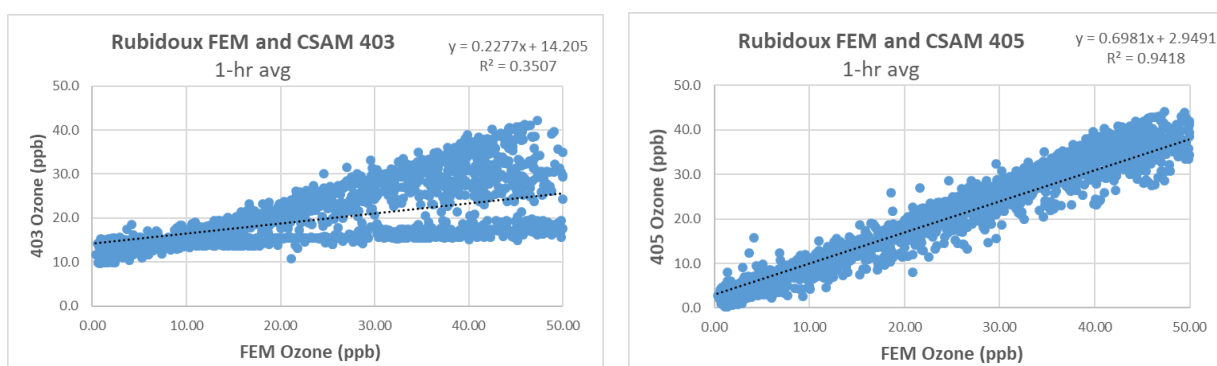

**Figure 3.28. Rubidoux FRM ozone and CSAM #403 and #405 comparison**

Coachella Valley
The Coachella Valley is in a desert region. Within the time frame of this study, the Indio AMS location indicated the highest 24-hour mean concentrations for ozone among the three Coachella Valley locations. The Coachella Valley's evening ozone readings rarely dropped below 10 ppb (Figure 3.29). This may be because the land in the region is primarily devoted to agricultural use and does not have significant

NO emissions from evening rush hour traffic that would titrate the ozone in the evening hours. During   the study period, the CSAM units did not report ozone concentrations that exceeded the NAAQS' 8-hour ozone standard of 70 ppb (Figure 3.30).
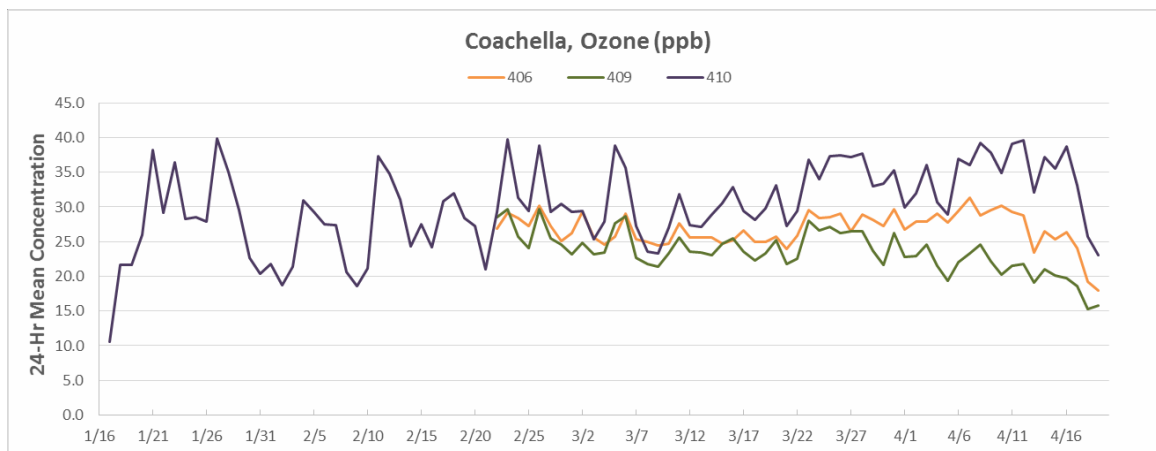

**Figure 3.29. Coachella Valley Ozone, 24-hour Mean**
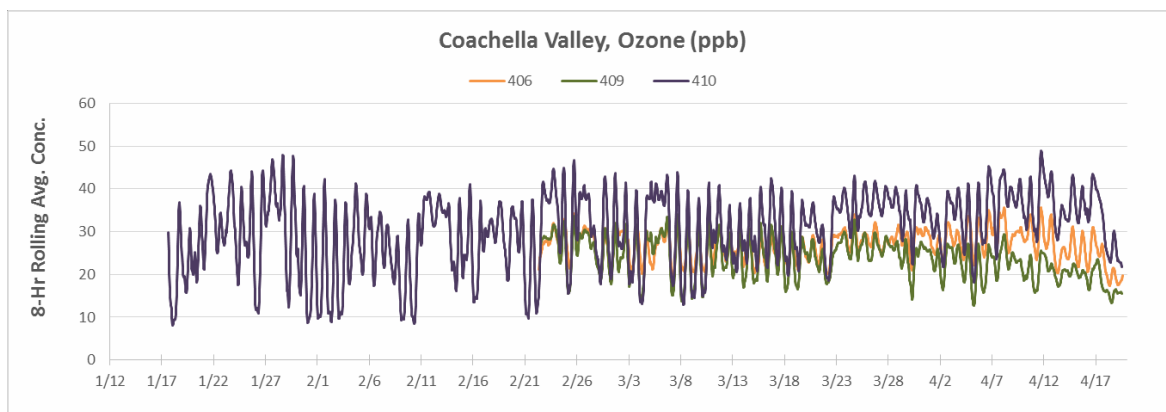
Figure 3.30. Coachella Valley Ozone, 8-hour rolling average

The Indio AMS employs an FEM instrument to measure ozone. Upon a comparison between the Indio AMS reference instrumentation and the CSAM #410, reduced sensor performance was observed over time, as indicated in the time series (Figure 3.31). The scatterplot between the FRM at Indio and CSAM #410 is shown in Figure 3.32.
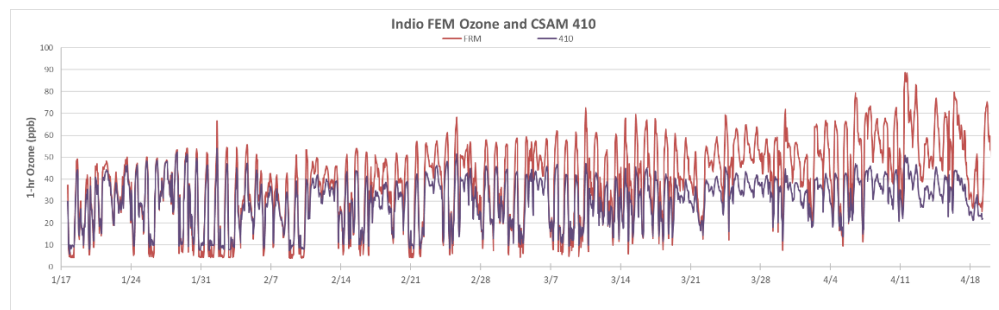
Figure 3.31. Indio FRM ozone and CSAM #410 time series
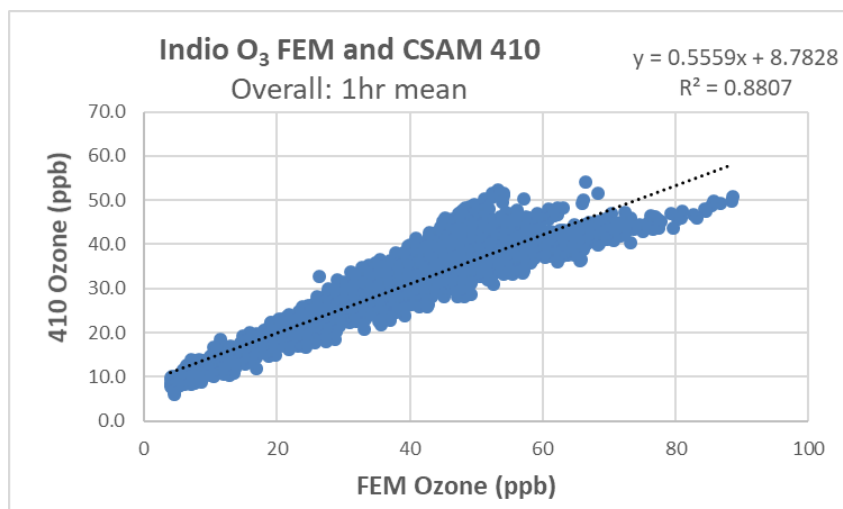
**Figure 3.32. Indio AMS FRM and CSAM #410 scatterplot**

The time series and scatterplot comparing CSAM #410 with the Indio AMS FRM for ozone indicates that the sensor lost sensitivity to ozone over time. Table 3.8 shows the changes in slope, intercept, and R^2 value between the FRM and CSAM #410 ozone sensor by examining the deployment month by month. Over four months, the slope between the reference and the CSAM was reduced from 0.84 in January to 0.47 in April, whereas the intercept increased from 4.1 to 10.1 over the same time period. The R^2 stayed consistent over the four months and was greater than 0.95.

Table 3.8. FRM and CSAM #410 ozone sensor regression parameters by month

Time period	Slope	Intercept	R^2
Overall	0.56	8.8	0.88
January*	0.84	4.1	0.98
February	0.69	5.4	0.97
March	0.57	7.7	0.95
April*	0.47	10.1	0.97

*CSAM not deployed entire month

When using the Indio AMS as a reference for the Coachella Valley region, it may appear that all three of the CSAM ozone sensors were losing sensitivity to ozone over time in an examination of the FRM ozone readings with the three monitors on a 24-hour average (Figure 3.33). However, such losses in responsiveness over time are to be expected with this type of sensor. CSAM units #406 and #409, which underwent laboratory testing at relatively high challenge concentrations, might have also experienced an impact on their lifespans. An underestimation of ozone concentrations in the region by low-cost sensors deployed in a community-based monitoring program will not provide accurate data without correction factors. The underestimation may miss potential days in which the NAAQS would have been exceeded if the sensor had been performing correctly.
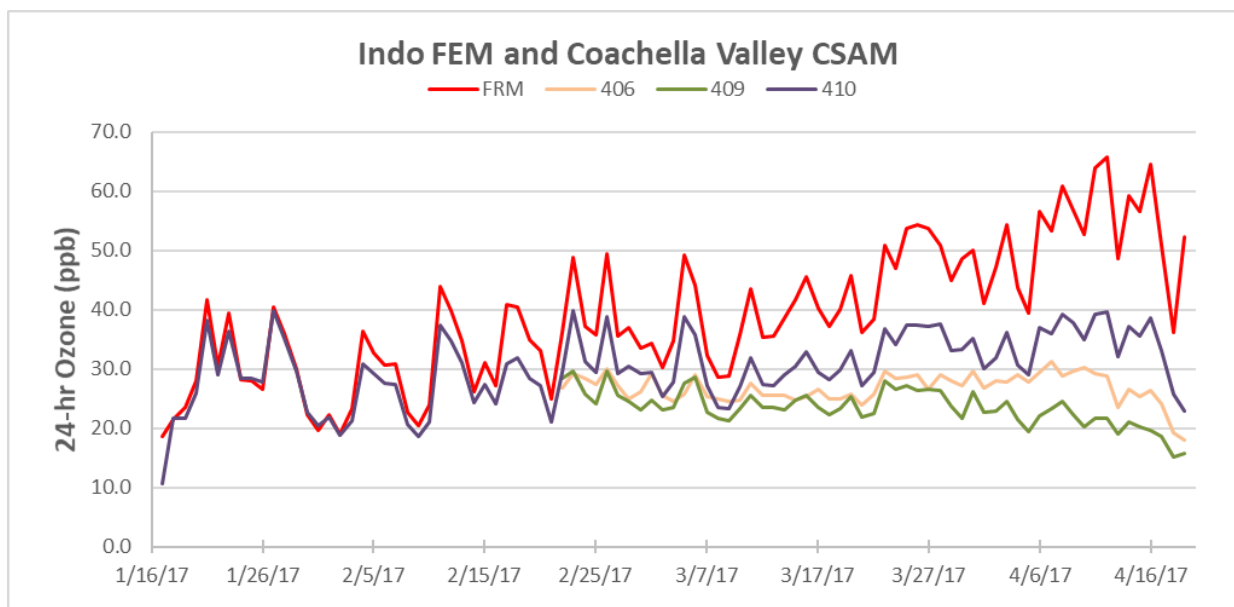
Figure 3.33. Time series of FRM and CSAM Pods #406, #409 and #410 (24-hour average)

### 3.2.3. Temperature and RH influences

Environmental factors, such as temperature and RH, may affect the measurement of air pollutants by low-cost sensing technology. Optical particle counters that measure scattered light from particles to count, size, and calculate a particulate mass value are susceptible to moisture affects. Particles containing high RH or moisture affect the light- scattering properties of measured aerosol; consequently, costly optical particulate counters typically include a dryer or heater to maintain the RH within a desired range for measurement. An estimation for dew point (DP), which includes both temperature and RH, provides the opportunity to determine if there is a combined effect of temperature and RH on the sensor's response. An approximation for the DP temperature suggested by Lawrence (2005) is useful for moist air (RH > 50%) and valuable for examining the dew point temperature with respect to the OPC measurement response, as the concern for measurement influences with RH < 50% is low.

$$D_p \approx t - \left(\frac{100 - RH}{5}\right)$$

The measurement of $PM_{2.5}$ and ozone are plotted against temperature, RH, and dew point. Temperature, RH, and dew point do not affect the measurement of ozone. The following three plots represent the Indio CSAM #410's ozone response with the three environmental parameters. These plots are characteristic of the ten CSAM pods for ozone. Figure 3.34 indicates ozone response to temperature: as temperature rises, the ozone values rise as well. This trend is expected, as sunlight is necessary for the production of ozone. As humidity decreases, the ozone values increase, as shown in Figure 3.35. This trend also is expected, as ozone concentrations peak during the early afternoon hours, which is also a time period characteristic of low humidity. No trend or correlation is evident between ozone and the approximation for dew point, as shown in Figure 3.36.
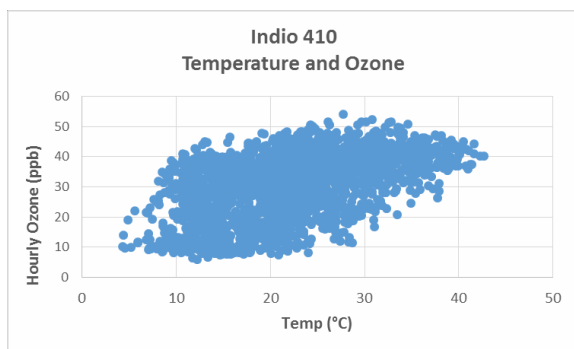
Figure 3.34. Indio 410 Temperature vs. Ozone
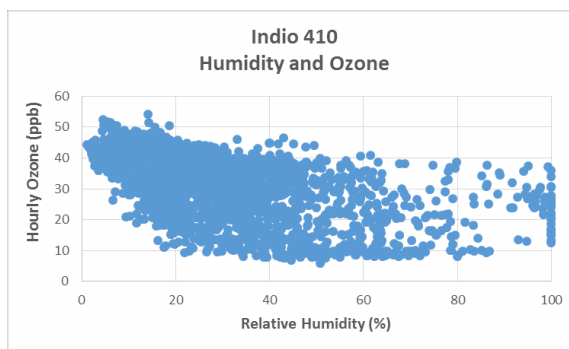

Figure 3.35. Indio 410 Humidity vs. Ozone
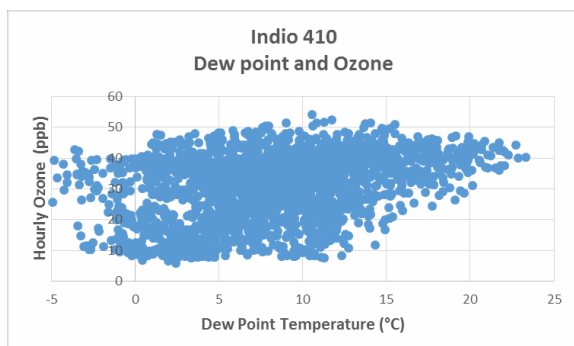
**Figure 3.36. Indio 410 Dew Point and Ozone**

The $PM_{2.5}$ mass concentrations of the OPC sensor were plotted against the three environmental factors of temperature, RH, and dew point (Figures 3.37-3.45). Plots for one sensor from each of the three major geographical areas (Long Beach, Jurupa Valley, and Coachella Valley) are shown below. The plot for CSAM #401 at Hudson AMS in the Long Beach region indicates that high PM concentrations are associated with high RH values. When reviewing the dew point, which includes both temperature and RH, a more refined peak than the T/RH plots is observed, with a peak centered in the 11-13 $^{\circ}$C range for high PM concentrations.
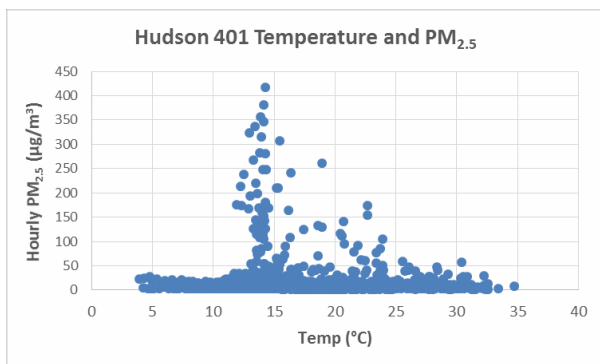

Figure 3.37 Hudson 401 Temp and PM
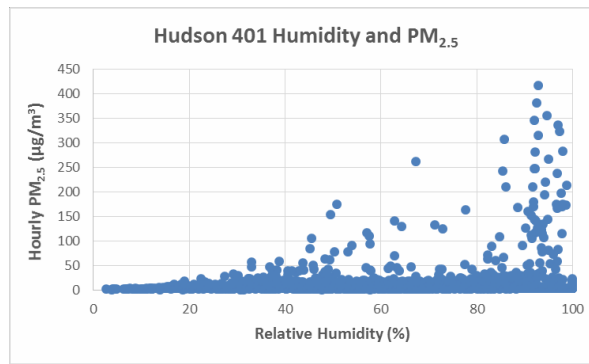
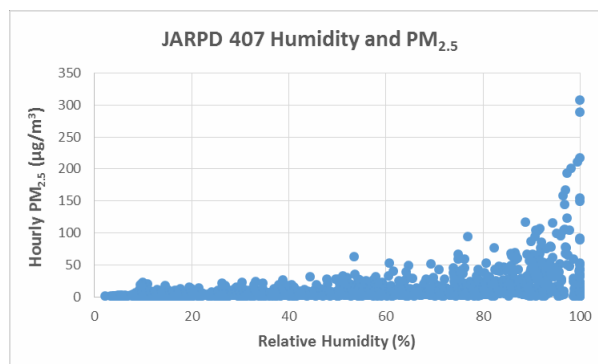**Figure 3.38. Hudson 401 Humidity and PM**
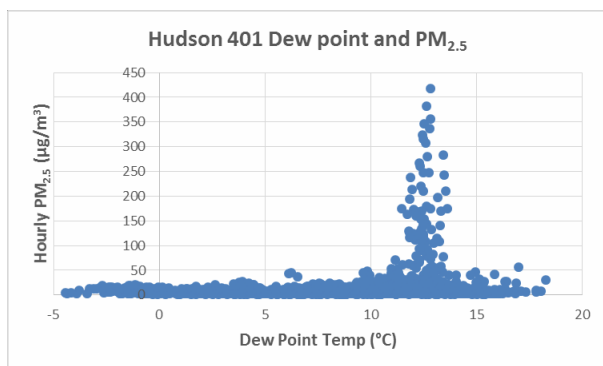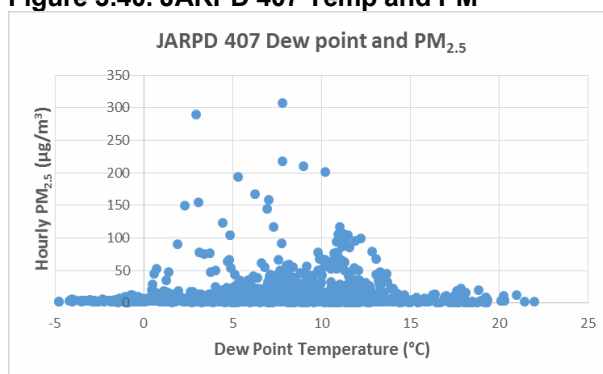
Figure 3.39. Hudson 401 Dew Point and PM

The plot for CSAM #407 in the Jurupa Valley region indicates that high PM concentrations are associated with high RH values and low temperatures. The comparison between temperature and dew point in the Jurupa Valley indicates more scatter than the Long Beach sites. This may be because the inland valleys experience more extreme weather conditions than the ocean communities, where conditions are tempered by the ocean's influence.
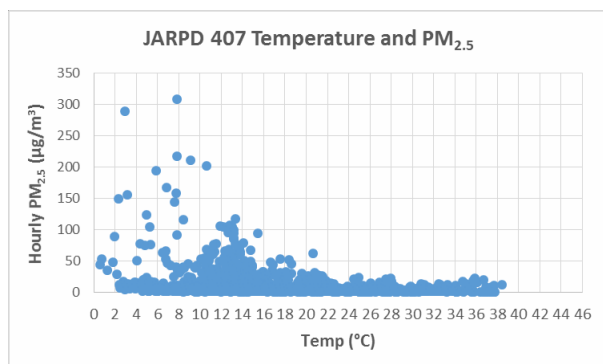

Figure 3.40. JARPD 407 Temp and PM

Figure 3.41. JARPD 407 Humidity and PM

Figure 3.42. JARPD Dew Point and PM

The plot for CSAM #410 at the Indio AMS in the Coachella Valley region indicates that high PM concentrations are associated with high RH values. The high RH events coincided with temperatures around 11.5 °C, which also indicated high PM values. As a result, Figure 4.45 represents the dew point in comparison to the PM concentrations and indicates a resolved peak around 11.5 °C. This is similar to the values observed for the Long Beach area.
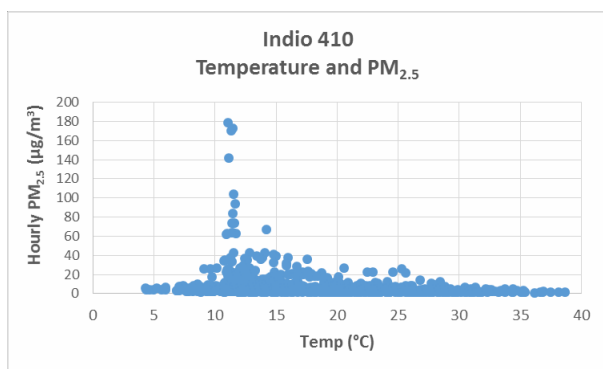
Figure 3.43. Indio 410 Temp and PM
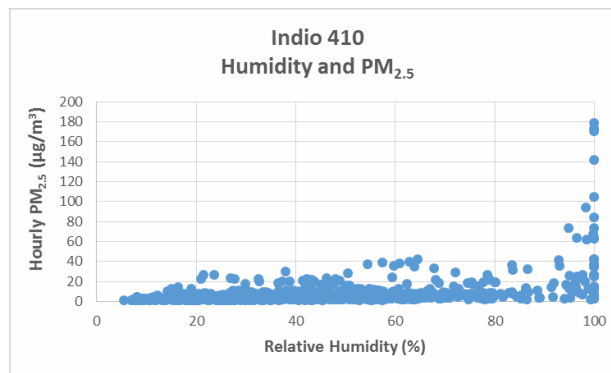
Figure 3.44. Indio 410 Humidity and PM
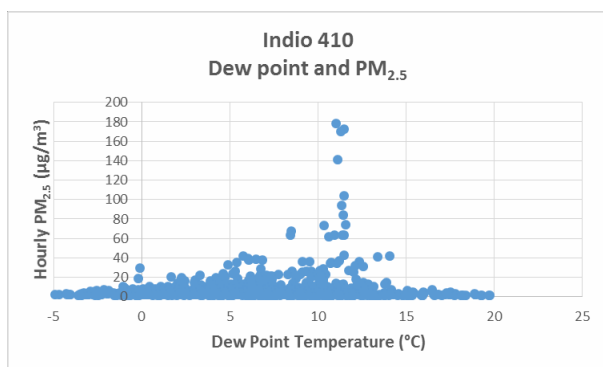
Figure 3.45. Indio 410 Dew Point and PM

In summary, no correlation between the temperature, RH, or dew point was found for the ozone or PM sensors. Additional research could further investigate the effects and potentially apply filters for specific temperature and RH values that may lead to invalid measurements by the OPC.

3.3. QA summary for field deployment

Throughout the CSAM field deployment, the Atmospheric Measurements (AM) Branch at SCAQMD operated and maintained the regulatory air monitoring stations across the air basin. Seven of the CSAM pods were located at six regulatory air monitoring stations. The ozone and particle instrumentation at these monitoring stations were maintained and operated in accordance with standard air monitoring practices. The FEM ozone instruments were maintained and checked weekly by station operators to verify that the instrument was operating according to the specifications defined in the SCAQMD's SOPs. The ozone instruments were subjected to daily precision and weekly span checks to verify the instrument was operating within 7% of the expected values for precision and span checks. During the field deployment, the ozone instruments at the Indio AMS and Rubidoux AMS were all within 7% of the expected values for all precision and span checks. These instruments were calibrated every six months or as needed if found to be out of tolerance. The ozone instrument at Indio was calibrated on December 10, 2016 and the instrument at Rubidoux was calibrated on November 2, 2016. The quality assurance branch at SCAQMD performs an ozone concentration ramping audit on the ozone analyzers annually. The combined maintenance, calibration schedule, and audit schedules performed on the station ozone instrumentation provides assurance that the data are of high quality.

The equivalent method particle instrumentation at the stations were subjected to flow, leak, temperature,

and pressure verifications monthly. Throughout the course of the field deployment, the flow, leak, temperature, and pressure verifications performed on the BAM units were found to be within specifications. The Metone BAM also automatically performs a span check each hour with a reference membrane to ensure that the instrument is not drifting over time. The Metone BAM units are calibrated every six months and the quality assurance branch performs audits of the BAM twice a year. The MLVB BAM was calibrated on December 6, 2016 and the Rubidoux BAM was calibrated on June 24, 2016 and February 10, 2017. The Grimm 180EDM undergoes flow checks monthly and is calibrated annually. The most recent calibration of the Grimm 180EDM was performed by the factory on November 29, 2016. The combined maintenance, verifications, and checks on the FEM equipment provides assurance that the instrumentation was operating in good condition and producing quality data.

The CSAM units were checked once every two weeks to ensure proper data logging and to verify date and timestamps. No further quality assurance checks or verifications were performed during the field deployment.

Conclusions

The AQ-SPEC group successfully evaluated the performance of EPA-designed CSAM pods both in the field and laboratory. The pods were then successfully deployed at nine locations across southern California in three distinct areas including Long Beach, Jurupa Valley, and Coachella Valley. The extended deployment and subsequent data analysis revealed some of the concerns related to long-term sensor deployment, including measurement sensitivity change and sensor degradation over time. The AQ-SPEC group recommends re-engineering the pods to include built-in data communication. The ability to remotely access the data would allow data validation and analysis procedures to be built into cloud-based applications that could detect sensor performance losses and failures on a timelier basis. This would reduce the need for staff members to visit the sites to download and compile the data, and then to perform statistical analysis weeks after the measurements have been taken. In addition, the AQ-SPEC recommends performing extended sensor performance testing before entering into sensor selection and subsequent sensor development for ambient air quality monitoring. Care should be taken to identify the raw sensor with the best fit within the allocated budget that provides an adequate sensor life time for the duration of the study. Minimizing down time to reduce data losses is also important when selecting sensors for in-field deployment. The AQ-SPEC also recommends that sensors that have undergone extensive field and laboratory testing should not be used in subsequent field deployments. Extensive testing in areas characterized by elevated air pollution levels may damage or alter the sensors' performance, which could result in significant data loss after the sensors have been deployed in the field for specific air monitoring applications.

References

Barzyk, T., R. Williams, A. Kaufman, M. Greenberg, M. OShea, P. Sheridan, A. Hoang, A. Teitz, C. Ash, M. Mustafa, AND S. Garvey. 2016. Citizen Science Air Monitoring in the Ironbound Community. U.S. Environmental Protection Agency, Washington, D.C., EPA/600/R-16/049. https://cfpub.epa.gov/si/si_public_record_report.cfm?dirEntryId=315154, last accessed September 18, 2017.

Jiao, W., Hagler, G., Williams, R., Sharpe, B., Brown, R., Garver, D., Judge, R., Caudill, M., Richard, J., Davis, M., Weinstock, L., Zimmer-Dauphinee, S., Buckley, K. 2016. Community air sensor network (CAIRSENSE) project: Evaluation of low-cost sensor performance in a suburban environment in the southeastern United States. Atmospheric Measurement Technology, DOI:10.5194/amt-9-5281-2016.

Jiao, W., Hagler, G., Williams, R., Sharpe, B., Brown, R., Garver, D., Judge, R., Caudill, M., Richard, J., Davis, M., Weinstock, L., Zimmer-Dauphinee, S., Buckley, K. "Community Air Sensor Network (CAIRSENSE) Project: Lower Cost, Continuous Ambient Monitoring Methods", presented at the 108th Annual Meeting of the Air & Waste Management Association, June 22-25, 2015 in Raleigh, NC. https://www.epa.gov/sites/production/files/2015-07/documents/cairsense.pdf, last accessed September 18, 2017.

Lawrence, M.G. 2005. The relationship between relative humidity and the dewpoint temperature in moist air: A simple conversion and applications, American Meteorological Society, DOI:10.1175/BAMS-86-2-225.

Papapostolou, V., Zhang, H., Feenstra, B.J., and Polidori A. 2017. Development of an environmental chamber for evaluating the performance of low-cost air quality sensors under controlled conditions. Atmospheric Environment, 171: 82-90.

Polidori, A., Papapostolou, V., Zhang, H. 2016. Laboratory Evaluation of Low-Cost Air Quality Sensors – Laboratory Setup and Testing Protocol. South Coast Air Quality Management District, Diamond Bar, CA.

South Coast Air Quality Management District Final 2016 Air Quality Management Plan (2016 SCAQMD AQMP). http://www.aqmd.gov/home/library/clean-air-plans/air-quality-mgt-plan/final-2016-aqmp, last accessed September 18, 2017.

Williams, R., A. Kaufman, and S. Garvey. 2015a. Next Generation Air Monitoring (NGAM) VOC Sensor Evaluation Report. U.S. Environmental Protection Agency, Washington, DC, EPA/600/R-15/122 (NTIS PB2015-105133). https://cfpub.epa.gov/si/si_public_record_report.cfm?dirEntryId=308114, last accessed September 18, 2017.

Williams, R., A. Kaufman, T. Hanley, J. Rice, and S. Garvey. 2015b. Evaluation of Elm and Speck Sensors. U.S. Environmental Protection Agency, Washington, DC, EPA/600/R-15/314. https://cfpub.epa.gov/si/si_public_record_report.cfm?dirEntryId=310285, last accessed September 18, 2017.

Williams, R., T. Barzyk, and A. Kaufman. 2015c. Citizen Science Air Monitor (CSAM) Operating Procedures. U.S. Environmental Protection Agency, Washington, DC, EPA/600/R-15/051. https://cfpub.epa.gov/si/si_public_record_report.cfm?dirEntryId=307111&simpleSearch=1&searchAll=CSAM+Operating+Procedures, last accessed September 18, 2017.

Williams R., A. Kaufman, T. Hanley, J. Rice, and S. Garvey. 2014a. Evaluation of Field-deployed Low Cost PM Sensors. U.S. Environmental Protection Agency, Washington, DC, EPA/600/R-14/464 (NTIS PB 2015-102104). https://cfpub.epa.gov/si/si_public_record_report.cfm?dirEntryId=297517, last accessed September 18, 2017.

Williams, R., R. Long, M. Beaver, A. Kaufman, F. Zeiger, M. Heimbinder, I. Hang, R. Yap, B. Acharya, B. Ginwald, K. Kupcho, S. Robinson, O. Zaouak, B. Aubert, M. Hannigan, R. Piedrahita, N. Masson, B. Moran, M. Rook, P. Heppner, C. Cogar, N. Nikzad, and W. Griswold. 2014b. Sensor Evaluation Report. U.S. Environmental Protection Agency, Washington, D.C., EPA/600/R-14/143 (NTIS PB2015-100611), https://cfpub.epa.gov/si/si_public_record_report.cfm?dirEntryId=277270, last accessed September 18, 2017.

U.S. Environmental Protection Agency (EPA). 2016. Village Green and AirMapper Fact Sheet. https://www.epa.gov/air-research/village-green-and-airmapper-fact-sheet, last accessed September 18, 2017.